

THE EFFECTS OF GLUTAMATERGIC ACTIVATION
OF THE LATERAL SUPRAMAMMILLARY NUCLEUS AND
THE MEDIAL SEPTUM COMPLEX ON PERFORANT
PATH-EVOKED POTENTIALS, AND OTHER
PHYSIOLOGICAL PARAMETERS, IN THE DENTATE GYRUS OF THE RAT

CENTRE FOR NEWFOUNDLAND STUDIES

**TOTAL OF 10 PAGES ONLY
MAY BE XEROXED**

(Without Author's Permission)

GEOFFREY PHILIP CARRE







National Library
of Canada

Acquisitions and
Bibliographic Services Branch

395 Wellington Street
Ottawa, Ontario
K1A 0N4

Bibliothèque nationale
du Canada

Direction des acquisitions et
des services bibliographiques

395, rue Wellington
Ottawa (Ontario)
K1A 0N4

Your file *Votre référence*

Our file *Notre référence*

The author has granted an irrevocable non-exclusive licence allowing the National Library of Canada to reproduce, loan, distribute or sell copies of his/her thesis by any means and in any form or format, making this thesis available to interested persons.

L'auteur a accordé une licence irrévocable et non exclusive permettant à la Bibliothèque nationale du Canada de reproduire, prêter, distribuer ou vendre des copies de sa thèse de quelque manière et sous quelque forme que ce soit pour mettre des exemplaires de cette thèse à la disposition des personnes intéressées.

The author retains ownership of the copyright in his/her thesis. Neither the thesis nor substantial extracts from it may be printed or otherwise reproduced without his/her permission.

L'auteur conserve la propriété du droit d'auteur qui protège sa thèse. Ni la thèse ni des extraits substantiels de celle-ci ne doivent être imprimés ou autrement reproduits sans son autorisation.

ISBN 0-315-86660-8

Canada

**THE EFFECTS OF GLUTAMATERGIC ACTIVATION OF THE LATERAL
SUPRAMAMMILLARY NUCLEUS AND THE MEDIAL SEPTUM COMPLEX
ON PERFORANT PATH-EVOKED POTENTIALS, AND OTHER
PHYSIOLOGICAL PARAMETERS, IN THE DENTATE GYRUS OF THE RAT**

BY

© **Geoffrey Philip Carre**

**A thesis submitted to the School of Graduate
Studies in partial fulfilment of the
requirements for the degree of
Doctor of Philosophy**

**Psychology Programme
Memorial University of Newfoundland
May 1993**

St. John's

Newfoundland

ABSTRACT

A large number of cells from the lateral aspect of the supramammillary nucleus (SUML) and the medial septum complex (MSC) innervate the dentate gyrus of the hippocampus. It has been demonstrated that electrical prestimulation of the SUML or the MSC enhances perforant path-dentate gyrus evoked field potentials. Considering the large number of fibres that pass through these regions, the effects glutamatergic stimulation of these regions had on dentate gyrus field potentials in urethane-anaesthetized rats was investigated. The perforant path was stimulated at a rate of 0.1 Hz, evoking an EPSP and a population spike in the dentate gyrus granule cell layer. L-glutamate was delivered by pressure injection (500 mM, 100-150 nl). In a second experiment, concomitant measures of hippocampal EEG, spontaneous unit activity, and the evoked potential recorded at the molecular layer were also taken. As well, the effects of glutamatergic activation of these areas on paired-pulse inhibition was investigated.

Glutamate ejection to the SUML and MSC produced a significant enhancement of the population spike. The duration of enhancement ranged from 2 to 54 min ($\bar{X} = 18.4$ min) and from 1 to 49 min ($\bar{X} = 10.5$ min) after SUML and MSC activation respectively. A consistent, but relatively short increase in the EPSP slope was demonstrated after MSC activation but not

after SUML activation. No consistent effects were found on the 2 latency measures.

SUML and MSC activation induced theta in 4 of 7 (duration = 10-45 s) and 7 of 10 animals (duration = 20-112 s), respectively. Theta induction preceded spike enhancement and occurred for a shorter duration than the enhancement.

After either SUML or MSC activation the effects on spontaneous unit activity were mixed. However, all changes in firing rate preceded spike enhancement, and their duration rarely coincided with the duration of the spike enhancement.

Results of paired-pulses (ISI = 20-30 ms) given during SUML activation demonstrated evidence of reduced feed-back inhibition, despite an absence of the enhancement of the first spike of the pair. MSC activation produced a reduction of feed-back inhibition in one of three animals where the first spike of the pair was enhanced.

ACKNOWLEDGEMENTS

I am deeply indebted to Dr. Carolyn Harley for supervising this thesis, for her advice, encouragement, and infinite patience. I am also grateful to the other members of my committee, Drs. Bob Adamec and Dale Corbett for their constructive and critical comments.

Special thanks are due to Beth Perry, for her logistical and emotional support, especially in the dying hours.

Thanks are also due to Graduate Studies, who provided financial support in the form of a Graduate Fellowship.

Finally I would like to thank my parents, whose constant encouragement and support made the submission of this thesis a reality.

TABLE OF CONTENTS

ABSTRACT	i
ACKNOWLEDGEMENTS	iii
LIST OF TABLES	vi
LIST OF FIGURES	vii
CHAPTER 1: INTRODUCTION	1
1.1 The Hippocampus	4
1.1.1 Gross Anatomy	5
1.1.2 Cells of the Dentate Gyrus	7
1.1.3 Connections	12
1.1.3.1 The Entorhinal Connection	12
1.1.3.2 The Trisynaptic Circuit	16
1.1.3.3 Local Circuitry of the Dentate Gyrus	17
1.1.3.3.1 Somatostatin-immunoreactive Aspiny Cells	18
1.1.3.3.2 Basket Cells	20
1.1.3.3.3 Calretinin-immunoreactive Spiny Cells	21
1.1.3.3.4 Mossy Cells	23
1.1.3.3.5 Conclusion	24
1.1.4 Electrophysiology of the Hippocampus	26
1.1.4.1 Evoked Field Potentials	26
1.1.4.1.1 Single Evoked Field Potentials ..	26
1.1.4.1.2 Paired-pulse Evoked Potentials ..	28
1.1.4.1.3 Long-term Potentiation	31
1.1.4.2 Hippocampal Theta	37
1.2 This Study	38
CHAPTER 2: THE LATERAL SUPRAMAMMILLARY NUCLEUS	41
2.1 Introduction	41
2.2 Methods	46
2.2.1 Experiment 1	46
2.2.2 Experiment 2	50
2.3 Results	53
2.3.1 Experiment 1	53

2.3.2 Experiment 2	61
2.4 Conclusions	80
CHAPTER 3: THE MEDIAL SEPTUM COMPLEX	88
3.1 Introduction	88
3.1.1 Anatomy	88
3.1.2 Influence of the MSC on Hippocampal Evoked Potentials	93
3.2 Methods	100
3.2.1 Experiment 1	100
3.2.2 Experiment 2	100
3.3 Results	101
3.3.1 Experiment 1	101
3.3.2 Experiment 2	107
3.4 Conclusion	122
CHAPTER 4: DISCUSSION	129
REFERENCES	149
APPENDIX I	183
APPENDIX II	204

LIST OF TABLES

Table 2-1. Listing of each unit recorded, its spontaneous firing rate, whether it fires in bursts or not, whether it fired rhythmically in the theta frequency, the effects of glutamate ejection in the SUML, and the magnitude of the accompanying population spike facilitation.	76
Table 2-2. Listing of each unit recorded and its relationship in time to the population spike enhancement and EEG (if it was recorded, - indicates no recording).	78
Table 3-1. Listing of each unit recorded, its spontaneous firing rate, whether it fired in bursts, whether it fired rhythmically in the theta frequency, the effects of glutamate ejection in the medial septum complex, and the magnitude of the accompanying population spike facilitation.	118
Table 3-2. Listing of each unit recorded and its relationship in time to the population spike enhancement and EEG (if it was recorded, - indicates no recording).	120

LIST OF FIGURES

FIG. 1-1. A transverse view of the hippocampus	6
FIG. 2-1. Diagram showing the parameters measured for an evoked potential recorded in the granule cell layer/hilar region	49
Fig. 2-2. Diagram illustrating how up to 4 parameters were recorded in the dentate gyrus during the same session	51
FIG. 2-3. Glutamate micropipette placements for hypothalamic sites which exhibited significant facilitation of the perforant path population spike amplitude	54
FIG. 2-4. Mean percent changes in population spike amplitude, EPSP slope, spike onset and peak latencies for the 12 sites exhibiting spike amplitude facilitation after glutamate ejection to the SUML	56
FIG. 2-5. Percent change in population spike amplitude for an animal exhibiting a relatively long-lasting potentiation after glutamate ejection to the SUML	57
FIG. 2-6. Glutamate micropipette placements for sites which exhibited significant facilitation of the perforant path population spike amplitude in the thalamus	59
FIG. 2-7. Mean percent changes in population spike amplitude, EPSP slope, spike onset and peak latencies for the 8 sites exhibiting spike amplitude facilitation after glutamate ejection to the medial thalamus	60
FIG. 2-8. Two examples of theta rhythm induction as a result of glutamate injected into the SUML	62
FIG. 2-9.(a-c) Three examples of units isolated by cluster-cutting and characterized by software analysis	63-66
FIG. 2-10. Time course and effect of glutamate ejection to the SUML on units and population spike	68

FIG. 2-11. Paired-pulse results from one experiment during glutamate ejection to the SUML 71-72

FIG. 2-12. Paired-pulse results from a second experiment 75

FIG. 3-1. Diagram illustrating the ejection sites directed at the medial septum complex 102-103

FIG. 3-2. Mean percent changes in population spike amplitude (area), EPSP slope, spike onset and peak latencies for the 19 sites associated with the MSC exhibiting spike amplitude facilitation 104

FIG. 3-3. An example of long-lasting perforant path-dentate gyrus spike facilitation as a result of L-glutamate ejection into the medial septum complex 105

FIG. 3-4. Representative examples of theta induction and frequency elevation as a result of medial septum complex activation by glutamate 108

FIG. 3-5. Time course and effect of glutamate ejection to the medial septum complex on units and population spike 110

FIG. 3-6. Paired-pulse results from one experiment during glutamate ejection to the MSC 113-114

FIG. 3-7. Paired-pulse results for a second experiment 115

FIG. 3-8. Paired-pulse results for a third experiment, where glutamate ejection did not produce an enhancement of the amplitude of the first population spike 116

CHAPTER 1: INTRODUCTION

A great deal is known about the anatomical connections that make up the neural circuitry of the brain. Only recently, however, have neuroscientists turned their attention towards the integration and modulation of impulse flow in any given circuit, properties that define the functional activity of the system.

The two cortical systems that have received the greatest attention in this regard are the visual cortical system (neocortex) of the cat and the hippocampus (allocortex) of the rat. The latter represents a structurally simple cortex that serves as a model for cortical organisation and cell physiology. It's structure is relatively uncomplicated, because the principal neurons, the pyramidal and granule cells, are each arranged in separate, compact layers, with dendrites emanating in a parallel manner. Excitatory cortical inputs are directed towards specific dendritic regions, allowing one to directly test the consequences of activation of these fibres to determine the excitability, or "state" of the principal cells.

Attention has also been drawn to the hippocampus because of its apparent role in learning and memory, and a large literature has accumulated in an attempt to determine its precise role. While researchers disagree on detail,

they agree that the hippocampus is important for the acquisition of certain categories of new information.

The role of the hippocampus in learning and memory has received a great deal of attention since H.M. developed severe anterograde amnesia as a result of the surgical removal of the medial portion of both his temporal lobes, which included the hippocampus (Scoville and Milner, 1957). Animal studies have identified several areas in which the hippocampus appears to play an important role. Special forms of conditioning, such as trace conditioning and discrimination reversal, appear to depend on the hippocampus (Lavond et. al., 1981; Berger and Orr, 1982), especially whenever a conditioned response needs to be unlearned or inhibited (Kimble, 1968). Recordings show that individual neurons in the hippocampus become active only when the animal is in a specific place in the environment, leading to the theory that the task of the hippocampus is to store all spatial memories tied together into a cognitive map of the animal's environment (O'Keefe and Nadel, 1978). If one distinguishes between working memory, a rapidly fading set of engrams that stores just recent events, and reference memory, all the relatively unchangeable facts that have been learned, the hippocampus appears to be critical for working memory (Olton, 1983).

The role of the hippocampus in sensory information processing is supported by an expanding knowledge of cortical circuitry. The connectivity of the

cortex suggests that each modality is processed through a sequence of connections, from unimodal areas, towards multimodal associational areas increasing the complexity of the information en route. It has been proposed that since these multimodal areas funnel their information into the hippocampal formation through the entorhinal cortex, it constitutes a final cascade of cortical sensory information processing - a supramodal associational cortex where cortical channels converge (Witter et al., 1989b).

Any model of learning and memory would require an accounting of the animal's behavioural condition, which would influence the state of information processing. The hippocampus receives widespread projections from relatively small groups of neurons in the basal forebrain and brainstem. Most of these systems are associated with a single neurotransmitter, such as the cholinergic basal forebrain system, the noradrenergic locus coeruleus, the serotonergic raphe system, and the dopaminergic ventral tegmental area. Each of these neurotransmitters appears to affect target neurons in a manner distinct from classical excitation or inhibition, and each has been implicated in the modulation of global behavioural states such as vigilance, mood, motivation, and arousal.

The intent of this thesis is to advance our knowledge of the effects of putative "arousal" systems on hippocampal physiology in the dentate gyrus. Two systems were of interest: the lateral supramammillary nucleus of the

hypothalamus, which, despite a large projection to the hippocampus and other cortical areas, has received little attention from neuroscientists, and the medial septum/diagonal band, which has received a great deal of attention.

This chapter will review the anatomy and physiology of the rat hippocampus, with emphasis on the portion of the hippocampus under investigation, the dentate gyrus.

1.1 The Hippocampus

The hippocampal formation can be divided into three major subdivisions: the dentate gyrus, Ammon's horn (Cornus ammonis, or CA), and the subiculum complex, which in turn can be subdivided into the subiculum, presubiculum, and parasubiculum. Some choose to add the entorhinal cortex as a fourth subdivision of the hippocampal formation (Amaral and Witter, 1989), whereas others group the subiculum complex and the entorhinal cortex together as the parahippocampus (or retrohippocampus), and the dentate gyrus and Ammon's Horn as the hippocampal formation (Lothman et al., 1991). The latter organization will be used here. Extensive reviews of the anatomy of the hippocampal formation and the parahippocampus have recently been published (Amaral and Witter, 1989; Lopes da Silva et al., 1990; Witter et al., 1989b; Swanson et al., 1987)

1.1.1 Gross Anatomy

In the rat, the hippocampal formation is located between the thalamus and the neocortex. It is shaped like a cashew, its anterior pole starting just caudal to the septum, curving along its length laterally and ventrally to end in the lowermost aspect of the forebrain, just caudal and medial to the amygdala.

The hippocampal circuitry is traditionally viewed in a transverse plane (perpendicular to the longitudinal axis), as presented in Fig. 1-1. Two interlocking cell layers are easily distinguished in this section. The principal cells of the dentate gyrus, the granule cells, form a horizontal V shape whose tip points to the contralateral hippocampus. The principal cells of Ammon's Horn, the pyramidal cells, form an interlocking C shape, where the lower blade originates between the two blades of the dentate gyrus and subsequently curves out and above the dentate gyrus to end distally at the subiculum.

The basic arrangement of the hippocampal subfields are similar, for their apical dendrites arise from the principal cells and project in a parallel arrangement into a cell-poor region, the molecular layer in the dentate gyrus, and the stratum lacunosum-moleculare and stratum radiatum in Ammon's horn. Underneath the principal cell layers, the granule cell layer and the pyramidal cell layer, is a polymorph zone where cells of a variety of shapes

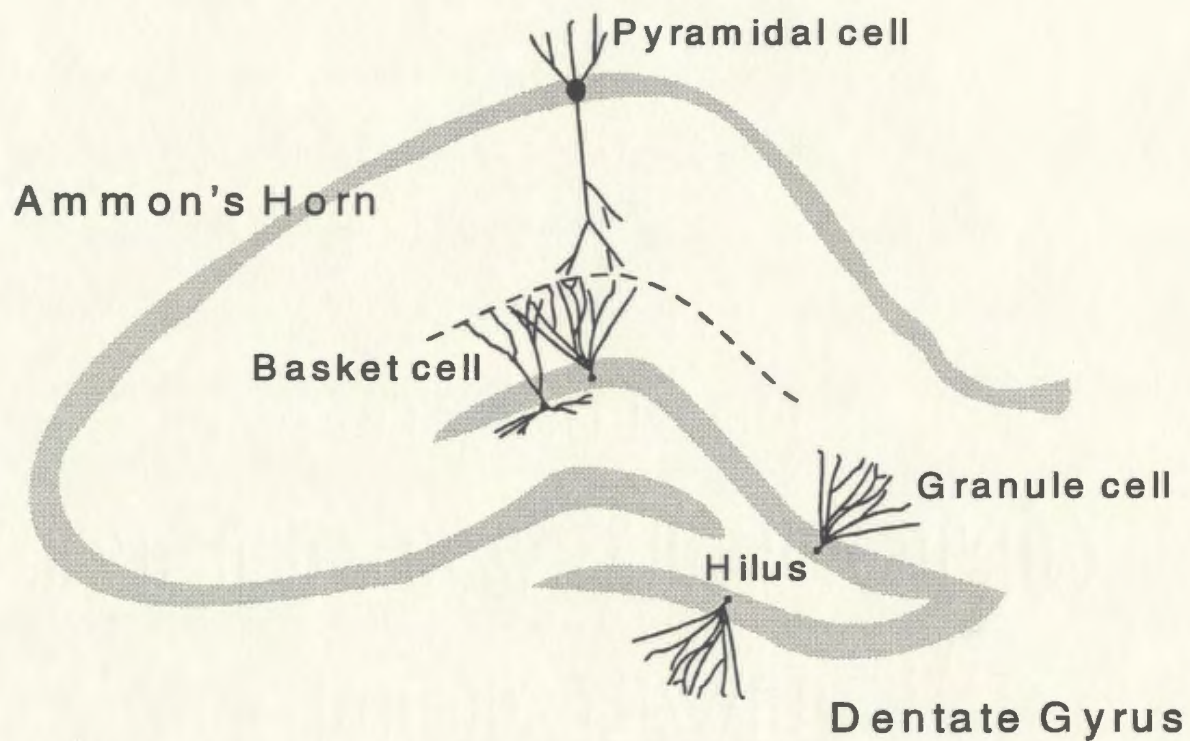


FIG. 1-1. Transverse view of the hippocampus. Shaded areas represent the principal cell layers with examples of each principal cell and a basket cell of the dentate gyrus.

lie scattered. The polymorph zone of the dentate gyrus lies between the blades of the granule cell layers and is called the hilar region or hilus.

The pyramidal cell layer of Ammon's horn was originally subdivided into four subfields, CA1 to CA4. CA1 starts at the subicular end of Ammon's horn and is characterized morphologically by smaller pyramidal cell bodies packed at a greater density than the other subfields. CA2 and CA3 pyramidal cells are greater in size and more loosely packed, and found along the back and lower blade of Ammon's horn. CA2 pyramidal cells can further be distinguished by a lack of dendritic spines on their proximal apical dendrites. In subfield CA4 the pyramidal cells become more scattered, and are mixed with a wider variety of cell types than in other CA subfields. Due to an apparent structural and functional relationship with the dentate gyrus (Amaral, 1978; Schwartzkroin et al., 1990), this area will be referred to as the dentate hilar region as opposed to Ammon's horn. The CA3 field can be further subdivided into three regions. The large pyramidal cells adjacent to the dentate hilus are called CA3c, while the approximate middle of the CA3 layer and the curved layer of CA3 cells adjacent to CA2 are called CA3b and CA3a, respectively.

1.1.2 Cells of the Dentate Gyrus

Granule cells have small cell bodies and few primary dendrites that arborize extensively into the molecular layer, forming a cone with the cell body at the

apex. Granule cells located deep in the granule cell layer give off a main apical shaft that branches immediately after entering the molecular layer (Frotscher and Leranth, 1986). Unlike pyramidal cells, they lack basal dendrites. All dendrites become densely covered with spines upon entering the molecular layer. Small spines and larger complex spines have been seen to emanate from the same dendrites, with larger complex spines being more numerous at the proximal portion (Frotscher and Zimmer, 1983). A single fine axon leaves the cell at the hilar end to join other "mossy fibres" which course through the hilus into Ammon's horn. Characteristic giant boutons on these unmyelinated axons give rise to the term "mossy fibres". Approximately 1,000,000 granule cells are found in the dentate gyrus of one hemisphere of the rat (Amaral et al., 1990).

The less numerous non-granule cells of the dentate gyrus are quite heterogeneous when characterized morphologically. They are sparsely distributed in the molecular layer, but are more numerous deep within the granule cell layer and in the underlying hilar region. Twenty-one different cell types have been identified in the polymorph or hilar region and they vary from medium sized stellate and pyramidal shaped cells to very large mossy cells (Amaral, 1978). The most numerous and best characterized non-granule cells are the basket cells, which are closely associated with the granule cell layer, and the mossy cells which are usually found in the deep hilus.

The mossy cells are one of the most distinctive and numerous of the hilar cell types (Ribak et al., 1985; Amaral, 1978), and derive their name from the fact that their proximal dendrites are covered with a dense coating of spines and "thorny excrescences" (Amaral, 1978). They have large multipolar cell bodies, and a very large dendritic tree that spans the hilus in all directions and extends into the dentate molecular layer (Amaral, 1978; Frotscher et al., 1991), where some will reach the outer zone (Scharfman, 1991).

The basket cells, have been subdivided into five different types that vary in regard to their somal location, their somal shape, and their dendritic arborization (Ribak and Seress, 1983). They all have smooth dendritic surfaces due to the lack of spines and their axons arborize within the granule cell layer to form a basket plexus (Amaral, 1978; Ribak and Seress, 1983), hence their name. Basket cells are found most often embedded in, or directly beneath, the granule cell layer. Their basal dendrites run parallel to this layer or descend into the hilar region. A single or branching dendrite ascends into the molecular layer. These cells are noticeably larger than granule cells and have a ratio of about one basket cell for every 180 granule cells (Amaral et al., 1990). It is not known whether a portion of deep hilar neurons participate in the "baskets" around granule cells (Ribak and Seress, 1983).

Basket cells have been classified as pyramidal, fusiform, horizontal, inverted fusiform or molecular layer basket cells (Ribak and Seress, 1983). The first

four category titles are indicative of their shape, and they are found predominantly in the granular or subgranular layers. The last category specifies cells of multipolar shape found in the molecular layer adjacent to the granule cell layer.

Immunocytochemical studies employing antibodies against the gamma-aminobutyric acid (GABA) synthesizing enzyme glutamate decarboxylase (GAD), suggests that all basket cells and 60% of the hilar cells are GABAergic (Ribak et al.,1978; Seress and Ribak, 1983; Gamrani et al.,1986). A subset of the basket cells are also immunoreactive for parvalbumin (Katsumaru et al.,1988; Nitsch et al.,1990; Soriano and Frotscher, 1989) or calretinin (Gulyas et al.,1992; Miettinen et al.,1992), two calcium-binding proteins. Furthermore, a subset of the basket cells are also positive for cholecystokinin (CCK) or vasoactive intestinal peptide (VIP) (Sloviter and Nilaver, 1987b).

Many somatostatin-positive cells surrounded by a plexus of GABA-, CCK-, and VIP- positive fibres have been identified in the hilus (Sloviter and Nilaver, 1987b). These cells are aspiny, often multipolar or spindle-shaped, and innervate the outer two-thirds of the dentate molecular layer (Bakst et al.,1986; Van der Zee et al.,1991). The majority of these cells (about 90%) contain the inhibitory neurotransmitter GABA or its synthesizing enzyme glutamate decarboxylase (GAD) (Kosaka et al.,1988; Schmechel et

al.,1984). Furthermore, a number of the somatostatin cells are immunoreactive for neuropeptide Y as well (Kohler et al.,1987). A set of cells that were generally small in soma size and number, were VIP-positive and found scattered throughout the dentate gyrus (Sloviter and Nilaver, 1987b).

On the basis of cell morphology, axonal targets, and resident neurotransmitters, it was postulated that three main populations of dentate interneurons exist (Sloviter and Nilaver, 1987b). One consists of GABA cells which are primarily basket cells with subsets containing VIP or CCK. The second population consists of the somatostatin aspiny cells, and the third are the hilar mossy cells, which are apparently GABA and peptide-negative.

An additional subpopulation of hilar cells has recently been characterized enough to warrant mention. These cells are immunoreactive to calretinin, a calcium-binding protein of the calmodulin family, and were found to form two distinct cell groups, spiny and spine-free cells (Gulyas et al.,1992; Miettinen et al.,1992). The majority of spine-free cells were immunoreactive for GABA, while few spiny cells (11%) were considered GABA positive. Many of the spine-free cells were characteristic of the basket cells of the dentate gyrus. The spiny cells can be compared to the long-spined multipolar hilar cells described by Amaral (Amaral, 1978). Their dendrites were restricted to the hilus.

1.1.3 Connections

1.1.3.1 The Entorhinal Connection

The entorhinal cortex plays a strategic role in relation to the hippocampal formation, since it provides the major extrinsic input to this area and serves as one of the primary targets of hippocampal output. The entorhinal cortex receives direct projections from the olfactory bulb and from other cortical areas that the olfactory bulb contacts, as well as from multimodal association areas of the temporal, prefrontal, cingulate, and insular regions (Swanson et al., 1987).

Within the entorhinal cortex six cortical layers are distinguished that are described as the superficial (layers I-III) and deep (layers IV-VI) layers. The entorhinal cortex is further subdivided into a lateral (LEC) or medial (MEC) entorhinal cortex based on differences in cytoarchitecture and projection sites (Hjorth-Simonsen, 1972; Steward, 1976; Ruth et al., 1982; Germroth et al., 1991). Layer II neurons of LEC are very densely packed and tend to be clustered in patches whereas in the MEC their distribution is more uniform, they are slightly larger, and less densely packed. A differential distribution of sensory modality inputs also distinguishes the two regions, as the olfactory input to the entorhinal cortex is denser in the LEC than in the MEC (Kosel et al., 1981; Haberly and Price, 1978).

As implied earlier, the entorhinal cortex gives rise to a massive projection to the hippocampal formation, whose trajectory is called the perforant path, which terminates predominantly in the dentate gyrus (Hjorth-Simonsen, 1972; Steward, 1976; Wyss, 1981; Ruth et al., 1982; Ruth et al., 1988). These axons arise from neurons of layers II and III, with the latter originating from predominantly pyramidal cells to contact Ammon's horn and the former from predominantly stellate cells to contact the dentate gyrus (Steward and Scoville, 1976; Eberhard et al., 1989; Germroth et al., 1991; Lingenhohl and Finch, 1991). A few neurons from the deep layers also innervate the hippocampal formation (Kohler, 1985b). Individual neurons within the entorhinal cortex may send collaterals to other sites, as well as the hippocampus (Lingenhohl and Finch, 1991).

To enter the hippocampal formation, the perforant path traverses the subiculum, and divides into two distinct branches (Witter, 1989a). One enters the dentate gyrus after "perforating" the hippocampal fissure, while the second stays within Ammon's Horn to synapse with pyramidal cells in CA3 and CA1.

The perforant path fibres have been shown to form asymmetric synapses on dendrites in the molecular layer of the dentate gyrus, and in fields CA1 and CA3 of Ammon's Horn, and these fibres use glutamate as their neurotransmitter (Hjorth-Simonsen, 1972; White et al., 1977; Bramham et

al., 1990; Grandes and Streit, 1991). The perforant path fibres make synaptic contact with granule cell dendrites, where virtually all excitatory contacts are found on spines (Andersen et al., 1966b). Entorhinal lesions produce electron-dense, degenerating terminals which synapse with characteristic spine formations (Matthews et al., 1976) that have been found to arise from identified granule cell dendrites (Frotscher and Zimmer, 1983; Lubbers and Frotscher, 1987). It has been estimated that each granule cell receives approximately 5,000 (Amaral et al., 1990) to 10,000 (West and Andersen, 1980) synapses, most of which are excitatory. A small population of GABAergic neurons also participates in the entorhino-hippocampal projection (Germroth et al., 1989). Since degeneration of perforant path fibres following entorhinal or perforant path lesions only involves asymmetric synapses on granule and pyramidal cells (Fifkova, 1975; Nafstad, 1967), it has been hypothesized that the perforant path fibres utilizing GABA terminate on local inhibitory neurons (Germroth et al., 1991).

The entorhinal fibres in the dentate gyrus show a laminated termination. Fibres arising from the MEC project to the middle third of the molecular layer and fibres arising from the LEC terminate in the outer third of the molecular layer. Within the MEC-middle zone projection, lateral parts of the MEC project to the outer part of the middle zone whereas medial parts of the MEC project to the inner portion of the middle zone (Witter, 1989a). Fibres of the

perforant path account for approximately 85% of the synapses in the outer two-thirds of the molecular layer (Hoff et al., 1982; Matthews et al., 1976).

The impetus to divide the molecular layer into thirds is supported by other evidence. The middle zone stains densely for cholecystokinin (CCK) whereas the outer zone is characterized by a strong enkephalin fibre plexus (Chavkin et al., 1985; Fredens et al., 1984; Gall et al., 1981; Stengaard-Pedersen et al., 1983). As well, immunostaining for different cell surface glycoproteins divides the three zones of the molecular layer on the basis of the segregated distribution of individual glycoproteins (Woodhams et al., 1992; Woodhams et al., 1991). Finally, immunocytochemical staining for the cellular and subcellular distribution of glutamate in the hippocampus demonstrates higher nerve terminal concentrations of glutamate in the outer zone of the molecular layer as opposed to the other two zones (Bramham et al., 1990). The functional significance of these zone distinctions has yet to be determined.

Entorhinal input to the dentate gyrus is not limited to the granule cells. Some perforant path fibres establish asymmetric (presumably excitatory) synapses on smooth dendritic shafts of inhibitory (GABAergic) neurons whose cell bodies are found in the hilar region (Zipp et al., 1989). As well, light projections from both the MEC and the LEC have been found in the hilar region (Wyss, 1981) where a subset give rise to fibre plexuses in the subgranular layer (Kohler, 1985a), which is populated mainly by basket cells.

1.1.3.2 The Trisynaptic Circuit

The perforant path-dentate connection gives rise to the first synapse of what is traditionally known as the trisynaptic circuit. The granule cells, in turn, send mossy fibres to synapse at the proximal dendrites of CA3 pyramidal cells, which in turn, send "Schaffer collaterals" to CA1 pyramidal cells to form the third synapse. All members of this chain probably use the neurotransmitter glutamate (Bramham et al.,1990). CA1 pyramidal cell fibres, according to this organizational concept, were seen as the major output pathway from the hippocampal formation. While this functional organization is essentially correct today, more studies are required to determine the contribution of the direct entorhinal inputs to both CA3 and CA1 [cf. (Yeckel and Berger, 1990)].

The early anatomical and physiological studies lead to the "lamellar" hypothesis to describe the three-dimensional organization of the major intrinsic hippocampal connections that make up the trisynaptic pathway (Andersen et al.,1971b; Rawlins and Green, 1977). They concluded that the four pathways of this circuit are all oriented in the same direction, transversely to the longitudinal axis. Stimulating a small area of the entorhinal cortex, according to this hypothesis, would lead to a small slice, or lamella, of tissue being activated by the four projections in rapid succession. They went on to suggest that small strips of the hippocampus

may then operate as independent functional sectors, noting that interconnections between neighbouring lamella may have a modulating influence. Indeed, this lamellar plan provided a catalyst for hippocampal slice studies which involved placing a transverse section of the hippocampal formation into a bath in order to study its intrinsic, and presumably intact, circuitry.

The advent and use of more sophisticated tract tracing techniques has demonstrated that this plan is oversimplified (Amaral and Witter, 1989; Witter et al., 1989b). The concept of lamellar organization holds true only for the mossy fibre projection to CA3. The perforant pathway, the Schaffer collaterals, and the CA1 axons form a relatively widespread terminal area along the longitudinal axis of the hippocampus.

1.1.3.3 Local Circuitry of the Dentate Gyrus

Hilar cells and the granular layer basket cells do not contribute to the trisynaptic circuit, but instead terminate in the dentate gyrus either ipsilateral or contralateral to the cell of origin. For this reason, the term "local circuit" or interneuron will be used for these cells, even though their axons may project out of the immediate vicinity. The fibres are called either associational, if they terminate ipsilaterally, or commissural, if they terminate contralaterally. The commissural fibres arise from the hilus only (Berger et al., 1980; Laurberg and Sorensen, 1981), mainly from the mossy cells

(Laurberg and Sorensen, 1981), and terminate in the inner third of the molecular layer and throughout the contralateral hilus of the dentate gyrus (Hjorth-Simonsen and Laurberg, 1977). Commissural and associational projections to the dentate gyrus can arise from the same neurons (Laurberg and Sorensen, 1981). Many of these local circuit cells send dendrites into the molecular layer to receive perforant path input and they also receive mossy fibre input from the granule cells. The local circuit neurons, in turn, feed back onto the principle cells to control the "gating" of information through the trisynaptic circuit. These neurons receive a number of subcortical inputs, many of which send a large portion of their fibres to these local circuit neurons, rather than to other hippocampal subfields. Therefore, understanding the local circuitry of the dentate gyrus is critical in understanding the mechanism by which subcortical inputs control the flow of information through the hippocampus.

In order to build a functional model of the local dentate circuitry, details about the connections of each cell type with the granule cells, the perforant path input, and each other are necessary. Furthermore, their neurotransmitters and mode of termination will also give clues about their role in this model.

1.1.3.3.1 Somatostatin-immunoreactive Aspiny Cells

Dendrites of somatostatin-immunoreactive aspiny cells have been observed in the molecular layer of the dentate gyrus (Leranth et al.,1990), which confirms earlier reports that some aspiny hilar cells send dendrites to the molecular layer (Amaral, 1978). These same dendrites are postsynaptic to perforant path fibres (Leranth et al.,1990), confirming a direct input from the entorhinal cortex.

Electrophysiologically, somatostatin-immunoreactive neurons have been shown to receive extremely powerful, monosynaptic short-latency inputs from the perforant path (Sloviter, 1987a). The dendrites of somatostatin-immunoreactive cells that are restricted to the hilus receive mossy fibre collaterals (Leranth and Frotscher, 1987; Leranth et al.,1990). The outer two-thirds of the molecular layer contain a plexus of somatostatin-immunoreactive fibres, whereas the inner third and the granule cell layers show only scarce fibres (Bakst et al.,1986). Neuropeptide Y fibres innervate the same area (Deller and Leranth, 1990) and are likely to arise from the same cells. These fibres originate from cells in the hilus, rather than from cells outside the hippocampus (Kohler et al.,1986; Bakst et al.,1986). Since 90% of somatostatin-immunoreactive cells apparently contain the inhibitory neurotransmitter GABA (Kosaka et al.,1988; Schmechel et al.,1984), and their synapses onto granule cell dendrites are symmetrical (Leranth et al.,1990), it is likely that these cells modulate the entorhinal input through

inhibition, although there is no physiological evidence that these cells are inhibitory. Preliminary evidence has been reported to demonstrate that somatostatin does depress perforant path excitatory postsynaptic potentials (EPSP) in granule cells when somatostatin is ejected in the outer molecular layer (Schwartzkroin et al., 1990). Somatostatin-immunoreactive terminals frequently form synapses with the base of the same spines that putatively receive entorhinal asymmetric synapses (Leranth et al., 1990), placing them in an ideal situation for controlling the amount of excitation generated by perforant path fibres. A small portion of somatostatin and neuropeptide Y cells (< 5%) send contralateral fibres to the dentate gyrus (Leranth and Frotscher, 1987; Bakst et al., 1986; Deller and Leranth, 1990; Kohler et al., 1986). These commissural fibres appear to terminate very lightly in the outer half of the molecular layer (Bakst et al., 1986), rather than the inner third which is normally the target of commissural fibres. Somatostatin/neuropeptide Y neurons form symmetrical (putative inhibitory) synapses on other hilar neurons (Deller and Leranth, 1990; Leranth et al., 1990) as well. Symmetrical synapses are commonly found on somatostatin-immunoreactive hilar cells, and they are therefore under inhibitory influences themselves.

1.1.3.3.2 Basket Cells

As discussed earlier, the unifying characteristic of basket cells is the distribution of their axons into a basket plexus on the soma and inner molecular layer of the granule cells (Ribak and Seress, 1983), and since most, if not all basket cells, are GABAergic, they likely produce a strong inhibitory effect upon granule cells. Basket cell axons usually branch close to the cell body and give rise to collaterals that innervate granule cells for relatively long distances on either side of the parent cell body (Ribak et al., 1978; Seress and Ribak, 1983). Their axons may extend for up to one millimetre in the longitudinal axis and may synapse with as many as 500 granule cells (Struble et al., 1978). There is no evidence that these granule layer basket cells innervate neurons in the hilus (Ribak and Seress, 1983).

Entorhinal projections have been found to make direct synaptic contact with the smooth dendrites of basket cells found in the molecular layer (Zipp et al., 1989), and basket cells may also receive sparse entorhinal input in the subgranular zone where most of their cell bodies are located (Kohler, 1985a). Furthermore, typical basket cells were shown to receive asymmetric synaptic contacts with recurrent mossy fibre collaterals (Lubbers and Frotscher, 1987; Ribak and Seress, 1983) and with commissural afferents from the contralateral hilus (Seress and Ribak, 1984).

1.1.3.3.3 Calretinin-immunoreactive Spiny Cells

The dendrites of calretinin-immunoreactive spiny cells never leave the hilus, running horizontally to the granule cell layer (Gulyas et al., 1992), therefore it is unlikely that they receive direct input from the entorhinal cortex. Calretinin-immunoreactive spiny cells are almost completely covered by asymmetrical synapses, an unusual property for hilar cells. It was estimated that 9,000 to 27,000 mossy fibres synapse onto a single calretinin-immunoreactive spiny cell, whereas symmetrical synapses were rarely found (Gulyas et al., 1992), another unusual feature for hilar cells. The lack of symmetric (putative inhibitory) synapses and the abundance of mossy fibre connections explains why spiny hilar cells, a broader category which includes mossy cells and calretinin-immunoreactive spiny cells, have been reported to be extremely sensitive to afferent excitation, and inhibitory postsynaptic potentials were rarely recorded (Scharfman and Schwartzkroin, 1988; Scharfman and Schwartzkroin, 1990; Scharfman, 1991). Calretinin-immunoreactive cells and mossy cells both contribute to the commissural projection to the contralateral dentate gyrus. (Miettinen et al., 1992).

The primary neurotransmitter for calretinin-immunoreactive cells has yet to be determined, but, a small number of these spiny cells (11%) were found to be immunoreactive to GABA (Miettinen et al., 1992). Their mode of termination onto granule cells may be restricted to the supragranular layer, which receives a significant input from calretinin-immunoreactive fibres.

However, since calretinin-immunoreactive cells in the supramammillary area of the hypothalamus also terminate in the supragranular layer, their site of termination remains speculative.

1.1.3.3.4 Mossy Cells

Isolated dendrites of mossy cells have been seen to enter the molecular layer and reach as far as the outer molecular layer (Scharfman, 1991), however, a majority of their dendrites remain in the hilus. Mossy cells likely use glutamate as their neurotransmitter (Storm-Mathisen et al., 1983; Fischer et al., 1986). Mossy cells give rise to a large portion of the commissural projections (Ribak et al., 1985; Frotscher et al., 1991). Numerous mossy fibres make synaptic contact with mossy cells which, in turn, send their fibres to make asymmetric synapses on other local circuit neurons in the hilus (Ribak et al., 1985; Scharfman et al., 1990), and on the inner molecular regions of the dentate gyrus (Laurberg and Sorensen, 1981; Frotscher et al., 1991). Mossy cell axons travel several millimetres along the longitudinal axis of the hippocampus before they terminate in the inner molecular zone (Amaral and Witter, 1989), thus avoiding contact with granule cells in the same transverse hippocampal segment. Symmetric synapses are also commonly found on mossy cells (Ribak et al., 1985), a significant portion of which are likely to be GABA-immunoreactive terminals (Sloviter and Nilaver, 1987b).

Despite the existence of symmetrical synapses onto mossy cells, like other spiny hilar cells, excitatory input dominates as a result of perforant path excitation (Scharfman, 1992). Perforant path stimulation currents that are subthreshold for granule cell activation will produce action potentials in identified mossy cells (Scharfman, 1991). Surprisingly, a study using combined intracellular recording from granule cells and mossy cells in the hippocampal slice found no evidence of synaptic connections in either direction despite slice orientations ranging from transverse to longitudinal (Scharfman et al., 1990). The authors concluded that it is unlikely that the relatively long axons were spared transection in the slice preparation before contacting granule cells. In another study, the burst activity of mossy cells (and other hilar cells) in the guinea pig slice was found to be associated with granule cell inhibition (Misgeld et al., 1992a).

1.1.3.3.5 Conclusion

Non-mossy cell local circuit neurons seem to share a number of important characteristics, regardless of their shape or position. Most appear to be inhibitory and have activation thresholds lower than granule cells (Scharfman, 1991). This makes them likely candidates for the role of feed-forward inhibition observed to be a factor in granule cell excitability (Buzsaki, 1984; Sloviter, 1991). The somatostatin-immunoreactive cells and basket

cells appear to fall into this category, since their dendrites have been shown to receive direct innervation by perforant path fibres.

All non-mossy local circuit cells are also likely candidates for feedback inhibition, since they receive mossy fibre input, and in turn project back to the granule cells. The calretinin-immunoreactive spiny cells may mediate feedback inhibition alone, since there is no evidence of a direct input to them arising from the entorhinal cortex, or they may mediate feedback excitation, since their neurotransmitter has not been identified, and the existence of an excitatory hilar interneuron other than a mossy cell has been described (Scharfman et al., 1990).

The circuitry of mossy cells implies a role in feed-back and feed-forward excitation of granule cells, however this modulation is likely to occur at some distance from the parent cell. Mossy cells innervate other local circuit neurons, thus if the preferential effect of mossy cell output were activation of inhibitory local circuit neurons, then the net effect upon granule cells would be inhibitory. A preferential inhibitory effect gains some support by the fact that the loss of mossy cells (and somatostatin-immunoreactive cells) correlates with the induction of granule cell seizure activity and a reduction in feedback inhibition (Sloviter, 1987a). The inhibition of granule cells associated with mossy cell bursts in the guinea pig slice (Misgeld et al., 1992a) also supports this hypothesis.

1.1.4 Electrophysiology of the Hippocampus

Most of the data arising from studies on the electrophysiology of the dentate gyrus have been obtained by means of field recordings of spontaneous slow activity, evoked potentials, and single unit activity. The following section will give a brief review of the data obtained from the first two methods whereas single units will be discussed in detail later.

1.1.4.1 Evoked Field Potentials

Stimulation of the perforant path to the dentate gyrus produces field potentials that can be recorded by means of extracellular electrodes. By field potential analysis of these evoked responses it is possible to determine the excitability changes of a population of granule cells (Andersen et al., 1966a; Lomo, 1971).

1.1.4.1.1 Single Evoked Field Potentials

Single stimulation of the perforant path evokes a glutamate-mediated monosynaptic field potential with at least two major components, the population EPSP and the population spike.

The population EPSP is mainly a recording of the current flow into the dendrites (sink) of the granule cells subsequent to their synaptic activation by perforant path fibres synapsing at the outer two-thirds of the molecular layer. At any location, the field potential depends on the linear sum of potentials from each of the current sources and sinks, weighted according

to distance and the extracellular conductivity (cf. Leung, 1990). If measured at the dendrites, this potential is seen as a negative deflection. As the electrode descends to the cell body the field potential "flips" at a reversal point, and the population EPSP is now seen as a positive wave.

The population spike is mainly a recording of the current flow into the axon hillock as a result of granule cell action potentials generated by a sufficient accumulation of dendritic EPSPs. Measured at the granule cell layer, this wave is seen as a negative deflection superimposed onto the positive wave generated by the dendritic EPSPs (Figure 2-1). The population spike reflects an averaged potential change of neurons in the vicinity of the recording electrode, the amplitude of which is dependent on the number of granule cells that discharge in synchrony (Andersen et al., 1971c; Lomo, 1971). Similarly, the amplitude or slope of the population EPSP reflects the number of perforant path fibres activated by the stimulus, and the efficacy of the synaptic process involving such determinants as the amount of neurotransmitter release and the sensitivity of postsynaptic receptors (Lomo, 1971).

It has been suggested that a third component contributes to the shape of the perforant path-evoked field potential (Andersen et al., 1966a). Adding to the second positive wave that follows a population spike, it reflects an outward current across the soma membrane as a result of inhibitory synaptic

activity that has been recorded intracellularly in granule cells (Andersen et al., 1966a). These IPSPs presumably arise from feed-forward and/or feed-back activation of inhibitory local circuit neurons, the majority of which contain GABA. Inward movement of chloride ions as a result of GABA receptor activation would represent an outward current, that, when measured at the granule cell layer, should add a positive deflection to the field potential. A significant contribution of soma inhibitory postsynaptic potentials (IPSPs) to the shape of an evoked field potential is, however, equivocal. Bicuculline, a GABA receptor antagonist, has been found to either abolish (Alvarez-Leefmans, 1976), or have no effect upon (Sloviter, 1991), the size and shape of the second positive wave.

1.1.4.1.2 Paired-pulse Evoked Potentials

Evoking two field potentials in quick succession can yield a series of changes in granule cell responses to the second stimulus. The impetus for such a paradigm is that the first input of any pair of stimuli in the train activates the local network, and the second input tests the modulatory influence of the network excited by the initial input. The use of this classic paired-pulse technique has led to the identification of three distinct phases identified by the interstimulus interval. While most of this work has been performed on anaesthetized animals, it has been found that their

manifestation in unrestrained animals is dependent on the animal's behavioural state (Austin et al., 1989).

Short perforant path stimulus intervals (approximately 10-40 ms) produce an early period of inhibition (Andersen et al., 1971a), where both the population EPSP and the population spike of the second field potential are depressed (Adamec et al., 1981; Sundstrom and Mellanby, 1990). Early inhibition can be demonstrated most clearly at a low interpair stimulus frequency of 0.1 Hz (Sloviter, 1991). While both the first and second field potential pairs will contain a measure of feed-forward inhibition, the second field potential is further reduced because of the addition of feedback inhibition, where recurrent mossy fibre collaterals activated by the first pulse have activated inhibitory local circuit neurons, which then feedback onto the granule cells.

Early inhibition is thought to be mediated by GABA, since during this phase inhibition can be enhanced by GABA-uptake blockers (Albertson and Joy, 1987) and reduced by picrotoxin and bicuculline (Tuff et al., 1983). Two GABA receptor types have been identified, the GABA-A receptor, which predominantly mediates increases in chloride conductance (Schofield et al., 1987), and the GABA-B receptor, which mediates an increase in potassium conductance (Gahwiler and Brown, 1985) and/or a decrease in the conductance of voltage-dependent calcium channels (Dolphin and Scott,

1974). As stated, picrotoxin and bicuculline, which are GABA-A receptor antagonists, reduce inhibition during the early inhibition phase, presumably by blocking postsynaptic receptors in the granule cells.

More recently it been shown that a GABA-B agonist, baclofen, reduces inhibition (Harris and Cotman, 1985; Burgard and Sarvey, 1991; Steffensen and Henriksen, 1991), and a GABA-B antagonist, CGP-35348, increases inhibition (Brucato et al., 1992) during the early phase. These results led the researchers to speculate that the critical GABA-B receptors are found on presynaptic GABA terminals, where it has been demonstrated that GABA-B receptor-activation on GABA terminals inhibits the release of GABA (Yoon and Rothman, 1991; Bowery et al., 1980; Potashner, 1978), and hence would produce disinhibition. The second phase is characterized by a facilitation of the second spike, and occurs with perforant path stimulus intervals of approximately 30 to 200 ms (Racine and Milgram, 1983). The final, or late inhibitory phase, is characterized by a marked depression of granule cell excitability if the second pulse is given approximately 200-1000 ms behind the first. Early studies suggested that late inhibition is not GABA mediated since it was not blocked by bicuculline or enhanced by diazepam (Tuff et al., 1983), which facilitates GABA binding to GABA-A receptors. More recent work suggests that the inhibition observed during the late phase is similar to that produced during the early phase (Steffensen and Henriksen,

1991). Not only did bicuculline reduce the paired-pulse inhibition, but baclofen increased it, leading the researchers to suggest that the early and late phases of paired-pulse inhibition represent one prolonged GABA-dependent process that is superimposed on an independent facilitatory process. The NMDA glutamate receptor (described in the next section) plays a dominant role in this facilitatory phase. Paired-pulse facilitation of the population spike is attenuated or blocked by the administration of NMDA receptor-ion channel blockers (Joy and Albertson, 1993).

1.1.4.1.3 Long-term Potentiation

Since the discovery that a brief high-frequency train of stimuli to the perforant path produces a lasting increase in the population EPSP and spike (Bliss and Lomo, 1973; Bliss and Gardner-Medwin, 1973), a phenomenon called long-term potentiation (LTP), an intense interest has developed in LTP largely because of its qualification for being a synaptic mechanism for memory (Alkon et al., 1991; Laroche et al., 1988; Jerusalinsky et al., 1992; Matthies et al., 1990; Watanabe et al., 1992; deToledo-Morrell et al., 1988; Krug et al., 1989; Eccles, 1988; Krug et al., 1991b; Kitajima and Hara, 1991; Krug et al., 1991a; Ruthrich et al., 1987; Ramirez et al., 1988; Laroche et al., 1991). The following represents a brief introduction to LTP. A number of reviews have recently been published (Kuba and Kumamoto, 1990; Sarvey et al., 1989; Eccles, 1988; Massicotte and Baudry, 1991).

LTP can be generated by applying a brief, high frequency repetitive stimulus train to any one of the fibre tracts that make up the trisynaptic circuit. The stimulus parameters used to generate LTP in the dentate gyrus are commonly one tetanus of 100 pulses or 5-8 tetani of 8 pulses at 100-400 Hz to the perforant path. Apparently the brief, patterned trains of stimulation are more efficacious than a single larger train, especially if the brief trains are separated by an interval of approximately 200 ms (Larson and Lynch, 1986; Larson et al., 1986; Larson and Lynch, 1988; Greenstein et al., 1988; Larson and Lynch, 1989), which matches the frequency of the spontaneously-occurring hippocampal theta rhythm (see next section).

The resulting potentiation can last for hours to days in vivo. LTP of either the population EPSP or population spike in the dentate gyrus has been observed to last for 80 days following the requisite tetanus to the perforant path (Racine et al., 1983). The intensity of the stimulus must exceed the intensity of a stimulus which produces a minimum postsynaptic response, suggesting a threshold determined by the number of afferents that must be coactivated (Bliss and Lomo, 1973; McNaughton et al., 1978). The threshold appears to be below the intensity required to produce a detectable population spike (McNaughton et al., 1978). The amount of postsynaptic depolarization is critical to the induction of LTP and achieved when the frequency of the stimulus train allows postsynaptic EPSPs to overlap and summate over time

(Gamble and Koch, 1987). Postsynaptic depolarization alone, however, does not produce LTP, for only at synapses in which depolarization is paired with activation of the synapse does LTP occur (Gustafsson et al., 1987; Wigstrom et al., 1986).

Another essential requirement for the induction of LTP involves an elevation of calcium levels in the postsynaptic cell. Injection of calcium chelators such as EGTA into postsynaptic neurons prevent the induction of LTP in those neurons (Lynch et al., 1983). Furthermore, increased release of calcium into postsynaptic neurons produces a potentiation of synaptic transmission (Malenka et al., 1988). More recent evidence suggests that the magnitude of postsynaptic calcium increase is a critical variable controlling the duration of synaptic enhancement (Malenka, 1991).

Possible sources for this calcium increase include voltage-dependent calcium channels, release from intracellular stores, and an influx through a glutamate receptor ionophore. The latter possibility has been shown to be critical for LTP at synapses that possess the NMDA receptor. Glutamate can bind to at least four receptors [see (Gasic and Hollmann, 1992) for a review], three of which are coupled to transmembrane ion channels and are identified by the selective agonists active at each type; N-methyl-D-aspartate (NMDA), quisqualate or AMPA (alpha-amino-3-hydroxy-5-methyl-4-isoxazole propionate), and kainate. The latter two are often called non-NMDA

receptors and are the principal receptor-ion channels that generate the EPSP at resting potential in all principal neurons of the hippocampus (Crunelli et al., 1983; Collingridge et al., 1983). The non-NMDA receptors are largely chemical-dependent, meaning their activation is dependent on the amount of glutamate that reaches the postsynaptic site. The NMDA receptors, however, are chemical- and voltage-dependent, for the presence of glutamate alone is not enough to allow ion passage through its ionophore. NMDA receptors are associated with an ion channel that is blocked by magnesium at the resting membrane potential (Mayer et al., 1984; Nowak et al., 1984). Hence, the temporal summation of EPSPs as a result of a tetanus brings the membrane potential to a level where magnesium ions no longer block the NMDA receptor channels, thereby allowing their functional activation. This explains the concomitant requirement of synaptic activity and postsynaptic depolarization for LTP to occur, at least at those excitatory synapses where NMDA receptors are involved.

This activation of the NMDA receptor-channel results in a considerable amount of calcium influx into the region of the cytoplasm beneath the activated synapses (Dingledine, 1983; Kudo and Ogura, 1986; Mody and Heinemann, 1986). The hypothesized role of NMDA receptors in the generation of LTP is confirmed by observations that NMDA receptor antagonists block the induction of LTP, but do not reverse LTP once it is

established (Errington et al.,1987; Morris et al.,1986). Therefore, four factors are important in the induction of LTP: (1) the amount and pattern of afferent stimulation, (2) postsynaptic activation of sufficient depolarization, (3) NMDA receptor activation, and (4) calcium influx.

The highest concentrations of NMDA receptors in the brain are found in the stratum radiatum of field CA1 and the molecular layer of the dentate gyrus (Cotman et al.,1987). The mossy fibre terminal zone on CA3 pyramidal cells is devoid of NMDA receptors (Monaghan and Cotman, 1985), which explains the inability of NMDA antagonists to block LTP induction at this site (Harris and Cotman, 1986). While some other sites in the brain are able to exhibit non-NMDA mediated LTP (Johnston et al.,1992), the receptor is critical for most aspects of LTP induction in the hippocampus.

In the dentate gyrus, the NMDA receptor may not mediate all aspects of LTP. Curiously, in the urethane-anaesthetized rat, NMDA receptor blockers have been shown to block the enhancement of the population spike when the tetanus is applied to the lateral perforant path, without blocking the enhancement of the population EPSP (Bramham et al.,1991). NMDA blockers successfully blocked both components of LTP in the medial path. In the guinea pig hippocampal slice, however, NMDA antagonists blocked both aspects of LTP in both pathways (Hanse and Gustafsson, 1992b). Either a

species difference or a preparation difference may underlie these contradictory results.

Since depolarization of the postsynaptic membrane is critical to the induction of LTP, it follows that interneuron-mediated inhibition, which limits postsynaptic depolarization during a stimulus train, may determine the threshold at which LTP can be induced. When inhibition is blocked with picrotoxin, a GABA-A receptor antagonist, depolarization during a stimulus train is enhanced, facilitating LTP induction (Wigstrom and Gustafsson, 1983). More recently, it was reported that GABA-B receptor-mediated disinhibition is required for LTP induction with stimulation in the frequency range of the theta rhythm (Mott and Lewis, 1991).

The mechanisms of expression or maintenance of LTP are less well understood, including whether it is predominantly a pre- or postsynaptic phenomenon. Since the induction of LTP is calcium-dependent, this second messenger may trigger the subsequent cascade of biochemical events responsible for sustaining LTP [for a review see (Abraham and Otani, 1991; Massicotte and Baudry, 1991; Kuba and Kumamoto, 1990)]. A fourth class of glutamate receptors, the metabotropic receptor (or family of metabotropic receptors (Tanabe et al., 1992)), has recently been reported [for review see (Baskys, 1992; Schoepp, 1993)] and may also be important for the induction of LTP (Stanton et al., 1991; Otani and Ben-Ari, 1991; Bortolotto and

Collingridge, 1992; Aniksztejn et al.,1992; Zheng and Gallagher, 1992; McGuinness et al.,1991), however its role in LTP induction is less clearly understood and awaits further clarification. The metabotropic receptor is not directly coupled to ion channels. Its activation generates diacylglycerol and inositol triphosphate, leading to the activation of protein kinase C and the release of calcium from intracellular stores (Schoepp et al.,1990).

1.1.4.2 Hippocampal Theta

The electroencephalographic (EEG) patterns produced by the hippocampus likely reflect different types of neural processing. The majority of studies have concentrated on one particular waveform, hippocampal rhythmic slow wave activity or theta. In addition to theta, it is also possible to record large irregular amplitude (LIA) activity at the same sites. Often the EEG patterns cycle between these two states. The following represents a very brief introduction to hippocampal theta, which has been extensively reviewed recently (Bland, 1986; Vanderwolf, 1988).

The theta rhythm is a 3-12 Hz, approximately sinusoidal, waveform. It is recorded maximally at two distinct sites within the hippocampus: the stratum oriens of CA1 and the molecular layer of the dentate gyrus (Bland and Wishaw, 1976; Buzsaki et al.,1986). Theta recorded at these two sites is approximately 180° out of phase, and evidence suggests that these two

sites represent separate and independent theta generators (Konopacki et al., 1987).

Two types of theta have been distinguished based on their behavioural correlates and pharmacological profiles. Type 1 theta occurs when the animal is walking, running, swimming, rearing, jumping, manipulating objects with forelimbs, shifts in posture, etc., all of which been described as instances of voluntary movement. In rats type 1 theta has a frequency range of approximately 7-12 Hz, it cannot be abolished by large doses of atropine sulfate, but is abolished by anaesthetics such as urethane and sodium pentobarbital. Type 2 theta is defined as theta that occurs in the absence of movement. In rats, type 2 theta has a relatively lower overall frequency of 4-9 Hz and is resistant to most anaesthetics but sensitive to large doses of muscarinic cholinergic receptor antagonists such as atropine sulfate and scopolamine (Kramis et al., 1975).

1.2 This Study

It has been demonstrated that subcortical deafferentation of the hippocampus induces severe learning impairments (Sutherland and Rodriguez, 1989; Wible et al., 1992; Li et al., 1992; Witter, 1989a; Sara et al., 1992; Matsuoka et al., 1991; Aggleton et al., 1990), and completely blocks or impairs the induction of LTP in the dentate gyrus (Buzsaki and Gage, 1989; Valjakka et al., 1991; Abe et al., 1992). Efforts to explore the

obviously critical influence of various subcortical inputs to the hippocampus have largely relied on electrical stimulation of the subcortical structure in question [see (Harley and Milway, 1986; Shin et al., 1987) for exceptions]. The two regions supplying the greatest subcortical inputs, the medial septum complex and the lateral supramammillary nucleus, have a large number of axons of passage, some of which also project to the hippocampus (Swanson et al., 1987). For this reason, glutamatergic stimulation of these two regions was employed to investigate the selective influence of cellular activation within these regions on the physiology of the dentate gyrus. Glutamate is an ubiquitous excitatory neurotransmitter in the mammalian brain and it has been demonstrated that injections of minute volumes of 0.5 M glutamate into selected sites within the medulla or midbrain of anaesthetized or conscious animals, respectively, elicited marked autonomic, somatomotor or behavioural responses, depending on the injection site (Goodchild et al., 1982). In contrast, glutamate microinjection into fibre tracts failed to elicit any response, whereas electrical stimulation applied to the same sites elicited marked responses (Goodchild et al., 1982). In this study, efforts were primarily directed at examining the effects of glutamate activation of cell groups on evoked potentials generated by perforant path stimulation. In an attempt to elucidate the mechanisms underlying the observed modulation,

data are presented on changes in dentate EEG and spontaneous activity of dentate units that accompanied changes in the evoked potential.

CHAPTER 2: THE LATERAL SUPRAMAMMILLARY NUCLEUS

2.1 Introduction

The supramammillary nucleus, more specifically the lateral portion of the supramammillary nucleus (SUML), and the smaller submammillothalamic nucleus (SMT), have been shown to have diffuse cortical projections (Saper, 1985; Haglund et al., 1984), and on that basis it has been hypothesized that they, along with other basal forebrain and brainstem groups which have diffuse cortical projections, function to selectively modify specific sensory, emotional, or behavioural patterns in a modulatory fashion (Saper, 1988).

Recently, the lateral hypothalamic portion of the medial forebrain bundle has been carefully parcellated into several cytoarchitectonically distinct cellular groups and subgroups (Geeraedts et al., 1990). The SUML consists of a heterogeneous group of cells that is caudally bounded by the ventral tegmental area and rostrally by the lateral hypothalamic nucleus. The SMT is a dense collection of medium-sized to large neurons that lie within the rostradorsal portion of the SUML, surrounding the caudal surface of the mammillothalamic tract (see Fig. 2-3).

The dentate gyrus receives a large number of extrinsic inputs, most notably from the entorhinal cortex and the medial septum. A large input from the SUML, and the smaller SMT, has also been described. Using the retrograde

HRP method in the rat, a direct projection to the hippocampus has been observed (Sakanaka et al.,1980; Pasquier and Reinoso-Suarez, 1976; Pasquier and Reinoso-Suarez, 1978; Riley and Moore, 1981; Segal and Landis, 1974; Wyss et al.,1979a). Combined retrograde transport-histochemical studies have demonstrated that most supramammillary area neurons projecting to the dentate gyrus contain acetylcholinesterase (Harley et al.,1983), while retrograde transport-immunohistochemical studies have revealed only small percentages of cells containing various peptides (Haglund et al.,1984). In the guinea pig and cat, the majority of SUML afferents to the hippocampus are immunoreactive for substance P (Gall and Selawski, 1984; Ino et al.,1988; Yanagihara and Niimi, 1989), however a similar constitution in the rat has not been seen (Davies and Kohler, 1985; Haglund et al.,1984). Therefore no principal neurotransmitter(s) have been identified in the SUML of the rat to date.

Anterograde transport studies have revealed that the supragranular layer of the dentate gyrus receives the largest proportion of supramammillary fibres (Haglund et al.,1984; Wyss et al.,1979b; Vertes, 1992) and electron microscope data indicate that the terminals contain small spheroidal vesicles and make direct asymmetric contact with granule cell bodies and their proximal dendrites (Dent et al.,1983). A more recent study using anterograde PHAL from the SUM found that the labelled terminals established asymmetric

synapses with a wide range of postsynaptic elements, including apical dendritic shafts and dendritic spines of granule cells, smooth, interneuron-like dendritic shafts, and, rarely, the somata of granule cells and local circuit neurons (Magloczky et al., 1991).

Electrical stimulation of the supramammillary area inhibits the activity of cells in the dentate gyrus (Mizumori et al., 1989; Segal, 1979) identified putatively as inhibitory cells (Mizumori et al., 1989), while enhancing the size of the population spike produced by electrical stimulation of the perforant path (Mizumori et al., 1989). Single pulse, low voltage (3-5 V, 0.2 ms), stimulation of the supramammillary nucleus in urethane-anaesthetized rats produced a short latency (3-5 ms) and temporally discrete (30-50 ms) inhibition of dentate cells located in the region of the granule cell layer (Segal, 1979). No field potentials were observed in the dentate gyrus in response to the supramammillary stimulation.

More recently, electrical stimulation of the supramammillary nucleus using twin pulses (2.5 ms apart, 0.1 ms duration) to the SUML, and not to the medial supramammillary nucleus, in the pentobarbital-anaesthetized rat was found to enhance the population spike if the pulses were given within 100 ms of, and prior to, the perforant path stimulus (Mizumori et al., 1989). The optimal interstimulus interval for enhancement was 10-15 ms, resulting in

a 75% increase to the population spike. No significant change was found in the EPSP amplitude or population spike peak latency.

Unit activity was also monitored, and units were identified as granule cells or basket cells according to several physiological criteria: the probability of activation with a stimulus intensity set just below population spike threshold, the likelihood of a driven cell firing to a second perforant path stimulus delivered during the early inhibition stage induced by the first stimulus (paired-pulse activation), mean spontaneous firing rate, and the latency to activation with a stimulus sufficient to elicit a population spike. Putative basket cells had significantly higher spontaneous discharge rates, fired in response to a stimulus that didn't evoke a population spike, fired at short latencies (usually before the population spike), and fired in response to a second stimulus given during the early inhibition stage. Putative granule cells had low spontaneous rates, did not fire in response to low stimulus intensities, did not fire in response to a second stimulus given during the early inhibitory stage induced by the first stimulus, and fired in response to a strong stimulus with a latency within the range of the population spike time window. The spontaneous activity of putative basket cells was inhibited by SUML stimulation for typically 15 ms whereas putative granule cells were either excited (15%) for the same time period or not affected at all. These investigators postulated that SUML stimulation produced population spike

enhancement through disinhibition of granule cells (i.e. inhibition of local circuit inhibitory neurons).

The above description of granule cell physiology does not concur with other studies done in awake or anaesthetized rats where putative granule cells identified by less rigorous criteria were found to exhibit relatively high discharge rates, above 10 Hz (Assaf and Miller, 1978; Bland et al., 1980; Buzsaki et al., 1983; Rose et al., 1983). However, electrophysiological recording of granule cells in the hippocampal slice, conclusively identified by lucifer yellow staining, have been found to have unusually high resting membrane potentials and a low spontaneous rate of firing (Scharfman et al., 1990; Scharfman, 1992), a finding consistent with Mizumori et al. (1989) [but see (Buzsaki and Czeh, 1992)]. Further, they found that spiny hilar cells and many aspiny hilar cells were more sensitive to perforant path stimulation. Granule cells identified morphologically in the slice preparation differ from other dentate cells by the absence of burst firing (Scharfman, 1992), even during pharmacological manipulation which causes spiny and aspiny hilar cells to burst (Misgeld et al., 1992a).

To avoid activating the large number of fibres passing through the SUML, the present work investigates the effects glutamatergic stimulation of the SUML has upon perforant path induced field potentials in the rat dentate gyrus. A portion of this work has appeared in abstract form (Carre and

Harley, 1990) and as a paper (Carre and Harley, 1991). In a second experiment, possible changes in dentate unit activity and in the EEG accompanying population spike enhancement were also investigated. Preliminary data on paired-pulse inhibition and changes in the molecular layer EPSP, following glutamate ejection to the SUMML, are also reported.

2.2 Methods

2.2.1 Experiment 1:

Subjects were 20 adult female Sprague-Dawley rats (Charles River Canada Inc, Montreal) weighing from 200 to 300 grams at the time of recording. Each rat was anaesthetized with urethane (1.5g/kg, i.p.), placed in a stereotaxic frame with skull flat, and maintained at a rectal temperature of 36.8-38°C with a circulating water blanket.

A coaxial stimulating electrode (Rhodes model NE-200) was aimed at the perforant path (7.1 mm posterior to bregma, 4.1 mm lateral to midline, and 3.5 mm below brain surface). A glass micropipette (tip size 10-15 μm) recording electrode filled with 2% pontamine sky blue in 0.5 M sodium acetate (1-5 M ohms), was aimed at the dentate gyrus (3.5 mm posterior to bregma, 2.0 mm lateral to midline, 3.5 mm below the brain surface). The depths for the stimulating and recording electrodes were determined by monitoring the perforant path-evoked population spike amplitude. A 0.2 ms monophasic square wave pulse, 5-25 V, delivered at 0.1 Hz served as the

perforant path stimulus. The field potentials were differentially amplified at a bandwidth of 1 Hz-3 KHz and displayed on a cathode ray storage oscilloscope.

A glass micropipette (tip size 10-35 μm) or a 30-gauge stainless steel cannula was filled with 0.5 M l-glutamic acid and aimed at the lateral supramammillary nucleus (4.2 mm posterior to bregma, 2.1 mm lateral to the midline angled at 21° from the vertical plane towards the midline). The pipette or cannula was positioned 7.0-8.5 mm ventral to the brain surface. In a majority of animals, glutamate was delivered at more than one site.

When using a glass pipette, a Neurophore BH II pressure ejection unit coupled to the glutamate filled pipette typically delivered a 300 ms, 30 psi nitrogen pulse to eject the glutamate solution. Ejection volumes were calibrated by measuring the spherical drop diameter. Volumes varied between 40-250 nl. The actual volume of glutamate injected intracerebrally under similar conditions has been reported to be approximately 68% of the volume estimated by drop diameter (Welzl et al., 1985).

When using a cannula, a Dynatech Precision Sampling 1 μl microsyringe was coupled to a 30 gauge stainless steel cannula with calibrated Micro-Line tubing. Using a bubble as a marker, 100-150 nl of glutamate was infused over a 10 s period.

To mark a glass pipette ejection site, the glutamate solution was aspirated

and replaced with a 2% solution of pontamine sky blue in 0.5 M sodium acetate and subsequently pressure ejected. For marking a cannula ejection site, dye had been placed in the tubing prior to glutamate loading, and was flushed out at the end of the experiment. The brain was removed and frozen. Forty μm coronal sections were taken through the region of the SUM. Sections were investigated for the dye ejection site before and after a metachromatic Nissl stain of 1% cresyl violet.

The perforant path was stimulated once every 10 s for 10 to 30 min prior to each glutamate ejection. The 10 min immediately preceding glutamate ejection constituted a control period. Each perforant path-evoked potential was displayed on an oscilloscope and digitized on an IBM-PC compatible computer (1 point/10 μs). Programs for acquisition and analysis were written in Asyst, a commercial package based on the language Forth (see appendix I and II for examples of an acquisition and an analysis program). The dependent variables extracted online for each evoked potential were EPSP slope, latencies for both the start and peak of the spike, and spike size measured as the area under a tangent drawn across the first two positive peaks, or the difference in amplitude between the first positive peak and the negative peak, or the difference in amplitude between the negative peak and the tangent (Fig. 2-1). Mean values for the six events were compared to two-tailed 95% confidence intervals based on the control period of ten

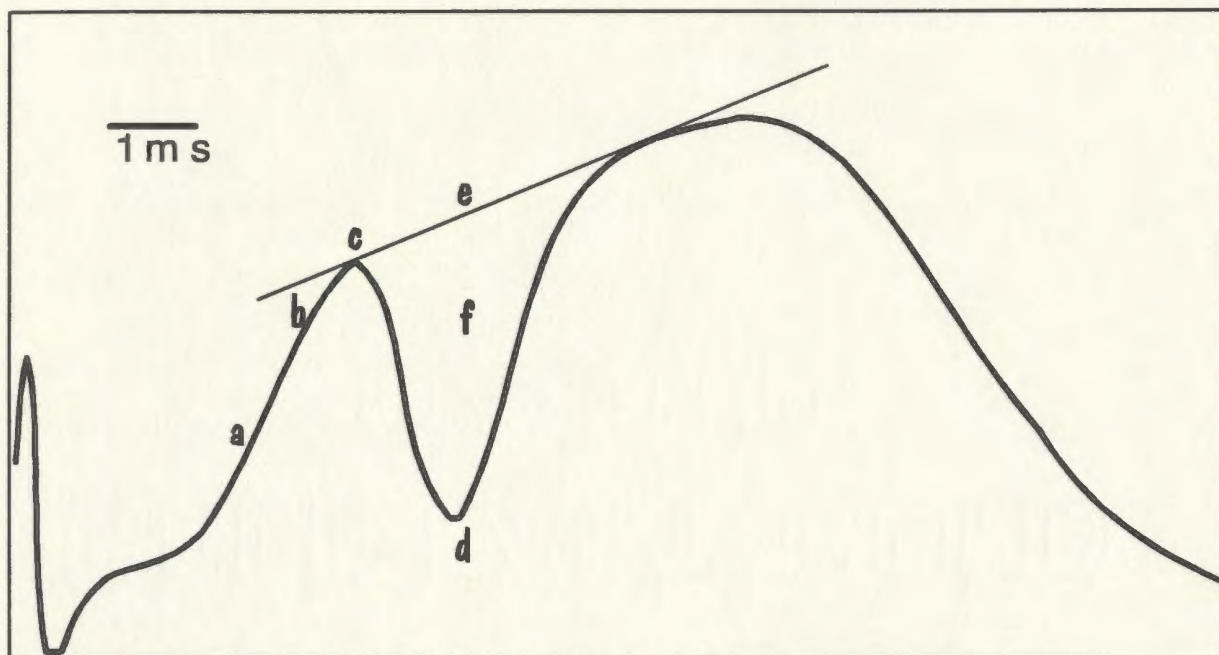


FIG. 2-1. Parameters measured for an evoked potential recorded in the granule cell layer/hilar region: population EPSP slope (difference in amplitude between points a and b divided by their difference in time), population spike onset latency (time at point c), population spike latency (time at point d), population spike height (difference in amplitude between points c and d), and population spike area (area under a tangent drawn between the 2 positive peaks -f), and population spike height to the tangent (difference in amplitude between points d and e).

means (10 means of six responses each, 10 min).

2.2.2 Experiment 2:

Thirteen female Sprague Dawley rats were prepared for evoked potentials as above except for the following differences. Two fine tungsten recording electrodes of approximately one megohm resistance and separated by about one mm were inserted into the dentate gyrus. Using a threaded microdrive (Biela), which allowed for the movement of one electrode with respect to the other, one electrode was placed in the molecular layer and the other in the granule cell layer or hilus. Placement was determined by monitoring the perforant path evoked potentials for characteristic waveforms, and the presence of a theta rhythm or unit activity. Using this arrangement, it was possible to record up to four parameters at one time as illustrated in Fig. 2-2. EEG waveforms and units were collected using the BrainWave Discovery software package. The EEG channel was amplified at a bandwidth of 1-100 Hz and the unit channel at a bandwidth of 600-3,000 or 10,000 Hz. Only units exceeding an experimenter-adjusted threshold were stored (at a rate of 31 KHz) for later off-line analysis. Unit and EEG data (the latter sampled at 300 Hz) were collected continuously beginning at 2 min prior to, and 5 to 25 min after, glutamate ejection into the SUML. The glutamate ejection event was entered into the computer by manually hitting a key, therefore the accuracy of the event in time is limited and precludes any discussion in

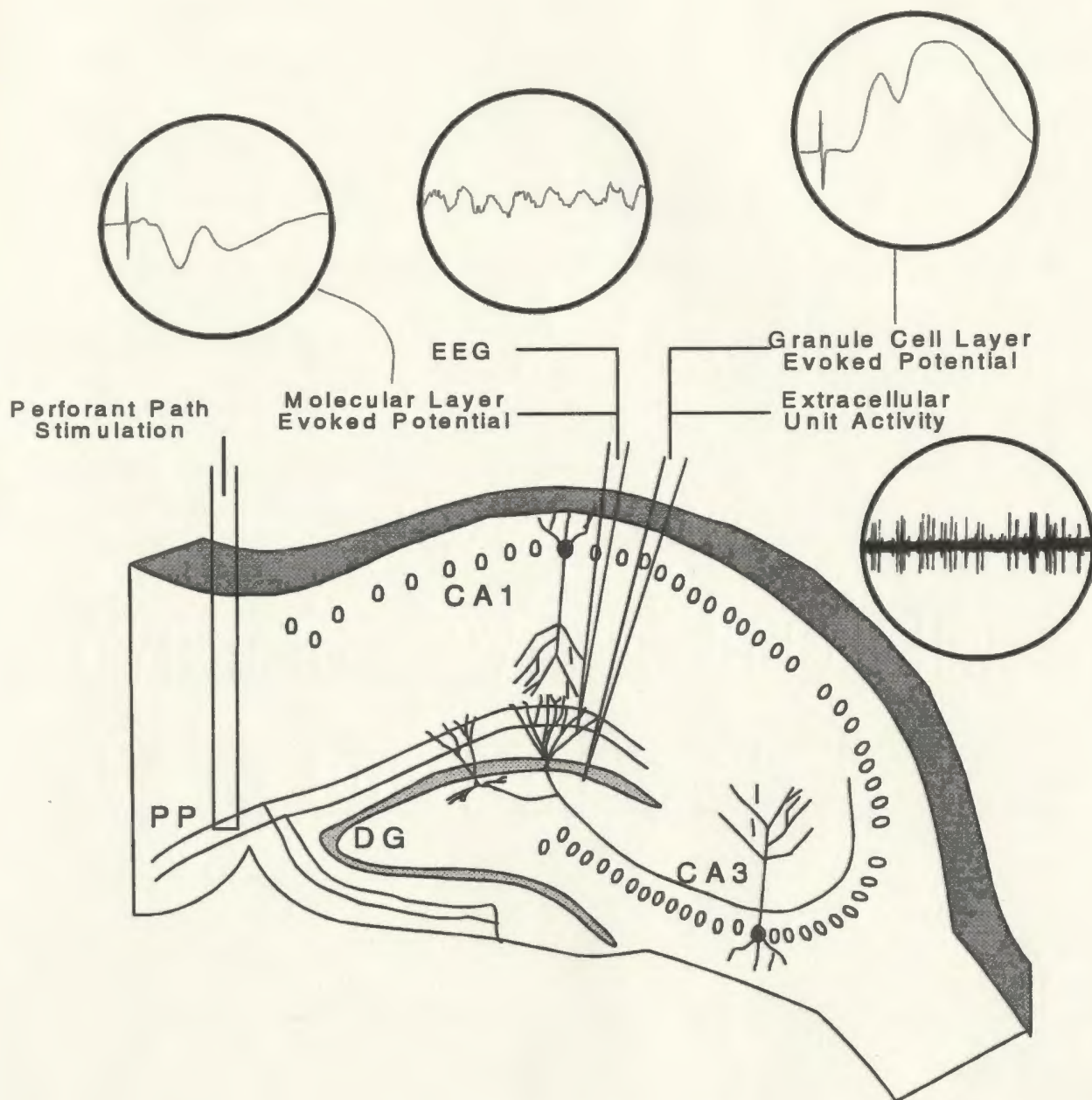


FIG. 2-2. Diagram illustrating how up to 4 parameters were recorded in the dentate gyrus during the same session. EEG and an evoked potential could be recorded from the same electrode placed in the molecular layer. A second electrode was placed in the granule cell layer/hilus to record both units and the evoked potential.

terms of milliseconds. Furthermore, it is not possible to know exactly when the SUML cells are activated using this approach without recording at the ejection site.

Evoked potentials recorded in the granule cell layer/hilus were analyzed as in experiment 1. EPSP responses recorded from the dentate molecular layer were assessed by measuring the negative-going slope of the population EPSP and its peak latency. The EEG and unit data was analyzed offline using BrainWave's analysis software package. The EEG samples were subjected to fast-Fourier analysis and 5 s averages of the frequency of maximum power was computed and plotted vs time to assess the possible influence of SUML-glutamate ejection.

For offline unit analysis using BrainWave software, units were scanned for the times and magnitudes of peaks and valleys. The following waveform parameters were calculated: peak magnitude, valley magnitude, spike height (peak - valley), spike width (time of peak - time of valley), time of valley, and time of peak. Individual units were then plotted using any 2 of the parameters involved. Distinct clusters of units could be identified and tagged by drawing a box around each cluster. Examples of this cluster cutting can be found in Fig. 2-9. Individual waveforms from each cluster were played back to ensure adequate cluster cutting. Autocorrelation, interspike interval, and perievent time histograms were then generated for each cluster.

In addition, after completion of the multiple parameter experiment 5 animals were subjected to paired-pulse stimulations, with pulse pairs delivered every 10 s. The paired-pulse interpulse interval (between 20 and 30 ms) was adjusted until a significant amount of inhibition was apparent in the second spike, but not enough to suppress the second spike totally. After 10 to 15 minutes, the stimulus intensity was reduced and glutamate was injected 10 min later. The first spikes of the pair were analyzed for evidence of enhancement as a result of glutamate ejection. Paired-pulse indexes (size of second spike/size of first spike) were calculated for all stimulus pairs as an index of the amount of inhibition. The initial period of higher-stimulus amplitude ensured comparison of paired-pulse indexes of any enhanced first spikes (as a result of glutamate) with other paired-pulse indexes with first spike sizes of equal magnitude.

2.3 Results

2.3.1 Experiment 1:

A total of 12 ejection sites were associated with a significant increase in the population spike. These sites are shown in Fig. 2-3 (filled stars) and are collectively called the INC group. Eleven ejection sites did not produce a significant enhancement (filled squares). All but 2 sites in the INC group were within the SUML whereas all of the control sites were scattered well outside of the SUML. The 2 effective sites that were outside the SUML

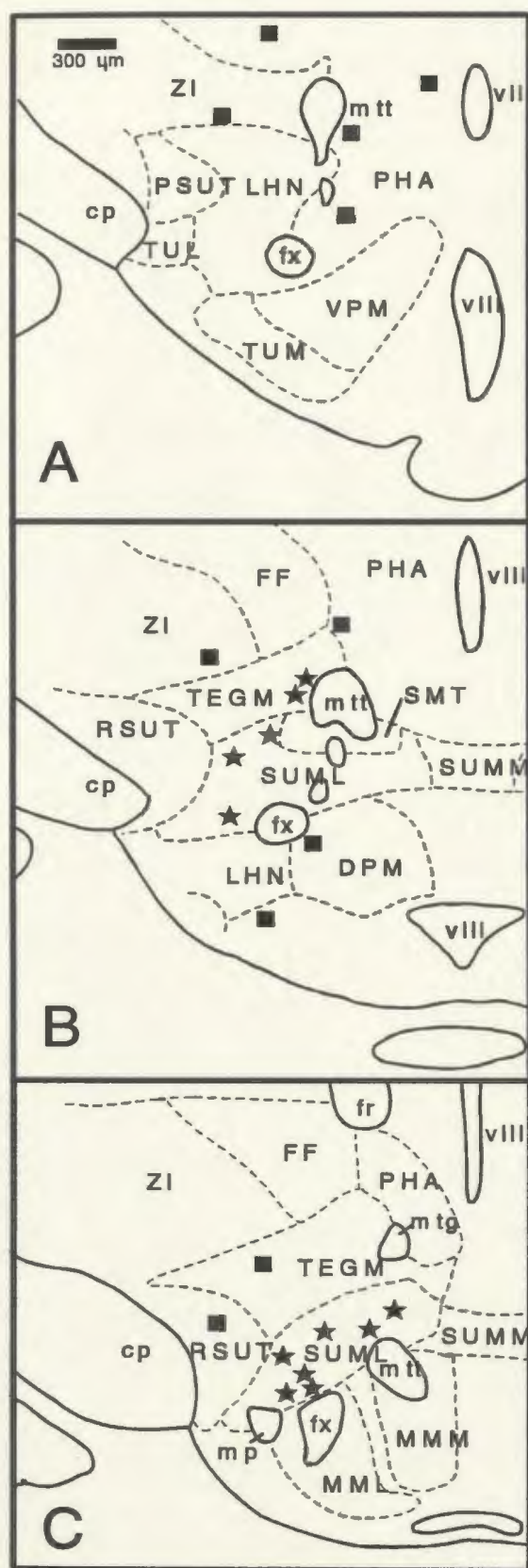


FIG. 2-3. Stars represent glutamate micropipette placements for sites which exhibited significant facilitation of the perforant path population spike amplitude. Filled squares represent ineffective glutamate placements. Representative sections are taken from Geeraedts et al (1990) and are spaced 300 μm apart. Abbreviations: cp; cerebral peduncle, DPM; dorsal pre-mammillary nucleus, FF; fields of Forel, fr; fasciculus retroflexus, fx; fornix, LHN; lateral hypothalamic nucleus, MML; medial mammillary nucleus (lateral division), MMM; medial mammillary nucleus (medial division), mp; mammillary peduncle, mtt; mammillotegmental tract, PHA; posterior hypothalamic area, PSUT; pre-subthalamic nucleus, RSUT; retro-subthalamic nucleus, SMT; submammillothalamic nucleus, SUML; lateral supra-mammillary nucleus, SUMM; medial supra-mammillary nucleus, TEGM; mesencephalic tegmentum, TUL; lateral tuberal nucleus, TUM; medial tuberal nucleus, viii; third ventricle, VPM; ventral pre-mammillary nucleus, ZI; zona incerta.

(illustrated in Fig. 2-3B) were within 200 μm of the SUML border.

The data in the INC group were pooled after conversion to a percentage of the control mean and plotted (Fig. 2-4). The area under the tangent was used as a measure of spike amplitude. The average maximal increase was 129% (range: 118-150%). The average time to termination of a significant enhancement was 18.4 min after glutamate ejection (range: 2 to 54 min). Thirty-three % of the INC group had enhancement durations exceeding 20 minutes (see Fig. 2-5 for an example).

To assess the latency to initial population spike enhancement, individual spike amplitudes were scrutinized. Enhancement of the first spike was observed in 4 (33%) of the INC group following glutamate to the SUML, whereas the rest varied from 2-5 ($\bar{X} = 2.3$) spikes before an enhancement was observed. In half the cases, enhancement was not seen until at least the third evoked potential.

Spike onset latency was significantly reduced in 5 out of 12 of the INC group (2-3% decrease) for an average duration of 8.8 min (range: 5-12 min). The significant reduction in onset latency rarely coincided in duration with that of the accompanying spike enhancement, ranging from half to twice the latter's length in time. The population EPSP slope was unchanged after glutamate at 11 of the 12 ejection sites, with a significant enhancement at one (106% of control for 2 min). Spike peak latency was marginally but

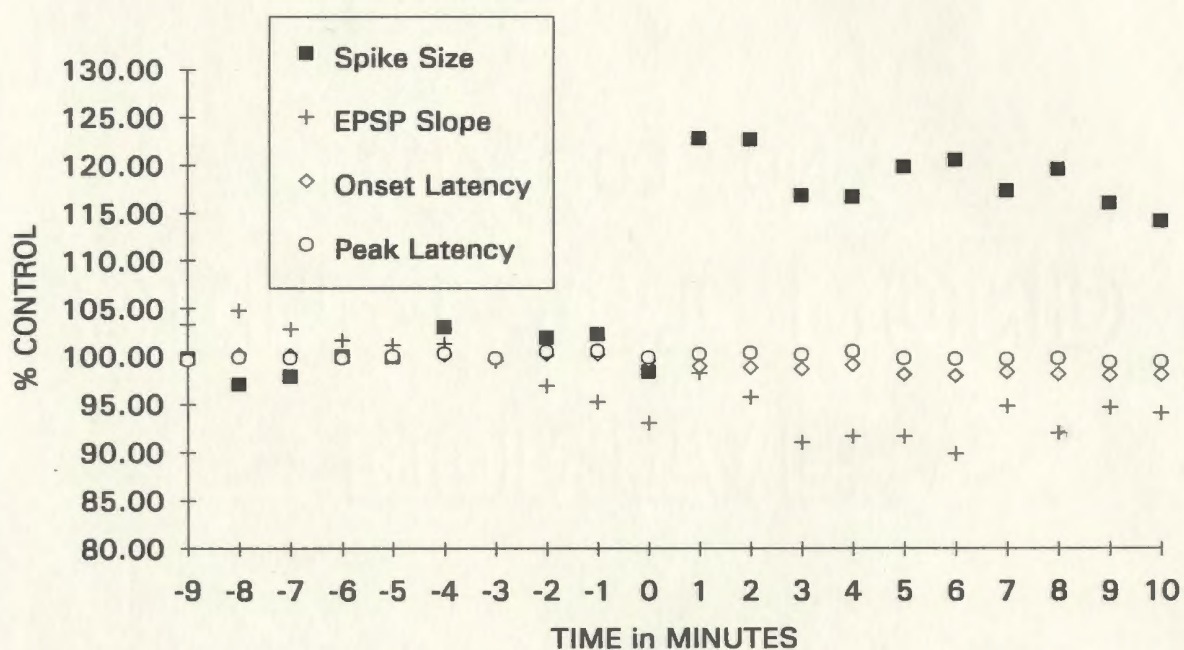


FIG. 2-4. Mean percent changes in population spike amplitude (area), EPSP slope, spike onset latency, and spike peak latency for the 12 sites exhibiting spike amplitude facilitation after glutamate ejection to the SUML. Each point represents a 1 min average.

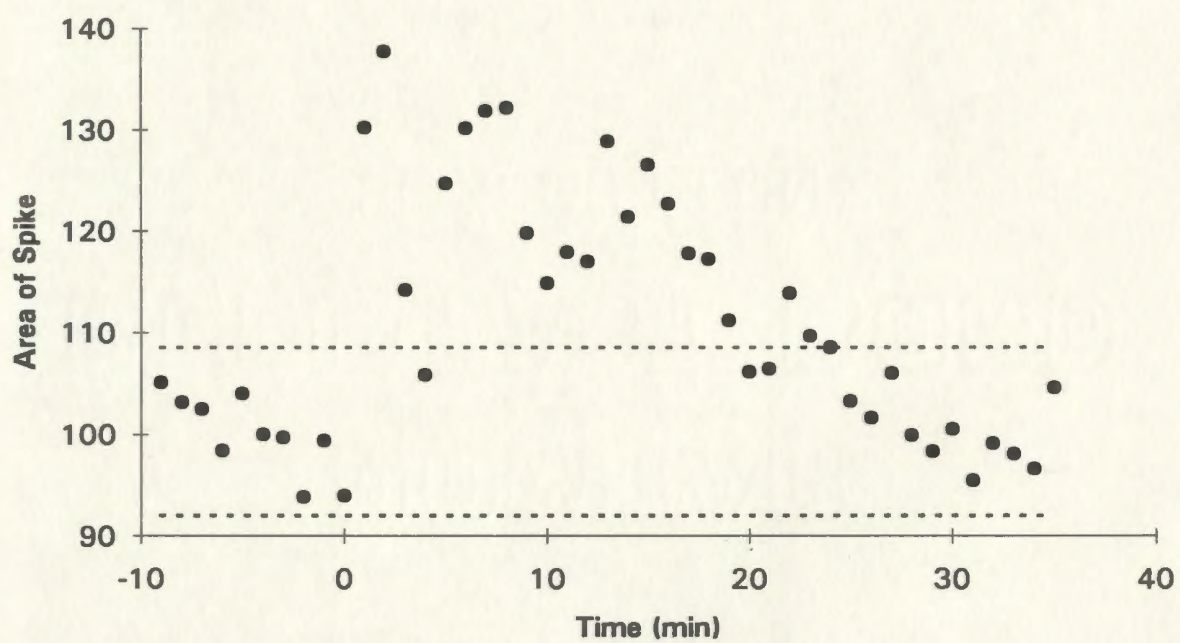


FIG. 2-5. Percent change in population spike amplitude (area) for an animal exhibiting an enhanced population spike for at least 20 min. Dashed lines represent 95% confidence limits based on the control period (first 10 minutes).

significantly increased (by 1%) in 25% of the INC group with an average duration of 1.3 min (range: 1-2 min), well below the duration of the enhanced population spike.

Unexpectedly, in addition to the 12 sites associated with the SUML, 8 sites in the thalamus also produced a significant enhancement in population spike size as a result of glutamate ejection ($\bar{X} = 165\%$). These sites are illustrated in Fig. 2-6 and are not clearly associated with any one nucleus. Average duration of spike enhancement was 15.9 min (range: 3-60 min) of which one exceeded 20 min in duration. A composite graph of 4 parameters for the 8 glutamate ejections is shown in Fig. 2-7.

Enhancement induced by glutamate ejections at thalamic sites never occurred by the first spike but took an average of 5.6 evoked potentials before enhancement was observed (range 3-8). Five of the 8 exhibited an increase in the EPSP slope ($\bar{X} = 112\%$; range: 109-116%) that usually lasted (3 of 5) for a shorter period of time than the spike enhancement. A significant reduction in spike onset latency was observed in half of the ejection sites ($\bar{X} = 97.3\%$; range: 96-98%) always lasting for a shorter period in time than the spike enhancement ($\bar{X} = 3$ min). Spike peak latency was marginally, but significantly, reduced in 3 and lengthened in 2 of the 8 spike enhancement studies, always for a relatively shorter period of time than the spike enhancement.

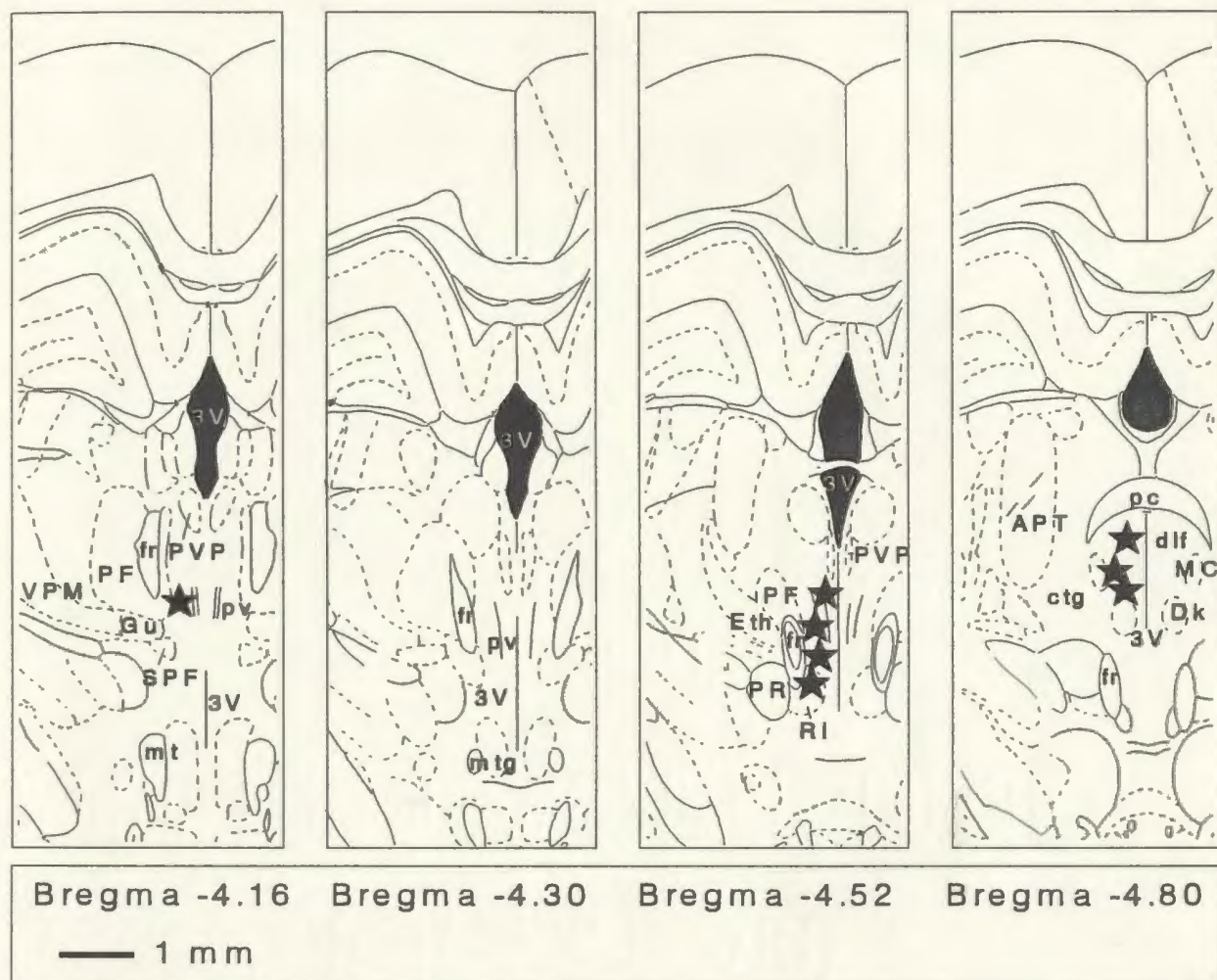


FIG. 2-6. Stars represent glutamate micropipette placements for sites which exhibited significant facilitation of the perforant path population spike amplitude in the thalamus. Representative sections are taken from Paxinos and Watson (1986). Abbreviations: 3V; third ventricle, ctg; central tegmental tract, Dk; nucleus Darkschewitsch, dlf; dorsal longitudinal fasciculus, Eth; ethmoid thalamic nucleus, fr; fasciculus retroflexus, Gu gustatory thalamic nucleus, MC; magnocellular nucleus of the posterior commissure, mt; mammillothalamic tract, mtg; mammillotegmental tract, pc; posterior commissure, PF; parafascicular thalamic nucleus, PR; prerubral field, pv; periventricular fiber system, PVP; posterior paraventricular thalamic nucleus, RI; rostral interstitial nucleus, SPF; subparafascicular thalamic nucleus, VPM; ventral posteromedial thalamic nucleus.

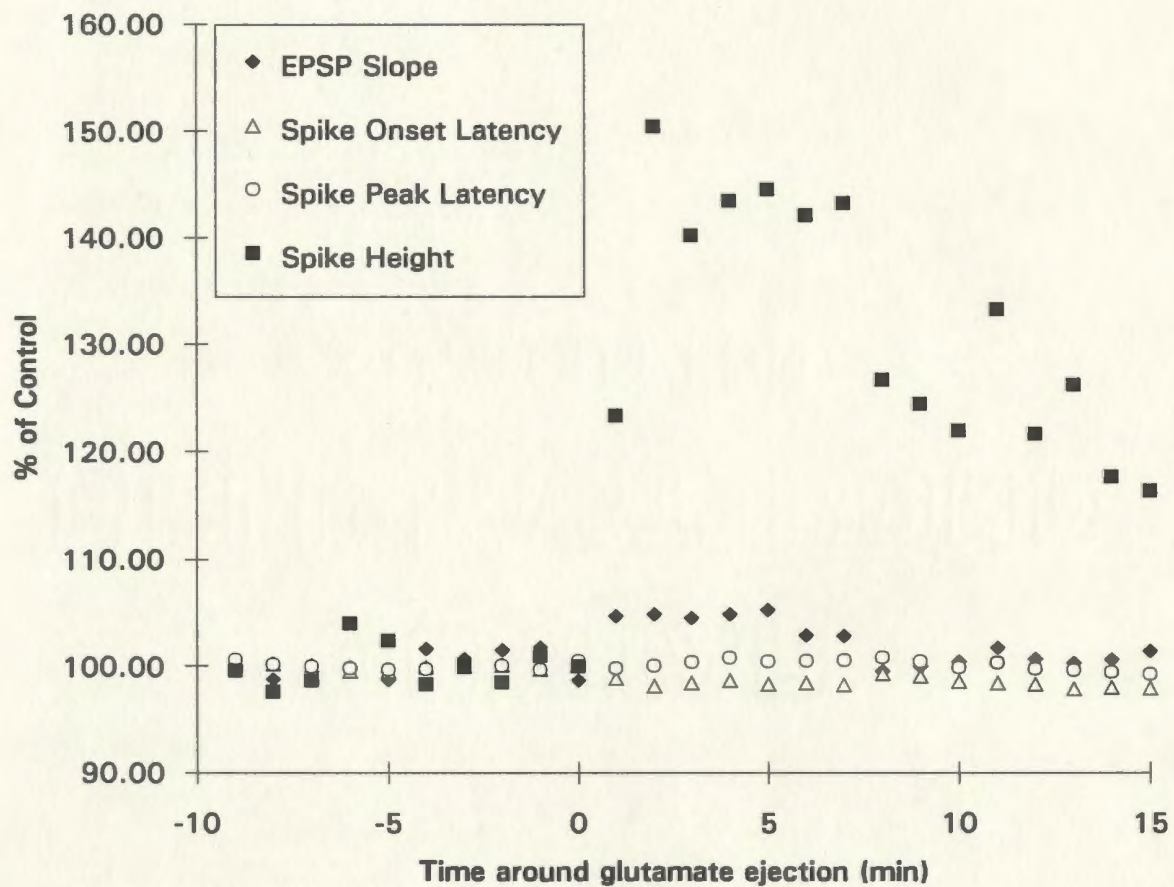


FIG. 2-7. Mean percent changes in population spike amplitude (area), EPSP slope, spike onset latency, and spike peak latency for the 8 sites exhibiting spike amplitude facilitation after glutamate ejection to the medial thalamus. Each point represents a 1 min average.

2.3.2 Experiment 2:

Ejection sites for animals experiencing population spike enhancement were similar to those shown in figure 2-3, being either in, or within 200 μm , of the SUML. Dentate EEG was recorded in 9 animals during population spike enhancement induced by glutamate ejection to the SUML. A theta rhythm was observed to occur spontaneously at each of these recording sites. Of the 9 animals, 2 were in theta at the time of ejection and neither exhibited a change in theta frequency as a result. Glutamate ejection in 4 of the remaining 7 induced theta (see fig. 2-8 for an example) while EEG frequencies were unchanged in the other 3. Therefore, in all situations where theta was absent, a SUML glutamate pulse produced theta in 57%. The longest latency to theta induction was 5 s (range 0-5 s) and the longest duration 45 s (range 10-45 s). Induced theta never lasted as long as the induced increase in the population spike.

Twenty-two units were recorded in 10 animals during population spike enhancement induced by glutamate ejection to the SUML. The results for two units are included after a second glutamate ejection. Units were considered repeats if the recording electrode was not moved between the two ejections and the spontaneous firing rates and bursting characteristics were similar. The characteristics of each unit are summarized in Table 2-1 (at end of Results section). Fig. 2-9 (a-c) illustrates 3 units and the method

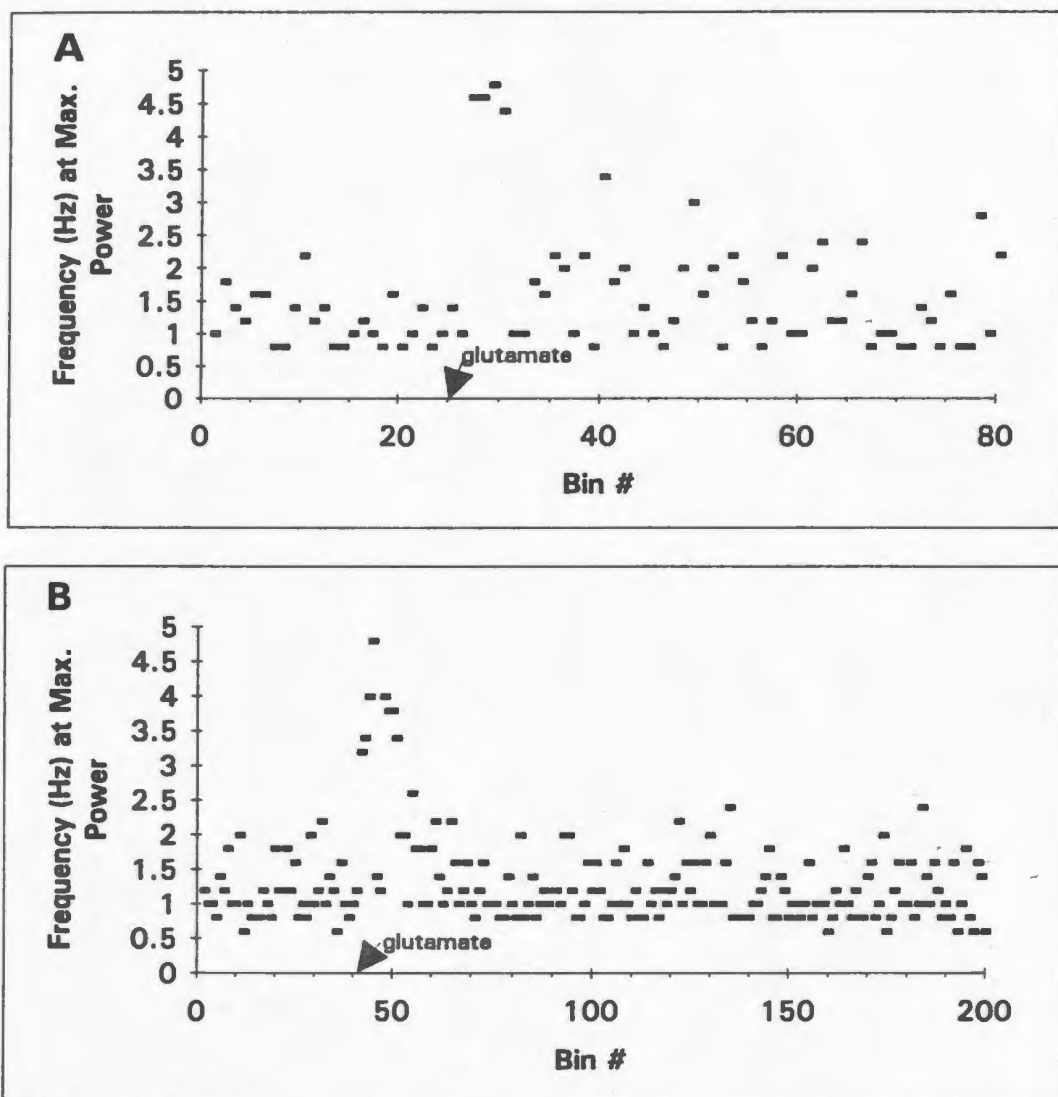
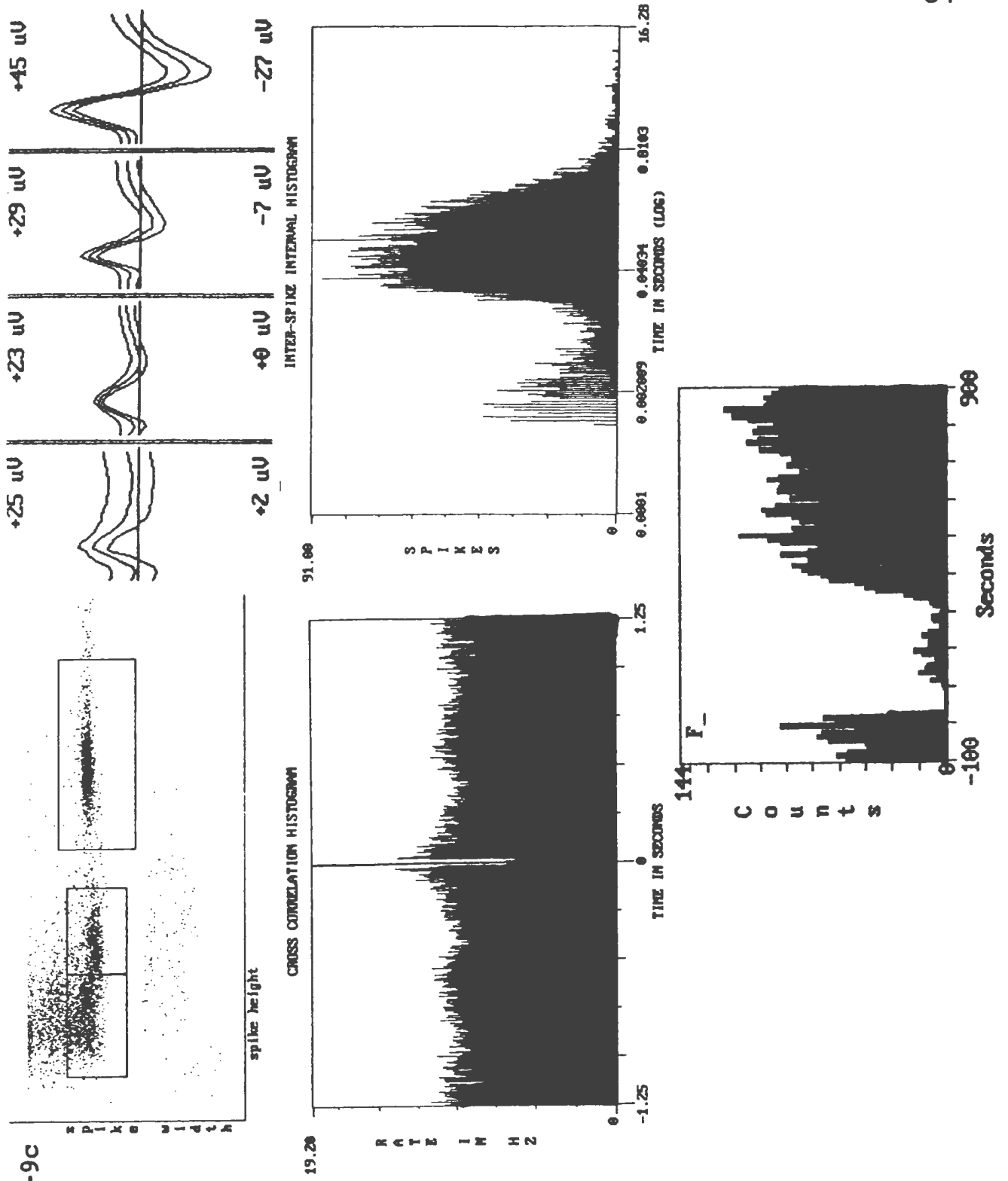


FIG. 2-8. Two examples of theta rhythm induction as a result of glutamate injected into the SUML. Arrows indicate the time of glutamate ejection. The frequency at maximum power is plotted against time. Each point represents a 5 s bin. Theta occurs at a frequency of 2.5 to 6 Hz in urethane-anaesthetized rats.

FIG. 2-9.(a-c) Three examples of units isolated by cluster-cutting (top left) and characterized by software analysis. The top right picture shows the "noise" and waveforms of each isolated unit bounded by its standard deviation. The two centre graphs are examples of autocorrelation functions (cross-correlation on the same cell) and interspike interval histograms (ISIH) for one of the units isolated by cluster cutting. A bimodal ISIH (Fig. 2-9c) with a short latency first peak is indicative of cells that fire in bursts. This burst pattern is also demonstrated by a centre peak arising from the autocorrelation histogram. Cells that do not have a tendency to fire in bursts have a unimodal ISIH and no centre peak in the autocorrelation (Fig. 2-9a). If a cell was rhythmically modulated due to the presence of theta, the autocorrelation is not flat but contains repeating peaks oscillating at about 3-4 Hz (Fig. 2-9b). The perievent time histogram (PETH) at the bottom shows the spontaneous firing of the unit before and after glutamate ejection to the SUML given at time 0. The first unit (Fig. 2-9a) was excited whereas the second and third units were inhibited.

Fig. 2-9c



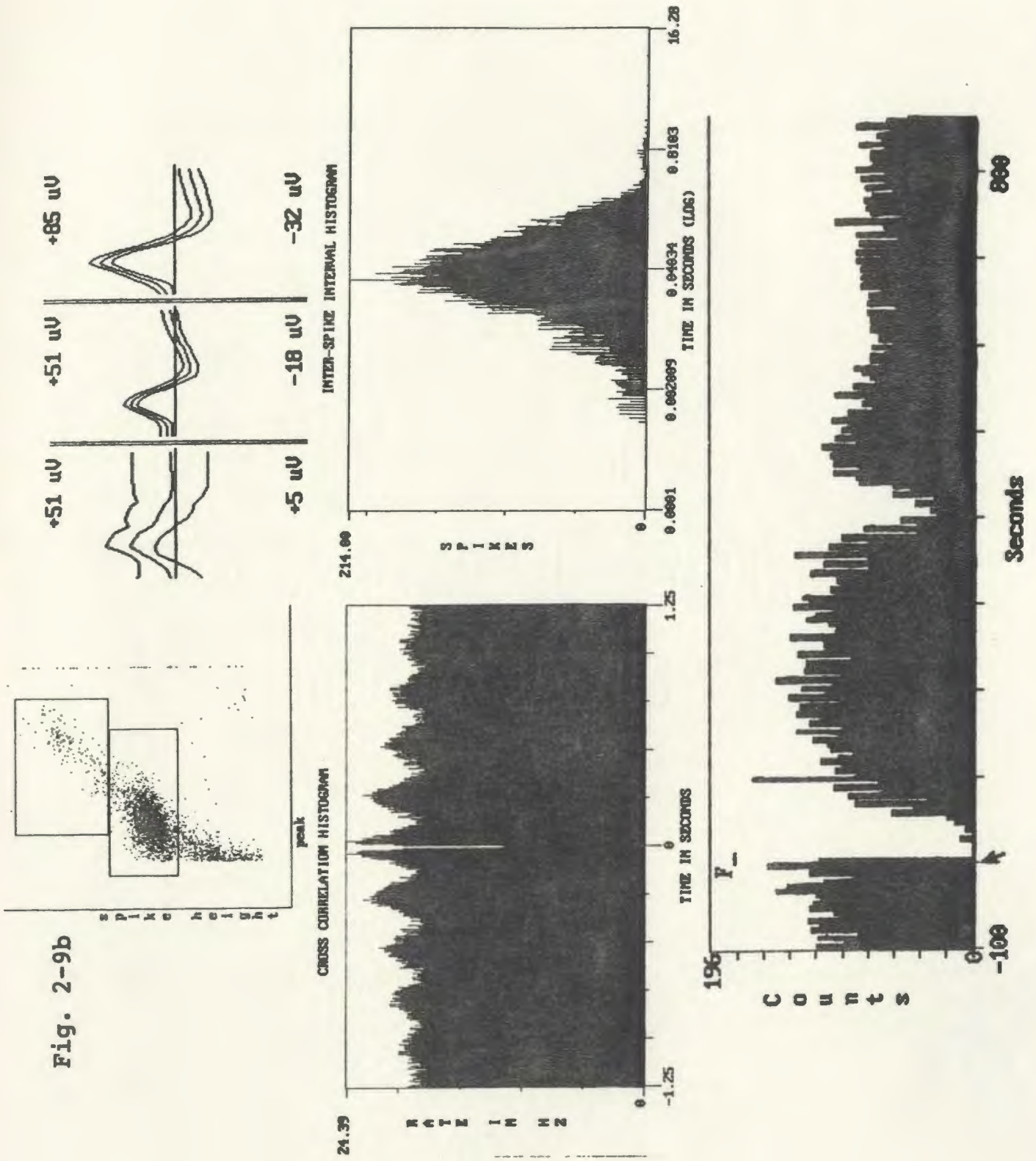
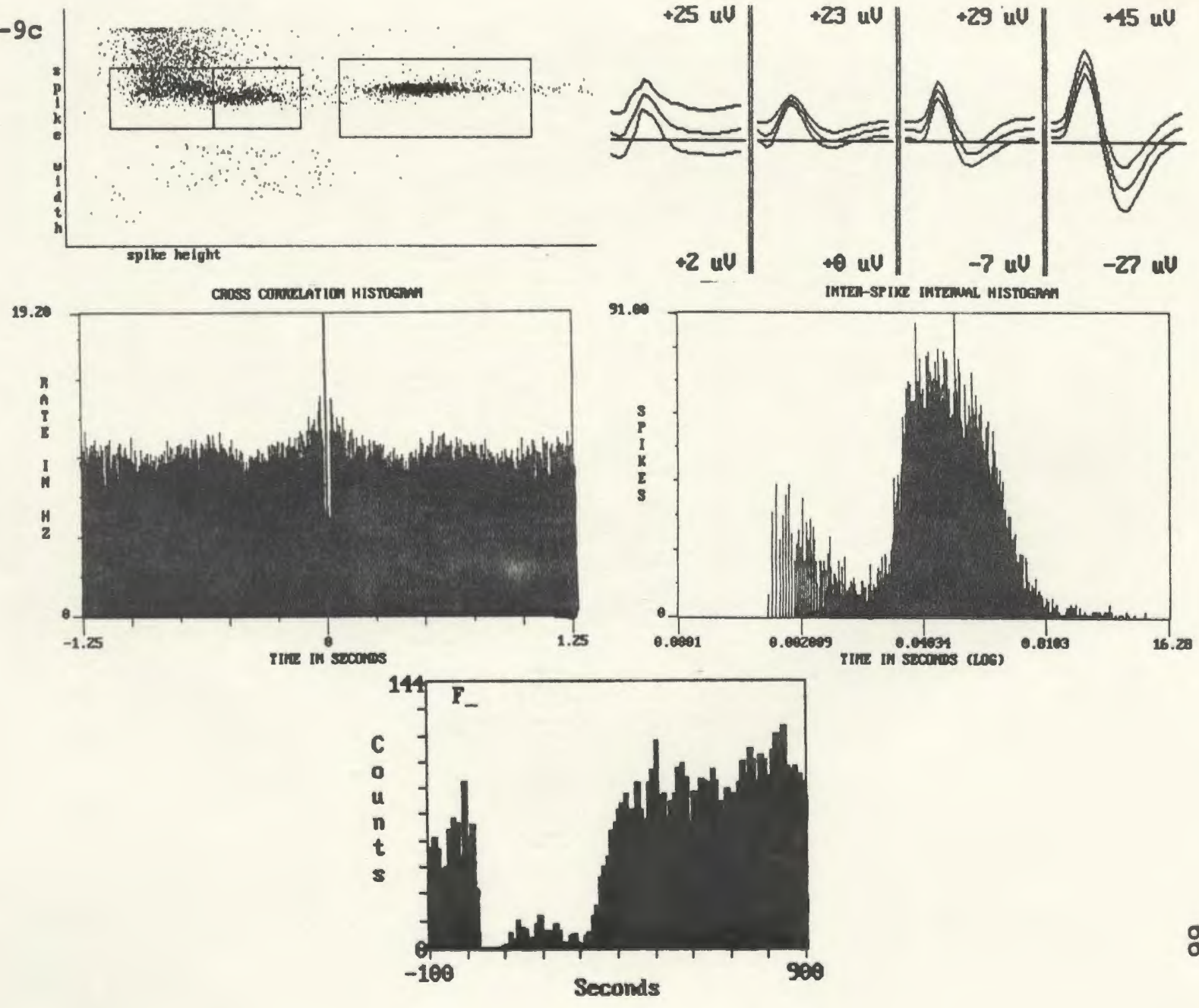


Fig. 2-9b

Fig. 2-9c



by which cells were characterized using the BrainWave Discovery program. With respect to table 2-1, if the peak at the centre of a units autocorrelation histogram (representing a short interspike interval) exceeded that of the other intervals, it was categorized as a bursting cell (fires repeatedly with an interspike interval of less than 6 ms). If bursting was indicated by the autocorrelation histogram but did not dominate, the cell was designated as a mild burster.

Eight of the units were inhibited, 13 excited, 2 exhibited a mixed response, and 1 showed no response to glutamate ejected in the SUML. Most of the unit effects were dramatic, as evidenced by the magnitude of the glutamate-induced effects given in column 5. A comparison of the magnitude of the unit effect and the magnitude of the population spike enhancement is also included in Table 2-1. There is no correlation between the two magnitudes (i.e. the magnitude of the unit effect did not predict the magnitude of the population spike enhancement).

The time course of the unit and population spike modulation as a result of glutamate ejection are presented in Table 2-2. If theta was recorded concurrently, the time course of its modulation is given as well. All but one unit (SUM15-2a) responded within 5 s of the glutamate pulse, and maintained their new level of activity for an average of 145 s (range 5-400 s). See Fig. 2-10 for a graphical representation of the time course for each

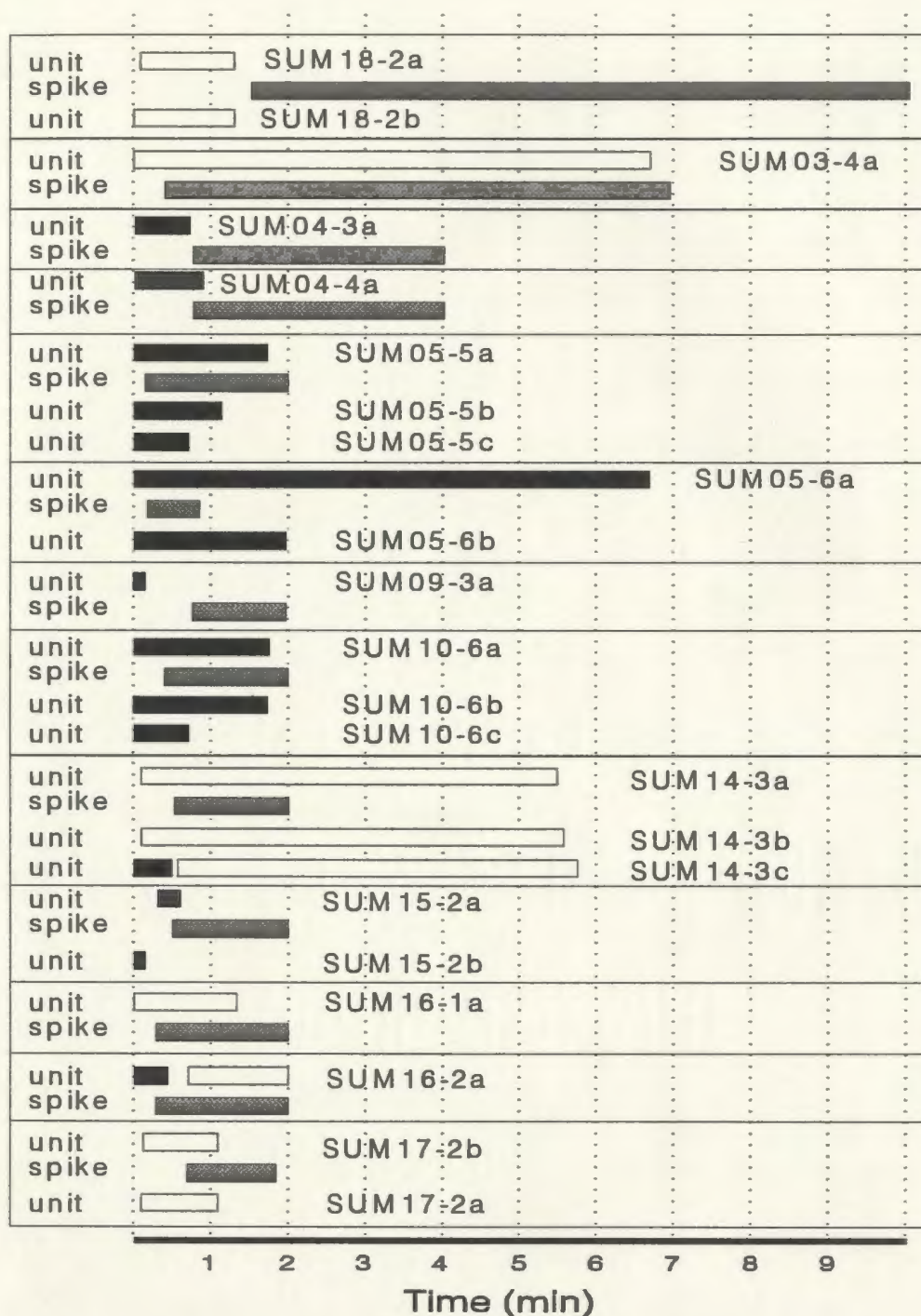


FIG. 2-10. Time course and effect of glutamate ejection to the SUML on units and population spike. Each rectangle delineates the results from one glutamate ejection. Shaded bars represent time course of population spike enhancement. Black bars represent excited units and white bars the inhibited units.

unit and the concurrent population spike changes as a result of glutamate ejection to the SUML. Regardless of whether the units were inhibited or excited, the period of change did not collectively predict the time period of population spike enhancement. Of the inhibited cells, unit SUM03-4a was inhibited for approximately the length of the population spike enhancement, but other units returned to baseline prior to spike enhancement (e.g. SUM18-2a) and others did not return until well after spike enhancement (e.g. SUM14-3a). The same is true of the excited cells with some returning to baseline prior to population spike enhancement (eg SUM09-3a) and others not returning until well after population spike enhancement (eg SUM05-6a).

Bursting cells were scrutinized for evidence of complex bursting, where each successive spike in a burst decreases in amplitude. A burst was defined as 2 or more action potentials with interspike intervals of less than 6 ms. Complex bursts are indicative of pyramidal cells (Fox and Ranck, 1975; Fox and Ranck, 1981), although CA3 pyramidal cells may burst in a non-complex manner as well (Scharfman, 1992). Complex bursting was only observed in unit SUM18-2b. Bursting cells that were excited by glutamate ejection to the SUML were scrutinized for a possible increase in bursting above that indicated by an increase in frequency. While bursting did increase, it was never above the proportional increase in frequency. There was no evidence

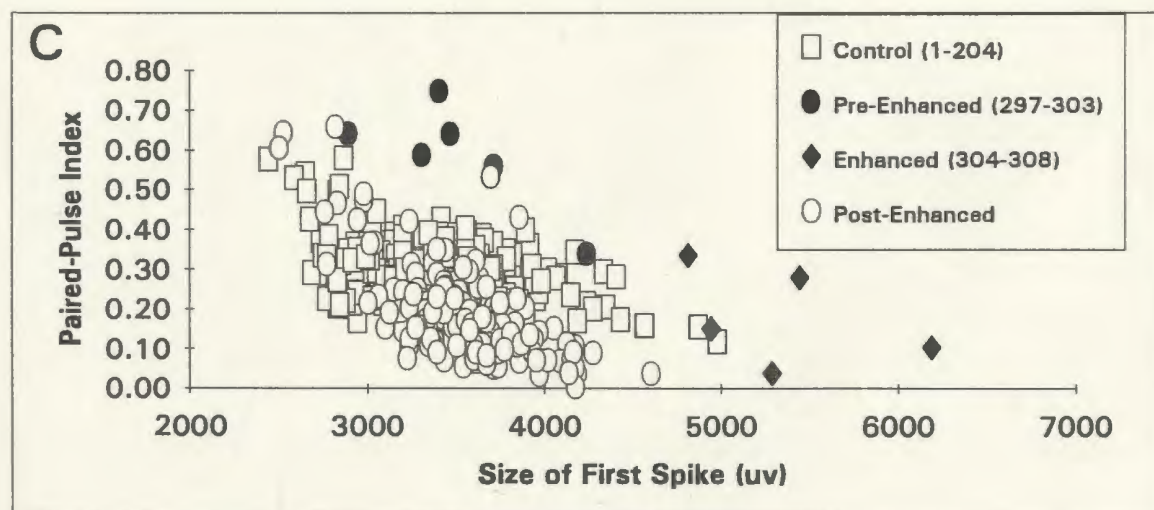
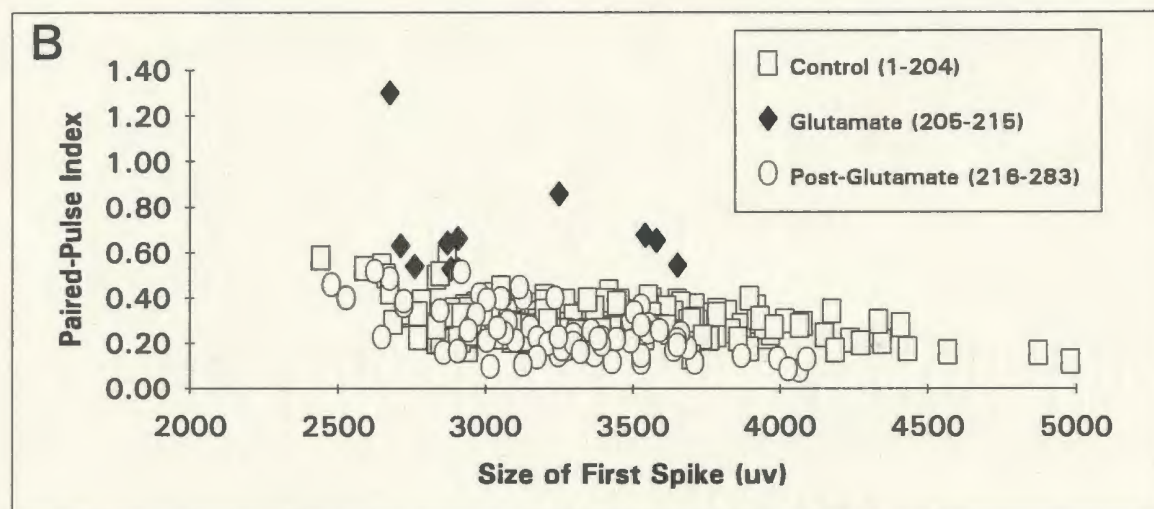
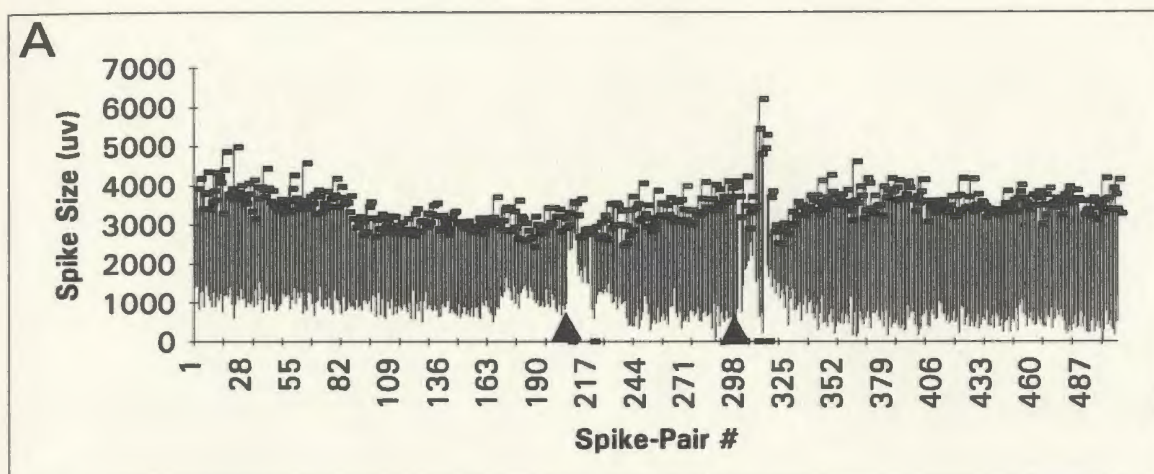
that the number of action potentials within a burst increased in number as a result of SUML activation as well.

All of the 6 non-bursting, low frequency (< 5 Hz) units were excited. On the basis of only these two criteria, these cells may be granule cells (Mizumori et al., 1989; Scharfman, 1992), as outlined in the introduction. The bursting cells, putative spiny hilar (e.g. mossy cells), aspiny hilar or CA3c pyramidal cells demonstrated mixed effects with 7 inhibited and 7 excited.

The molecular layer EPSP was recorded in two animals that exhibited population spike enhancement as a result of three different SUML stimulations. No significant change in the EPSP slope and latency to peak occurred measured concurrently at the cell layer and molecular layer.

Of the five animals subjected to paired-pulse stimuli following the multiparameter investigation, results from only one demonstrated a significant population enhancement due to glutamate ejection to the SUML, perhaps as a consequence of a reduced responsiveness to repeated ejections to the same site. In single spike experiments, repeated glutamate ejections were made at 4 sites that produced enhancement of the population spike on the first ejection. Two of the 4 ejections failed to reproduce the enhancement.

FIG. 2-11. A. Population spike size is plotted for each paired-pulse pair and a line connects the two points. Paired-pulse inhibition is evidenced by the reduced size of the second population spike. Arrows indicate the time of glutamate ejection to SUML. B. The ratio of the size of the second population spike to that of the first (paired-pulse index) is plotted against the size of the first. The data is taken from first glutamate ejection shown in 2-11A. The paired-pulse index for spike pairs immediately following glutamate injection (glutamate group) often fall well above those pairs with equivalent first spike sizes, indicating a reduction in feedback inhibition. C. The data are taken from the second glutamate ejection shown in 2-11A. In this case the 'glutamate' group was broken into a pre-enhancement and an enhanced category. Clearly, the pre-enhanced group had reduced feedback inhibition since their paired-pulse indexes were higher than those pairs with equivalent first spike sizes. Since the enhanced group had first spike sizes above any of those in the control group, clear evidence of a reduction of feedback inhibition is lacking. Numbers in the legends of B and C represent spike pairs numbered in A.



The results from the 'enhanced' animal are shown in Fig. 2-11. Two SUML glutamate ejections were given during the course of the experiment as indicated by the arrows in Fig. 2-11A. While only the second ejection produced a statistically significant enhancement of the first population spike, a reduction in feedback inhibition is apparent after both ejections, as evidenced by the increase in the size of the second or test population spike shown in Fig. 2-11A, and in the paired-pulse index plots in Figs. 2-11B and C. The mean paired-pulse index for the "glutamate" group in Fig. 2-11B is $0.69 (\pm .23)$ while the mean for the control group (using only those pairs with first spike sizes that fall within the range of those of the glutamate group) is $0.31 (\pm .07)$.

Even the first 6 spikes following glutamate ejection that were not enhanced in the second case (a delay consistent with the results given in experiment 1), show a reduction in feedback inhibition. This can be seen in Fig. 2-11A and C (the pre-enhanced group, paired-pulse index $\bar{X} = 0.53 \pm 0.19$). In this instance, the enhanced (first) population spikes were larger than most of the control (first) spikes therefore making it impossible to determine whether feedback inhibition was reduced. If the paired pulse indexes continued to decline in a linear fashion with an increase in first spike size, then it is likely that the enhanced pairs also exhibited a reduction in feedback inhibition.

Of the four paired-pulse experiments where no statistically significant enhancement of the first population spike of the pair was induced, three showed a reduction in feedback inhibition. An example is given in figure 2-12. When the perforant path stimulus intensity was turned down at spike pair number 84 (see Fig. 2-12A), the resultant feedback inhibition was weak as evidenced by a second spike of almost equal size with the first. When glutamate was ejected, the size of the first spike was not enhanced but clearly the second spike of the pair was, becoming almost three times the size of the first. The mean paired-pulse index for the "glutamate" group in Fig. 2-12B is $1.93 (\pm 0.57)$ while the mean for the control group (using only those pairs with first spike sizes that fall within the range of those of the glutamate group) is $0.68 (\pm .27)$.

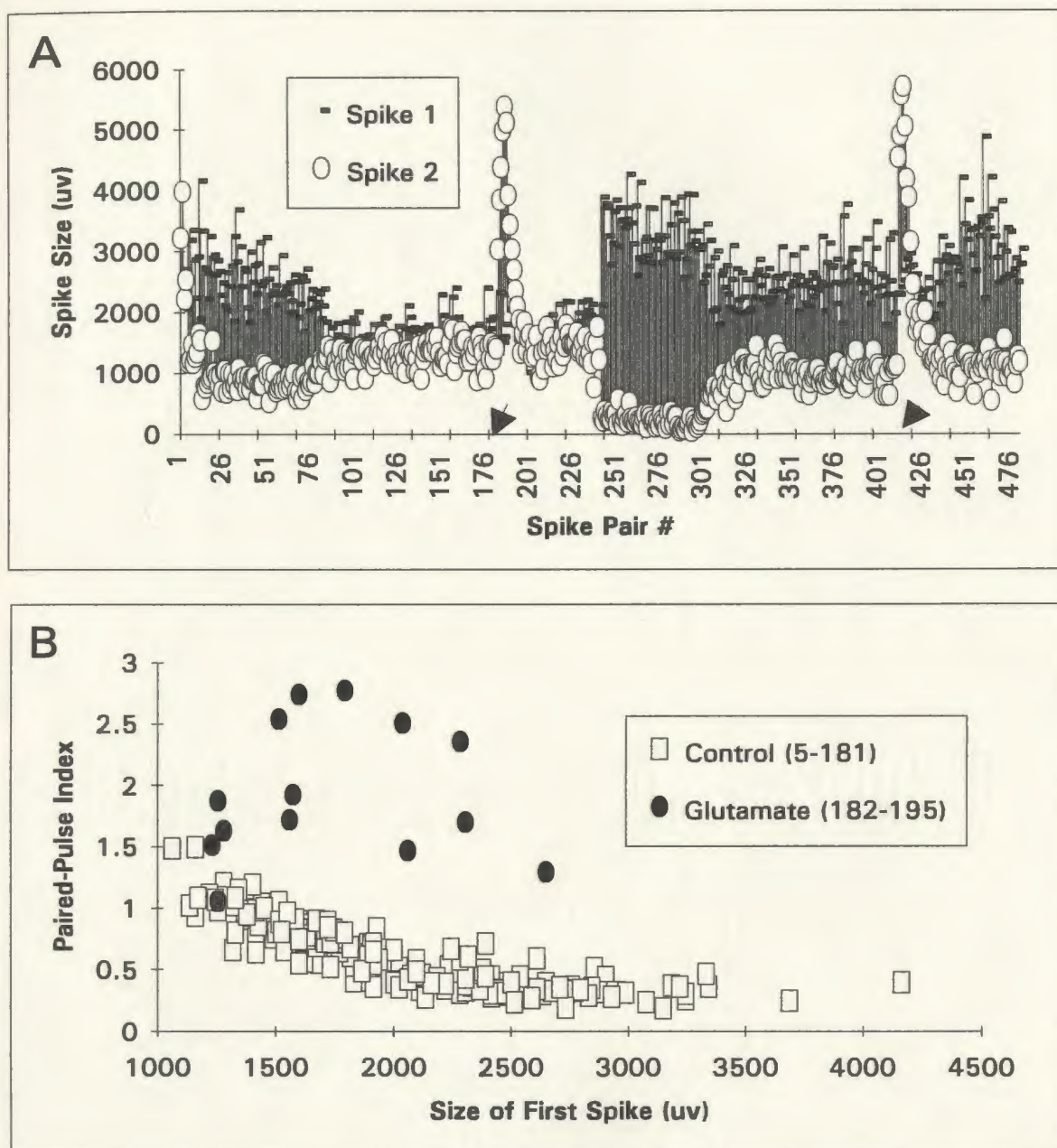


FIG. 2-12. See Fig. 2-11 for explanation of graphs. A. Without enhancing the size of the first spike, glutamate to the SUML induced paired-pulse facilitation, as evidenced by a second spike of the pair being larger than the first. B. The data are taken from the first glutamate ejection illustrated in 2-12A. Paired-pulse indexes for the glutamate group are much larger than those of the control group, once again indicating a reduction in feedback inhibition.

Table 2-1. Listing of each unit recorded, its spontaneous firing rate, whether it fires in bursts or not, whether it fired rhythmically in the theta frequency, the effects of glutamate ejection in the SUML, and the magnitude of the accompanying population spike facilitation.

Cell ID	Freq. (Hz)	Burst	Rhythmic	Effect (factor)	Spike (% of control)
SUM18 2a	16.0	mild	yes	Inhibition (complete)	145
SUM18 2b	2.0	yes	no	inhibition (complete)	145
SUM03 4a	2.0	mild	no	inhibition (complete)	152
SUM04 3a	3.8	yes	no	excitation (x8)	120
SUM04 4a repeat	4.0	yes	no	excitation (x10)	126
SUM05 5a	2.0	mild	no	excitation (x2.5)	118
SUM05 5b	4.4	mild	yes	excitation (x2.4)	118
SUM05 5c	5.0	no	yes	excitation (x1.8)	118
SUM05 6a	1.0	mild	no	excitation (x10)	110
SUM05 6b	.02	no	no	excitation (x500)	110
SUM09 3a	.40	mild	no	excitation (x3)	120
SUM09 2a	.53	yes	no	none	133

Cell ID	Freq. (Hz)	Burst	Rhythmic	Effect (factor)	Spike (% of control)
SUM10 6a	2.0	yes	no	excitation (x4)	174
SUM10 6b	4.2	no	no	excitation (x6)	174
SUM10 6c	0.8	no	no	excitation (x27)	174
SUM14 3a	14.3	yes	no	inhibition (complete)	125
SUM14 3b	9.0	yes	yes	inhibition (complete)	125
SUM14 3c	12.0	no	no	excitation (x4.6) inhibition (x0.25)	125
SUM15 2a	1.5	no	no	excitation (x5)	123
SUM15 2b	0.4	no	no	excitation (x15)	123
SUM16 1a	7.6	yes	no	inhibition (x0.2)	129
SUM16 2a repeat	6.0	yes	no	excitation (x2.6) inhibition (x.25)	181
SUM17 2b	6.0	no	yes	inhibition (complete)	111
SUM17 2a	1.2	yes	no	inhibition (complete)	111

Table 2-2. Listing of each unit recorded and its relationship in time to the population spike enhancement and EEG (if it was recorded, - indicates no recording).

Cell ID	Time of Unit Effect (s)	Time of max. effect (s)	Spike Enhance. time (s)	Time of max. effect (s)	Time of EEG effect (s)
SUM18 2a	5-80	5-30	90-600	120-180	no effect
SUM18 2b	0-80	0-35	90-600	120-180	no effect
SUM03 4a	0-400	0-100	25-420	60-120	no effect
SUM04 3a	0-40	15-20	45-240	180-240	no effect
SUM04 4a repeat	0-50	10-15	45-240	180-240	no effect
SUM05 5a	0-100	20-25	5-120	10-60	no effect -in theta
SUM05 5b	0-70	35-40	5-120	10-60	no effect -in theta
SUM05 5c	0-40	0-35	5-120	10-60	no effect -in theta
SUM05 6a	0-400	0-400	10-50	10-50	no effect -in theta
SUM05 6b	0-120	20-25	10-50	10-50	no effect -in theta
SUM09 3a	0-5	0-5	50-120	60-120	5-25
SUM09 2a	-	-	60-120	60-120	-

Cell ID	Time of Unit Effect (s)	Time of max. effect (s)	Spike Enhance. time (s)	Time of max. effect (s)	Time of EEG effect (s)
SUM10 6a	0-100	75-80	25-120	25-120	0-40
SUM10 6b	0-100	25-30	25-120	25-120	0-40
SUM10 6c	0-100	25-30	25-120	25-120	0-40
SUM14 3a	5-330	30-100	35-120	35-120	-
SUM14 3b	5-340	30-100	35-120	35-120	-
SUM14 3c	0-30 40-360	5-10 50-100	35-120	35-120	-
SUM15 2a	20-35	25-30	35-120	35-120	-
SUM15 2b	0-5	0-5	35-120	35-120	-
SUM16 1a	0-80	0-5	15-120	15-120	0-44
SUM16 2a repeat	0-25 45-120	15-20	15-120	15-120	0-30
SUM17 2a	5-65	5-20	45-110	45-110	0-10
SUM17 2b	5-65	5-45	45-110	45-110	0-10

2.4 Conclusions

Theoretical mechanisms by which SUML activation may enhance the physiology of the dentate gyrus will be explored in chapter 4. The following represents a summary of the experimental findings.

Glutamate ejection in or immediately adjacent to the SUML invariably produced a significant increase in amplitude of the perforant path-evoked population spike in the dentate gyrus, without affecting the EPSP. A similar finding was reported using electrical stimulation of the SUML (Mizumori et al., 1989). The lack of effect on the population EPSP slope, combined with a decrease in spike onset latency in approximately half of the SUML group, indicates that SUML afferents are increasing granule cell excitability rather than acting on perforant path fibres or their synapse with granule cells.

Synaptic current flow recorded from the major current source in or below the granule cell layer and from the site of activation in the molecular layer (the current sink) are generally assumed to parallel each other. Recent observations indicate that the two measures may not covary in a uniform manner under certain conditions (Dahl and Winson, 1985; Pavlides et al., 1988b). In the three cases where molecular layer EPSP slope changes were monitored concurrently with the evoked potential measured at or below the granule cell layer, no changes in both EPSP slopes were observed during population spike enhancement induced by glutamate ejection to the SUML.

Two ejection sites falling outside of the SUML, as cytoarchitectonically defined by Geeraedts et. al. (1990), produced increased population spikes. It is quite possible that the glutamate injected at these sites diffused to the SUML to stimulate a sufficient number of cells. Another explanation is that these sites near the mtt include cells projecting to the dentate gyrus. Evans Blue administered to the dentate gyrus labelled hypothalamic cells that capped the mtt at the level of Fig. 2-3B (Harley et al., 1983).

The duration of neurotransmitter release from the SUML afferents as a result of glutamate stimulation cannot be ascertained. It is unlikely, however, that the duration of neurotransmitter release due to glutamate-induced SUML cell activation matches the duration of population spike facilitation, which was over 20 min in one third of the experiments. Concurrent monitoring of SUML cell activity would be of interest. Glutamate excitation of locus coeruleus cells using comparable volumes and concentrations lasts for less than 1 s (Harley and Sara, 1992). Therefore, SUML afferents probably produce excitability changes in the granule cells of the dentate gyrus which exceed the duration of SUML activation.

Glutamate activation differs from electrical stimulation of the SUML in the time course of its effects on evoked potentials in the dentate gyrus. Electrical stimulation only produces an enhancement if given within 100 ms prior to the perforant path stimulus, optimally 10-15 ms prior to the stimulus

(Mizumori et al., 1989). Units recorded in the dentate gyrus during SUML electrical stimulation were affected for typically 10-15 ms (Mizumori et al., 1989). Both units and evoked potentials were modulated for minutes in this experiment, as a result of a brief pulse of glutamate to the SUML. Furthermore, a 30 s delay between the glutamate pulse and increases in spike amplitude was common in these experiments.

Glutamatergic stimulation of the SUML inhibited 36% and excited 59% of the cells recorded in the dentate gyrus for an average of 145s. Most responded immediately, prior to the spike amplitude enhancement. The time course of unit modulation rarely correlated with the time course of the spike enhancement. While this implies that changes in the spontaneous activity of the units recorded do not reflect the critical events that lead to an enhanced population spike, only a few cells were sampled from a large population. It is quite possible that the unit population response would reflect a mixture of unit responses in time, and hence their combined average may directly underlie the changes in the population spike amplitude.

SUML electrical stimulation prior to perforant path stimulation resulted in a decrease in putative inhibitory local-circuit neuron activity in the dentate gyrus and an increase in putative granule cell activity (Mizumori et al., 1989). This effect suggests a disinhibition mechanism mediates the population spike facilitation produced by SUML stimulation (Mizumori et al., 1989). Units

recorded in this experiment were not identified by the rigorous response properties employed by Mizumori et. al. (1989). However, assuming that granule cells, in relation to non-granule cells found in the dentate gyrus, fire at low rates (Mizumori et al., 1989; Scharfman, 1992), and are characterized by an absence of burst firing (Misgeld et al., 1992a; Scharfman, 1992), then it is noteworthy that all non-bursting cells that fired at a frequency of less than 5 Hz were excited by SUML activation. An excitatory action on granule cells by SUML afferents is indicated by the asymmetric, putative excitatory, synapses they make on granule cells (Dent et al., 1983). It is difficult to identify other cell types solely by their firing rates and burst propensity. A larger number of units sampled, coupled with the rigorous response properties employed by Mizumori et. al. (1989), would be more informative.

The mechanism by which the SUML influences hippocampal throughput was explored in this study using paired-pulse stimulation with interpulse intervals of 20-30 ms. While the threshold for a significant population spike amplitude enhancement appears to increase as a result of repeated glutamate ejections to the same site, as witnessed by the failure to reproduce spike amplitude enhancements in the paired-pulse paradigm, evidence for reduced inhibition was apparent nonetheless. A reduction in paired-pulse inhibition, without a concomitant increase in the amplitude of the first spike, implies

that feed-forward inhibition was not affected whereas feed-back inhibition was reduced.

The SUML projects to a number of sites (Behzadi et al.,1990; Vertes, 1992) that have previously shown to enhance perforant path-evoked potentials in the dentate gyrus including the medial septum complex (Mizumori et al.,1989) and the raphe nucleus (Klanchnik and Phillips, 1991). For this reason, it is possible that SUML activation enhances dentate population spikes in a disynaptic manner, however this seems unlikely given its direct and massive innervation of the dentate gyrus. Since the primary neurotransmitter of SUML cells is yet to be determined, direct pharmacological intervention cannot be carried out.

Glutamatergic activation of the SUML induced a brief (range = 10-45s) theta rhythm recorded at the molecular layer of the dentate gyrus in 57% of the experiments associated with a concomitant enhancement of the population spike. Enhancement of the perforant path-dentate evoked potential has been correlated with the induction of theta through sensory stimulation (Herrerias et al.,1988) and the theta rhythm may play a modulating role in the induction of LTP in the dentate gyrus (Pavlidis et al.,1988a; Ford et al.,1989). The production of theta is not necessary for the enhancement of the population spike here, given that the theta rhythm was not induced in 43% of the experiments. When induced, the theta rhythm lasted for a brief

period in time (10-45 s), therefore if it did play a role in spike enhancement, it was restricted to the induction of the event alone, and not the maintenance of the spike enhancement.

It is well established that the medial septum complex plays a critical role in the generation of hippocampal theta and that stimulation of the brainstem reticular formation can generate septal or hippocampal rhythms in the theta frequency range (Bland, 1986; Smythe et al., 1992; Vertes, 1986). Since critical brainstem sites do not directly innervate the medial septum complex, it has been postulated that the supramammillary nucleus acts as a relay station for hippocampal theta modulation originating from the brainstem (Vertes, 1986). Both SUML and the medial supramammillary nucleus (SUMM) project to the medial septal complex whereas only the SUML sends fibres to the hippocampus (Vertes, 1992). Recently, supramammillary cells more closely associated with the SUMM have been found to discharge synchronously in phase with hippocampal theta rhythm (Kirk and McNaughton, 1991). Reviewing their placements, it appears that they did not sample cells from the SUML region stimulated in this experiment. Alternately, the SUML placements that induced theta in this study were not clustered near the SUMM, therefore, a SUMM-mediated theta induction is unlikely. The induction of theta by SUML activation demonstrated here could be mediated by the medial septum complex or through its direct projections

to the dentate gyrus. The ability of GABA agonists ejected into the medial septum complex to block SUML activation-induced hippocampal theta would be of interest. Application of GABA agonists into the MSC, prior to SUML activation, should block SUML messages to the hippocampus relayed through the MSC, while leaving the direct route intact.

The results demonstrating the enhancement of population spikes by glutamate ejection into the thalamus were serendipitous and hence not systematically studied. The marking of sites in the thalamus that fail to produce population spike enhancements would help to identify the critical areas involved. The largest known projection from the thalamus to the hippocampus arises from the nucleus reunions (anterior to the glutamate ejection sites) where the projections are restricted to Ammon's Horn, avoiding the dentate gyrus (Herkenham, 1978; Pakhomova, 1992; Su and Bentivoglio, 1990; Wyss et al., 1979a; Sakanaka et al., 1980; Wouterlood et al., 1990). The parataenial and paraventricular nuclei of the thalamus also project to the hippocampus, however, unlike the nucleus reuniens, they innervate the dentate gyrus, particularly the hilus (Swanson et al., 1987). The rostral/caudal extent of the paraventricular nucleus contributes to the hippocampal projection (Wyss et al., 1979a) and therefore, as can be seen in Fig. 2-6, is the only thalamic site within the vicinity of the glutamate ejection sites that is known to project to the hippocampus. Since the ejection

sites range from 0.1 to 1.2 mm from the paraventricular nucleus, it is unlikely that stimulation of the paraventricular nucleus underlies all enhancement effects. It is possible that the critical site provides a multisynaptic input to the dentate gyrus.

Thalamic activation by glutamate stimulation shares many characteristics of SUML activation-induced modulation of dentate evoked potentials. The enhancement of the population spike lasted minutes and took time to develop. However, over 50% produced an enhancement in the slope of the population EPSP, differing from SUML effects, and suggesting that thalamic input may be modulating the perforant path synapse.

CHAPTER 3: THE MEDIAL SEPTUM COMPLEX

3.1 Introduction

The medial septum/diagonal band contains neurons which innervate several structures in the central nervous system, most notably the hippocampal formation, where it apparently serves a critical role in learning and memory [e.g. (Kesner, 1988; Bond et al.,1989; Mesulam, 1988)]. Relatively few pathways in the brain have been as extensively studied anatomically, histochemically and functionally as the projection from the medial septum/diagonal band to the hippocampus. A review of its anatomy, as well as its modulation of evoked potentials recorded in the dentate gyrus, follows.

3.1.1 Anatomy

On the basis of cytoarchitecture and connections, the septal region, which lies anterior to the hippocampus, is usually parcellated into 4 divisions; lateral, medial (which consists of the medial septal nucleus and the diagonal band nucleus), posterior, and ventral (Swanson et al.,1987). Since there is no clear cytoarchitectonic boundary between the medial septum nucleus and the nucleus of the diagonal band, they will be considered together as the medial septum complex (MSC) (Swanson et al.,1987).

Neurons in the MSC innervate all fields of the hippocampus, but the inputs to the dentate gyrus are particularly dense. Early work suggested that

projections from the MSC were cholinergic in nature and innervated both the hilus and molecular layer of the dentate gyrus. Combined silver-stained degeneration and acetylcholinesterase staining suggested cholinergic afferents innervated the dentate molecular layer and, more densely, the hilus (Mosko et al., 1973; Mellgren and Srebro, 1973). More sophisticated techniques have overcome limitations inherent in earlier studies, e.g., degeneration studies also characterize fibres of passage and acetylcholinesterase is not a selective indicator of cholinergic systems.

Anterograde transport of tritiated leucine or horseradish peroxidase (HRP) confirmed a medial septal projection to the dentate molecular layer and hilus, the projection to the former being more modest (Rose et al., 1976; Crutcher et al., 1981). Electron microscopic examination of anterograde HRP detected inputs to hilar cell dendrites and somata as well as to granule cell somata (Chandler and Crutcher, 1983). Using the more sensitive method involving the anterograde transport of the lectin *Phaseolus vulgaris* leucoagglutinin (PHAL) after injection into the MSC, one study confirmed a prominent projection to the hilus and a small projection to the molecular and supragranular layers of the dentate gyrus (Yoshida and Oka, 1990). Another study revealed that in the dentate gyrus, thick axons, with few boutons (type 1) were found to terminate in the hilus, while finer axons (type 2), with many en passant terminals, were found to terminate most densely in the

supragranular layer and in the middle third of the molecular layer (Nyakas et al., 1987).

PHAL anterograde studies have demonstrated that MSC afferents innervate calbindin-, parvalbumin-, and CCK-immunoreactive cells (Miettinen and Freund, 1992a), as well as somatostatin-immunoreactive cells (Yamano and Luiten, 1989), in the hilus.

Are the afferents arising from the MSC cholinergic, or are other neurotransmitters involved? The results of combined acetylcholinesterase staining and retrograde tracing experiments (Swanson, 1982; Baisden et al., 1984) and combined choline acetyltransferase (ChAT) immunoreactive staining and retrograde transport experiments (Rye et al., 1984; Wainer et al., 1985; Amaral and Kurz, 1985) have revealed that a substantial portion of MSC cells that project to the hippocampus are not cholinergic. At least 30% are immunoreactive to glutamic acid decarboxylase (GAD) (Kohler et al., 1984), a synthesizing enzyme for GABA, and are thus presumably GABAergic. There is virtually no colocalization of GAD with ChAT (Brashear et al., 1986).

As well, a subpopulation of ChAT immunoreactive cells in the MSC (over 50%) was found to be immunoreactive for the peptide galanin (Melander et al., 1985; Pasqualotto and Vincent, 1991), and these cells participated in the septohippocampal projections (Melander et al., 1985). Furthermore, a

subpopulation of GABAergic cells contains the calcium-binding protein parvalbumin (Freund, 1989). The fine structure of MSC cells participating in the septohippocampal projection is heterogeneous and the existence of ChAT- or parvalbumin-immunoreactivity did not differentiate between cell types based on their fine structure (Naumann et al., 1992).

The fact that the proportion of cells projecting to the hippocampus containing ChAT or GABA is well short of 100% prompted one laboratory to investigate the contribution of a wide variety of peptides to this pathway (Senut et al., 1989). Using a combination of retrograde transport and immunohistochemistry, they found that of the neurons projecting to the hippocampus, 42% were immunoreactive for ChAT, 22% for galanin (of which 26-52% double-labelled for ChAT), and 0.5% for the peptides luteinizing hormone-releasing hormone, calcitonin gene related peptide, and met-enkephalin. They concluded that other, unknown neurotransmitters likely participate in the septohippocampal projection.

What is the general distribution of cholinergic versus GABAergic septohippocampal terminals in the dentate gyrus? ChAT immunoreactive fibres were seen to predominantly innervate the supragranular layer and the portion of the hilus nearest the granule cell layer (Clarke, 1985; Houser et al., 1983; Matthews et al., 1987). These bands of staining were abolished by electrical lesions of the MSC. Combining ChAT immunocytochemistry with

electron microscopic examination of Golgi impregnated granule cells, both the soma and dendrites of the granule cells were found to receive ChAT-positive terminals (Frotscher and Leranath, 1986; Frotscher, 1992).

Somatostatin- and GAD-immunoreactive cells in the hilus were also found to receive ChAT immunoreactive terminals (Leranath and Frotscher, 1987; Lubbers and Frotscher, 1987). Half of the somatostatin-immunoreactive cells were recently shown to be immunoreactive for the muscarinic receptor protein, making up approximately one-third of the muscarinic-immunoreactive population in the hilus (Van der Zee et al., 1991). In general, ChAT immunoreactive terminals made symmetric synaptic contacts on dendritic shafts and cell bodies and mainly asymmetric contacts on dendritic spines (Clarke, 1985; Frotscher and Leranath, 1986; Leranath and Frotscher, 1987).

To demonstrate the specific distribution of septohippocampal GABA fibres, a number of recent studies have combined GABA immunohistochemistry with anterograde tracing of the lectin PHAL, allowing the researcher to differentiate extrinsic GABA projections from GABA terminals arising from cells intrinsic to the dentate gyrus. GABAergic axons arising from the MSC had type 1 fibres (thick axons with large spherical or oval boutons) and formed multiple basket-like contacts around cell bodies and proximal dendrites, predominantly in the hilus and granule cell layer (Freund and Antal, 1988). Hilar neurons immunoreactive for GABA (Freund and Antal, 1988),

neuropeptide Y (Miettinen and Freund, 1992b), CCK, somatostatin, and VIP (Gulyas et al., 1990) have all been found to receive the type 1, GABAergic, septohippocampal afferents. Calbindin-immunoreactive granule cells were never found to receive multiple synaptic input from GABAergic septohippocampal axons (Freund and Antal, 1988).

In summary, septohippocampal GABAergic fibres have been shown to innervate all dentate local circuit neurons tested so far and there is no evidence for a significant innervation of the granule cells as yet. The septohippocampal cholinergic fibres, however, have been found to be less selective, innervating both hilar and granular cells. ChAT fibres are distributed throughout the dentate gyrus but predominantly innervate the supragranular and subgranular layers. Studies involving combined ChAT immunocytochemistry with anterograde tracing need to be performed on tissue selectively stained to define select cell groups, to better characterize the cholinergic distribution.

3.1.2 Influence of the MSC on Hippocampal Evoked Potentials

It was first reported in anaesthetized rabbits that the size of the population spike evoked in the dentate gyrus can be altered by stimulating the MSC (Alvarez-Leefmans and Gardner-Medwin, 1975). Since then, several studies have explored the effects of electrical stimulation of the MSC on evoked

potentials in the dentate gyrus of the anaesthetized rat. This section reviews their findings.

Applying a single pulse to the MSC 10 ms prior to perforant path stimulation was found to augment the size of the population spike without altering the population EPSP in barbiturate-anaesthetized rats (Fantie and Goddard, 1982). Using interstimulus times ranging from 200 ms prior to, and 5 ms after perforant path stimulation, maximal spike augmentation was found to occur at 5 ms prior to perforant path stimulation. Augmentation occurred in a range of approximately 100 ms before, and 1 ms after perforant path stimulation. Muscarinic and nicotinic antagonists failed to block the effect.

In a follow up study, the influence of MSC stimulation on dentate evoked potentials was investigated using the paired-pulse paradigm or the presence of a GABA antagonist (Bilkey and Goddard, 1985). The infusion of picrotoxin into the dentate gyrus enhanced the population spike (without affecting the population EPSP slope), presumably due to a general decrease in GABA-mediated tonic or feed-forward inhibition, and blocked the enhancement of the population spike that normally occurs with a preceding (5 ms) septal stimulus. In the second portion of the experiment, the perforant path paired-pulse interstimulus time was adjusted to provide a measure of early inhibition, and a septal conditioning pulse was applied at an interval varying

from 8 ms before to 11 ms after the first perforant path stimulus. They found, for both barbiturate- and urethane-anaesthetized rats, that the inhibition apparent in the second evoked potential was reduced only if the septal conditioning pulse occurred within 3-4 ms before or 1-2 ms after the population spike of the first evoked potential. Since septal facilitation was blocked by a GABA antagonist, and since it reduced feed-back inhibition, they concluded that septohippocampal projections inhibit the inhibitory interneurons in the dentate gyrus, thus reducing feed-forward or tonic inhibition of granule cells seen in the single perforant path stimulus paradigm.

The results of the paired-pulse study require a closer look, because at first glance one would have to question why a septal pulse would not demonstrate disinhibition if it preceded the second pulse by zero to 100 ms, as seen in the single pulse studies. Since this study did not employ paired-pulse ratios in their analysis of the data, the size of the first spike was not accounted for. In other words, a septal pulse that precedes the first spike by more than 4 ms would have enhanced the first spike and subsequently produced feed-back inhibition of a greater magnitude, thereby reducing the size of the second spike further. On the other hand, a direct facilitation of the second spike might also be predicted, since all septal pulses preceded the second perforant path pulse by less than 100 ms. If both a disinhibitory and facilitatory process were operating, complex outcomes might follow. In

this way, a partial disinhibitory effect by the septal pulse may have been masked. At the time period where a septal pulse produced disinhibition, ranging from 4 ms before to 2 ms after the first population spike, the first spike was not enhanced and disinhibition was observed. This still does not explain why disinhibition was not observed when the septal pulse followed the first population spike by more than 2 ms. Furthermore, it is significant that the critical septal pulse time window was tied to the timing of the first spike and not the second, since the paired-pulse interstimulus intervals varied. The authors argued that this restricted time window could be accounted for by the requirement of the MSC input to arrive almost concurrently with the mossy fibre excitation on the inhibitory interneurons (feed-back circuit).

Using urethane-anaesthetized rats, Robinson and Racine (1986) reported that a septal conditioning pulse (1.2 mA) produced maximal population spike enhancement when it preceded the perforant path pulse by 20 ms (range tested was 20-1000 ms) Facilitation occurred at all interstimulus intervals including 1000 ms. In their paired-pulse paradigm, they found that neither a septal pulse delivered 6-10 ms prior to the first population spike, or immediately prior to the first spike (3-5 ms after the first pulse), had any effect on the size of the population spike produced by a second perforant path stimulus 20 or 30 ms after the first (Robinson and Racine, 1986b).

These results contradict those of Bilkey and Goddard (1985), since the septal pulse given immediately prior to the first spike would have occurred in the time window critical for the disinhibition found in their study. The Robinson and Racine results of no change in feed-back inhibition may be explained by invoking an interaction of both disinhibition and facilitatory processes. Again, paired pulse ratios were not evaluated in order to account for the size of the first spike of a pair. Robinson and Racine (1986) did however find an enhanced depression of the second pulse following septal stimulation immediately prior to the first population spike if the second pulse was given during the time window of the late inhibitory phase.

More recently, the application of twin pulses (2.5 ms apart, 0.1 ms duration) to the MSC in barbiturate-anaesthetized rats was also reported to produced an enhancement of perforant path-induced population spikes in the dentate gyrus (Mizumori et al., 1989), with no clear effect on the population EPSP, confirming the results presented above. Furthermore, the interstimulus interval of maximum enhancement proved to be 5 ms (range studied was 3-3000 ms), and the enhancement was not seen at intervals of 100 ms or greater. Putative basket cells were inhibited as a result of MSC stimulation, while 15% of the putative granule cells were excited, prompting the authors to conclude that the septohippocampal projection suppresses inhibitory interneurons thereby enhancing population spike size.

In summary, electrical stimulation of the MSC induces population spike facilitation. In all but one study, the stimulus time window required to produce the facilitation was 0-100 ms prior to perforant path stimulation, and there was evidence of disinhibition. Robinson and Racine (1986) found enhancement at septal-perforant path pulse intervals longer than 100 ms, and no evidence of disinhibition. These discrepancies may be explained by the larger stimulus intensity used by Robinson and Racine (1986) to activate the MSC which was strong enough to elicit an evoked potential in the dentate gyrus, a result which was rarely observed in the other studies. Their longer time window for enhancement (20-1000 ms) and the lack of observed changes in paired-pulse early inhibition may be accounted for by the activation of additional cells in the MSC that have a high threshold of activation, and hence were not activated in the other studies. The response of neurons to electrical stimulation has been shown to vary as a result of such cell characteristics as membrane resistance, axonal conduction velocities, and other variables (Ranck, 1975).

These four studies all utilized electrical stimulation of the MSC and therefore cannot rule out the possibility that their effects were due to stimulation of fibres of passage arising from other subcortical areas that pass through this region. Enhancement of the population spike induced in the dentate gyrus has been obtained after stimulation of the locus coeruleus

(Harley et al.,1989; Harley and Milway, 1986), raphe nucleus (Winson, 1980; Assaf and Miller, 1978), and the supramammillary nucleus [(Mizumori et al.,1989), present paper]. All of the projections arising from these areas, and targeting the hippocampus, pass through the MSC, at least in part (Swanson et al.,1987). However, 6-hydroxydopamine treatment of the dorsal noradrenergic bundle that destroyed the noradrenergic fibres of the locus coeruleus failed to block the enhancement produced by MSC stimulation (Fantie and Goddard, 1982). Furthermore, lesions of the MSC failed to block the enhancement produced by stimulation of the SUML (Mizumori et al.,1989). Therefore, enhancement of population spikes produced by electrical stimulation of the MSC may not involve fibres arising from the locus coeruleus or the SUML, but may involve fibres arising from the raphe nucleus, or other regions.

To avoid stimulation of axons of passage, glutamate was injected into the MSC during a period of low frequency stimulation to the perforant path with the concomitant recording of the evoked potentials in the dentate gyrus, in or below the granule cell layer. Results on the effects of septal activation on evoked potentials recorded in the molecular layer, dentate EEG, and on paired-pulse potentials are also presented, as well as preliminary data on unit responses.

3.2 Methods

3.2.1 Experiment 1:

Subjects were 16 adult female Sprague-Dawley rats (Charles River Canada Inc, Montreal) weighing from 225 to 325 grams at the time of recording. Each rat was anaesthetized with urethane (1.5g/kg, i.p.), placed in a stereotaxic frame with skull flat, and maintained at 36.8-38°C with a circulating water blanket.

The methods were the same as those outlined in chapter 2 except that glutamate was always pressure ejected using the glass micropipette technique. The pipette was filled with 0.5 M l-glutamic acid and aimed at the MSC (0.3 mm anterior to bregma and 0.1 mm lateral to the midline. The pipette was positioned 4.5-6.5 mm ventral to the brain surface. In a majority of animals, glutamate was delivered at more than one site.

Following a successful enhancement of the population spike after glutamate ejected in the MSC, a subset of animals were injected with scopolamine (scopolamine bromohydrate in 0.9% saline, 1 mg/kg, ip.) and glutamate was ejected again at the same site 25-45 min later.

3.2.2 Experiment 2:

Fifteen female Sprague Dawley rats were prepared for multiparameter investigation as in chapter 2, experiment 2. In addition, after completion of

the multiple parameter experiment 5 animals were subjected to paired-pulse stimulations.

3.3 Results

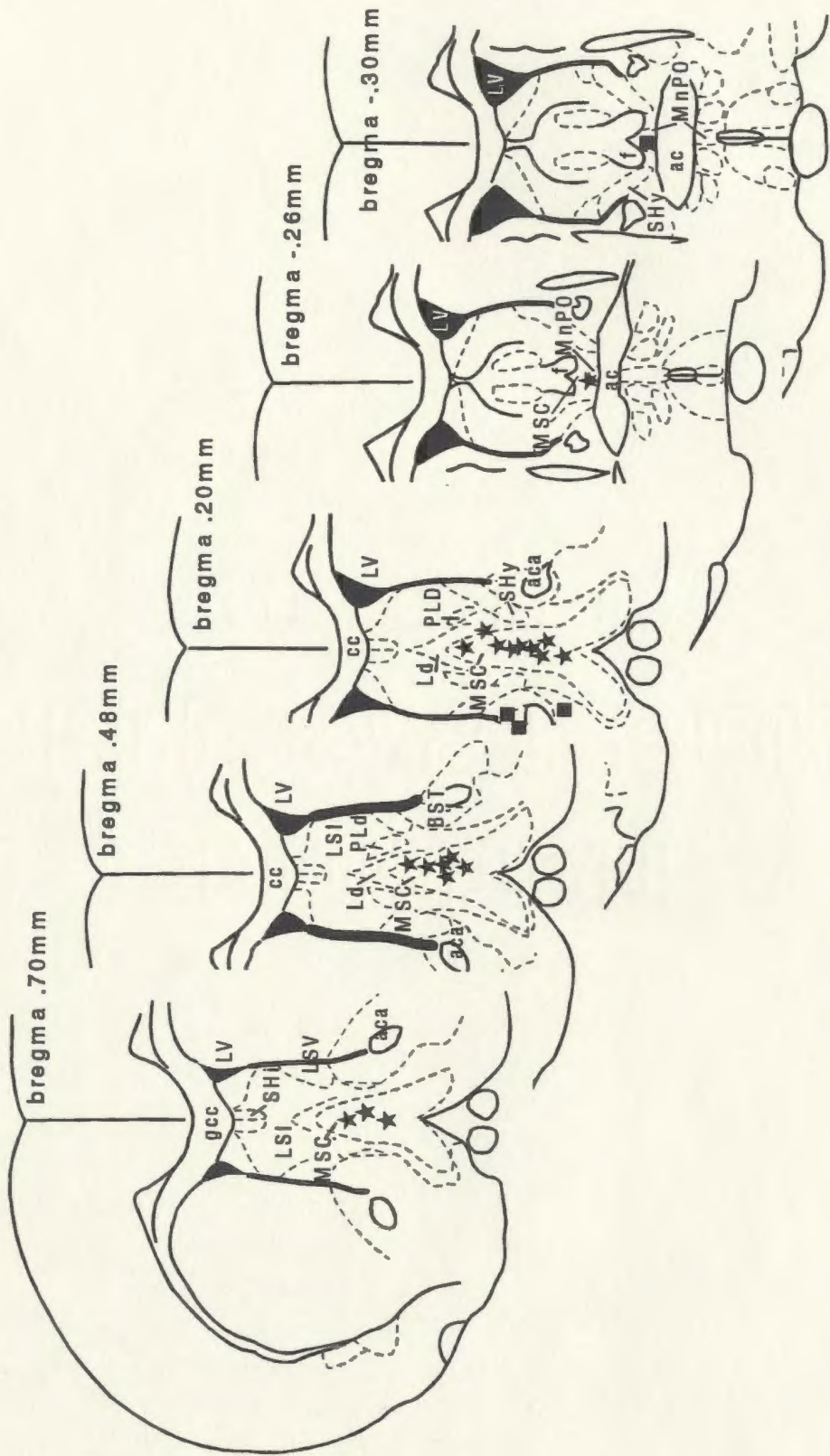
3.3.1 Experiment 1:

A total of 19 ejection sites were associated with a significant increase in the population spike. These sites are shown in Fig. 3-1 (filled stars). All were found to be in, or immediately adjacent to, the MSC. Four ejection sites did not produce a significant enhancement (filled squares), and were found well outside the complex.

The data from the 19 ejection sites were pooled after conversion to a percentage of the control mean and plotted (Fig. 3-2). Glutamate ejection in the MSC consistently produced an enhancement of the population spike reflected in all 3 measures of spike size. The population spike height, averaged over 1 min., was significantly enhanced from 113 to 169% ($\bar{X} = 132\%$) of the control mean. The period of the enhancement ranged from 1 to 49 min ($\bar{X} = 10.5$ min). The number of post-glutamate spikes until enhancement ranged from 1 to 4 ($\bar{X} = 2.32$). Three of the ejections (16%) produced a spike enhancement exceeding 20 min. in duration.

The amplitude of the EPSP slope was also significantly increased (range = 105-141% of control, $\bar{X} = 112$) for typically 1-2 min (range = 1-3 min., $\bar{X} = 1.31$ min.) following MSC activation at 16 of the 19 sites that

FIG 3-1. Ejection sites directed at the medial septum complex. Stars represent glutamate micropipette placements for sites which exhibited significant facilitation of the perforant path population spike amplitude. Filled squares represent ineffective glutamate placements. Representative sections are taken from Paxinos and Watson (1986). Abbreviations: aca; anterior commissure (anterior), ac; anterior commissure, cc; corpus callosum, BST; bed nucleus of the stria terminalis, f; fornix, gcc; genu corpus callosum, Ld; lamboid septal zone, LSI; lateral septal nucleus (intermediate), LSV; lateral septal nucleus (ventral), LV; lateral ventricle, MSC; medial septum complex, MnPO; median preoptic nucleus, PLd; paralamboid septal nucleus, SHi; septohippocampal nucleus, SHy; septohypothalamic nucleus.



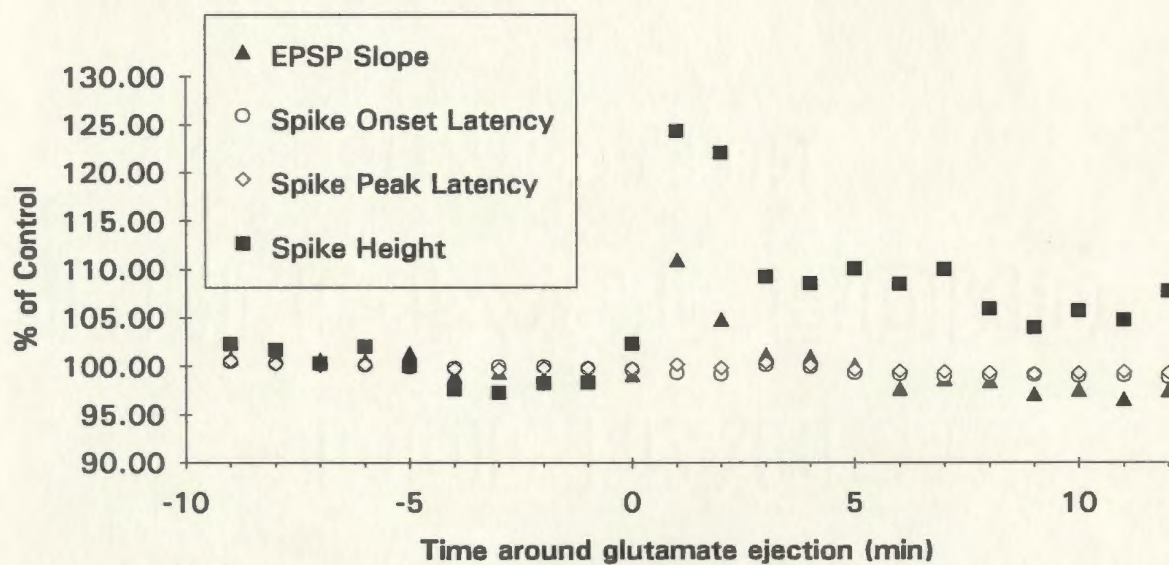


FIG. 3-2. Mean percent changes in population spike amplitude (area), EPSP slope, spike onset latency, and spike peak latency for the 19 sites exhibiting spike amplitude facilitation. Both the spike amplitude and EPSP slope were significantly enhanced. Each point represents a 1 min average.

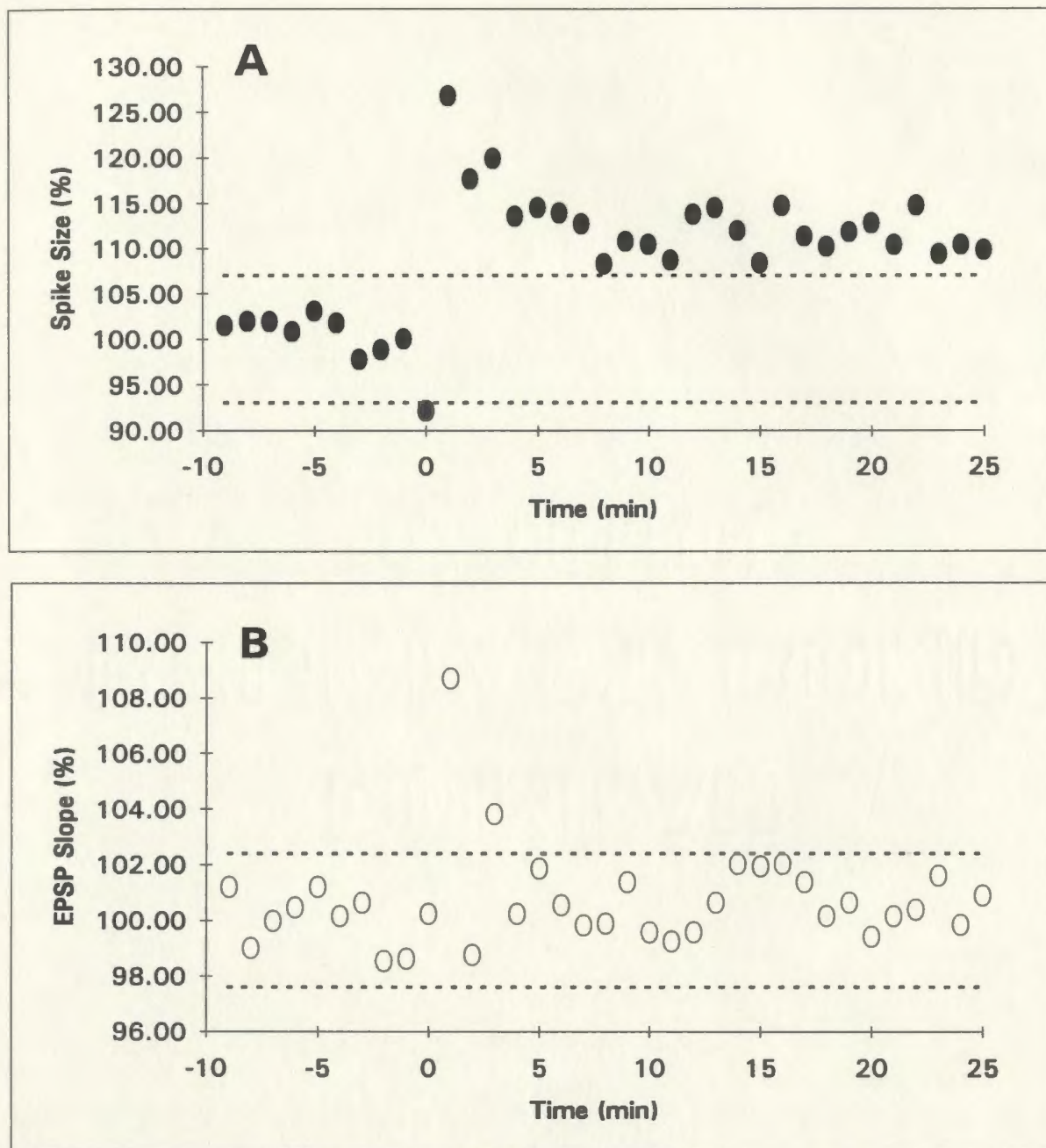


FIG. 3-3. An example of long-lasting perforant path-dentate gyrus spike facilitation by ejection of L-glutamate into the medial septum complex. EPSP slope changes were short lived. Mean values for six events (1 min. of data) were compared to 95% confidence intervals (dashed lines) based on the ten means prior to injection (time 0).

produced spike enhancement. The latency to an EPSP slope increase was shorter, on average, than the latency to produce a spike enhancement (range = 1-3 spikes, $\bar{X} = 1.5$). Fifty percent exhibited a significant increase by the first evoked potential following glutamate ejection. The EPSP slope increase was always shorter in duration than the spike amplitude increase unless the latter was for 2 min. or less. Fig. 3-3 illustrates a long-lasting (defined as 20 min. or greater) spike amplitude enhancement accompanied by a short-lasting EPSP slope amplitude enhancement.

Spike onset and spike peak latencies were marginally but significantly changed at 5 of the 19 MSC sites that produced spike enhancement. Four of 5 exhibited a reduction in onset latencies ($\bar{X} = 98\%$) and 1 exhibited an increase (103%). Of the 4 that exhibited an onset latency decrease, 3 exhibited a spike peak latency increase ($\bar{X} = 102\%$) and one exhibited a decrease (98%).

Six animals were subjected to scopolamine injections after glutamate to the MSC induced a spike enhancement. A second ejection of glutamate to the same site produced an enhancement in the population spike in 5 of the 6 animals for a reduced duration when compared to the duration of the first ejection ($\bar{X} = 18\%$ of duration as a result of the 1st ejection). To ensure that the reduced duration was not due to a normal loss of potency as a result of a second ejection, these data were compared to data where a second

glutamate ejection was made to the same site without the intervening scopolamine injection. Six animals received a second ejection at the same site. All six repeated ejections produced a second population spike enhancement, and the mean duration of the second effect when compared to the first was 57%. While this data suggests that scopolamine attenuated the duration of spike enhancement, a 2-way analysis of variance indicated no interaction between the scopolamine versus control group and first versus second glutamate ejection on the duration of the spike enhancement ($F_{1,20} = 1.86, p > .05$). More data will be needed before the absence of a significant attenuation by scopolamine can be concluded.

3.3.2 Experiment 2:

Injection sites for animals experiencing population spike enhancement were similar to those shown in figure 3-1, being in the MSC. Dentate EEG was recorded in 13 animals during population spike enhancement induced by glutamate ejection to the MSC. Of these, 3 were in theta at the time of ejection of which 2 exhibited an increase in theta frequency (see Fig. 3-4 for an example). Glutamate ejection to 7 of the remaining 10 induced theta (see fig. 3-4 for an example) and had no effect in the other 3. Therefore, in situations where theta was absent, a glutamate pulse to the MSC produced theta in 70%. The longest latency to theta induction was 12 s (range 0-12 s) and the longest duration 112 s (range 20-112 s).

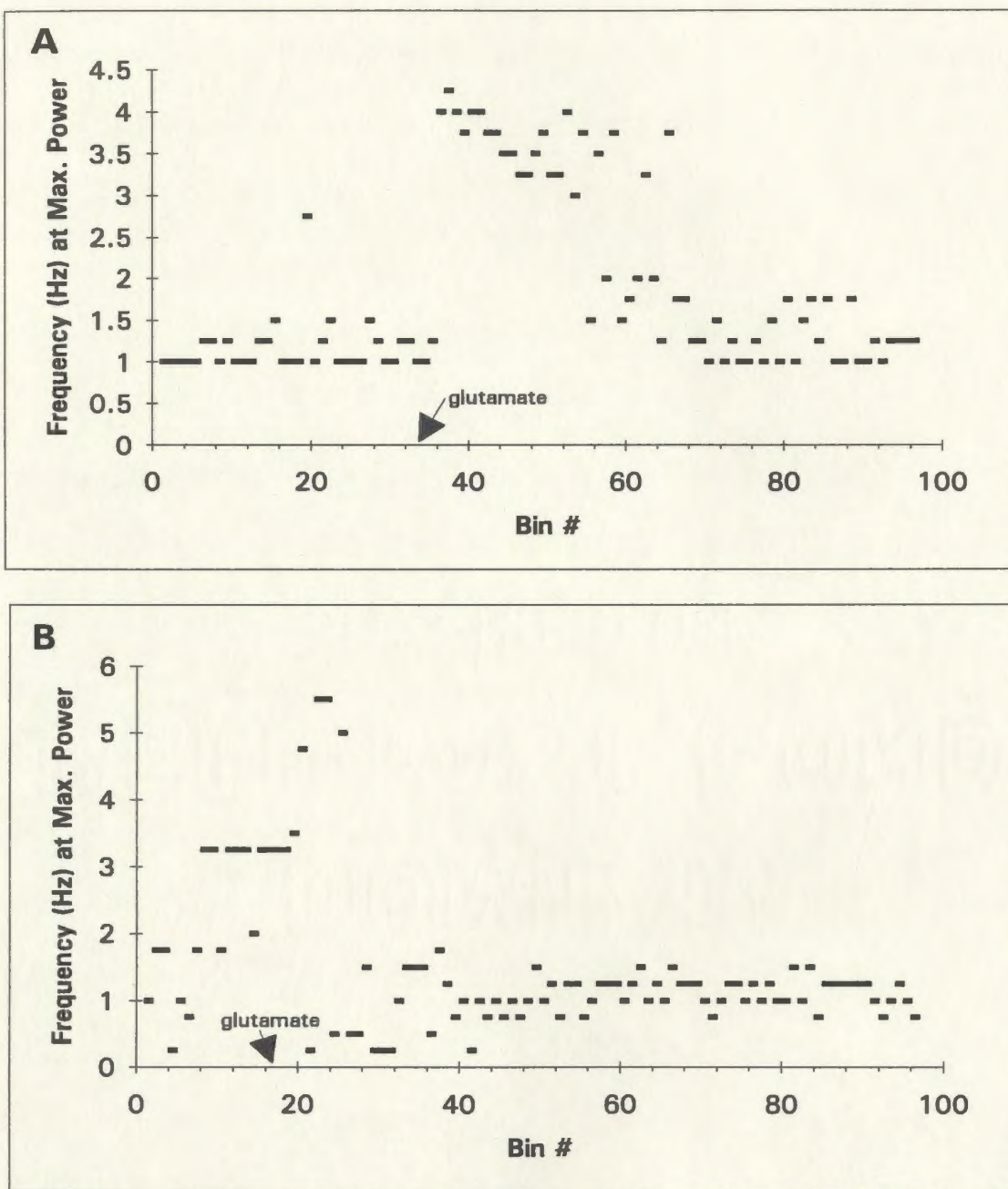


FIG. 3-4. Representative examples of theta induction (A) or frequency elevation (B) as a result of medial septum complex activation by glutamate. Four second bins were analyzed using FFT and power spectrum analysis and the frequency of maximum power for each bin plotted over time.

Twenty-five units were recorded in 10 animals during population spike enhancement induced by glutamate ejection to the MSC. The characteristics of each unit are summarized in Table 3-1. These units were characterized using the BrainWave Discovery program as illustrated in chapter 2. Thirteen of the units were inhibited, 8 excited, and 3 showed no response to glutamate ejected in the MSC. One unit was recorded during a repeat glutamate ejection to the complex and the results were similar to the first (marked repeat in table 3-1). Most of the unit effects were dramatic, as evidenced by the magnitude of the glutamate-induced effects given in column 5. A comparison of the magnitude of the unit effect and the magnitude of the population spike enhancement is included in Table 3-1. There is no correlation between the two magnitudes (i.e. the magnitude of the unit effect did not predict the magnitude of the population spike enhancement).

The time course of the unit and population spike modulation as a result of glutamate ejection are presented in Table 3-2 and illustrated in Fig. 3-5. If theta was recorded concurrently, the time course of its modulation is given in Table 3-2 as well. Most of the units responded within 5 s of the glutamate pulse, and maintained their new level of activity for an average of 125 s (range 5-600 s). Regardless of whether the units were inhibited or excited, the period of change did not collectively predict the time period of population

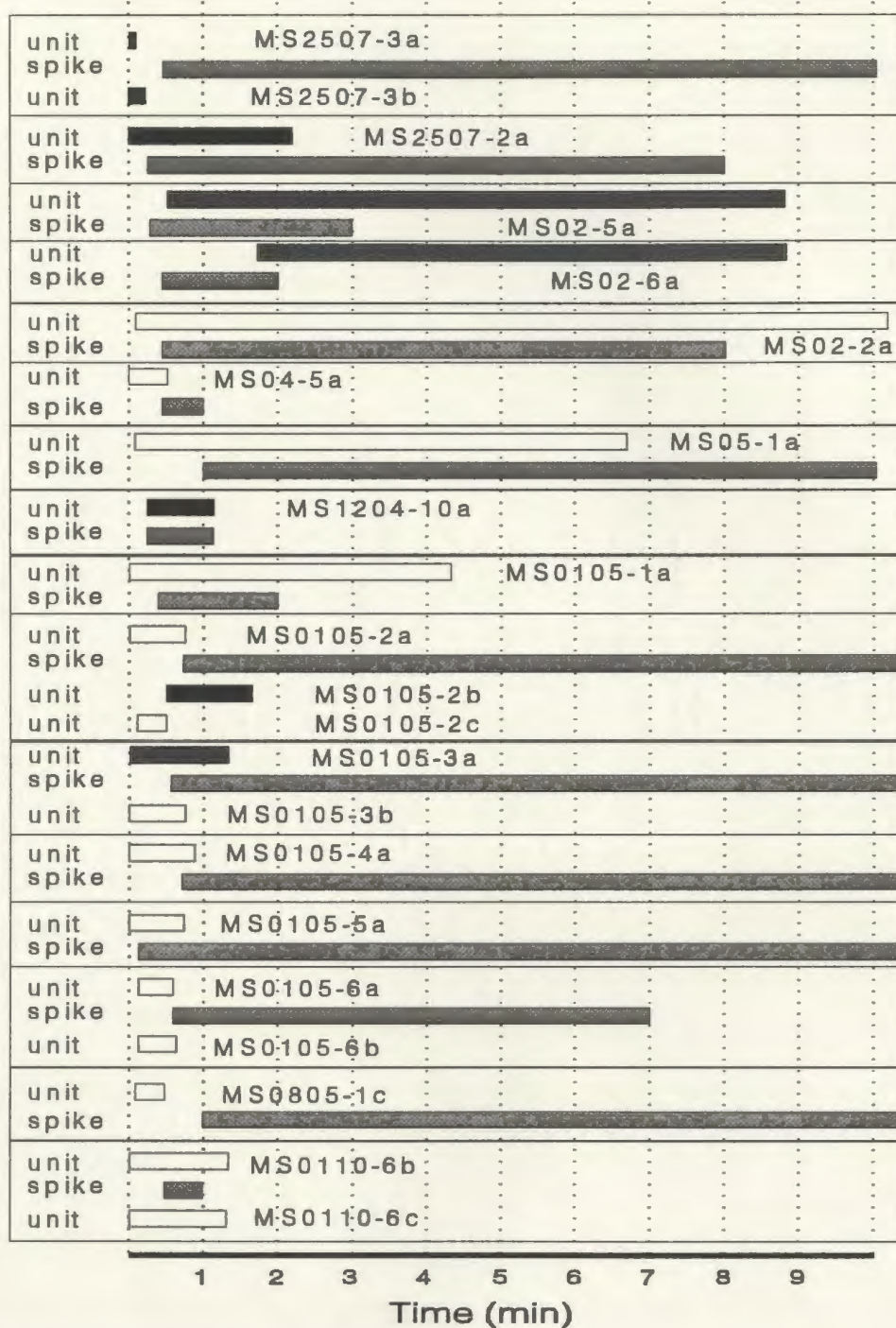


FIG. 3-5. Time course and effect of glutamate ejection to the medial septum complex on units and population spike. Each rectangle delineates the results from one glutamate ejection. Shaded bars represent time course of population spike enhancement. Black bars represent excited units and white bars the inhibited units.

spike enhancement. Of the inhibited cells, some units returned to baseline prior to spike enhancement (e.g. MS0805-1c) and others did not return until well after spike enhancement (e.g. MS02-2a). The same is true of the excited cells with some returning to baseline prior to population spike enhancement (e.g. MS2507-3b) and others not returning until well after population spike enhancement (e.g. MS02-5a). One unit (MS1204-10a) displayed an increase in firing rate that matched the time course of population spike enhancement.

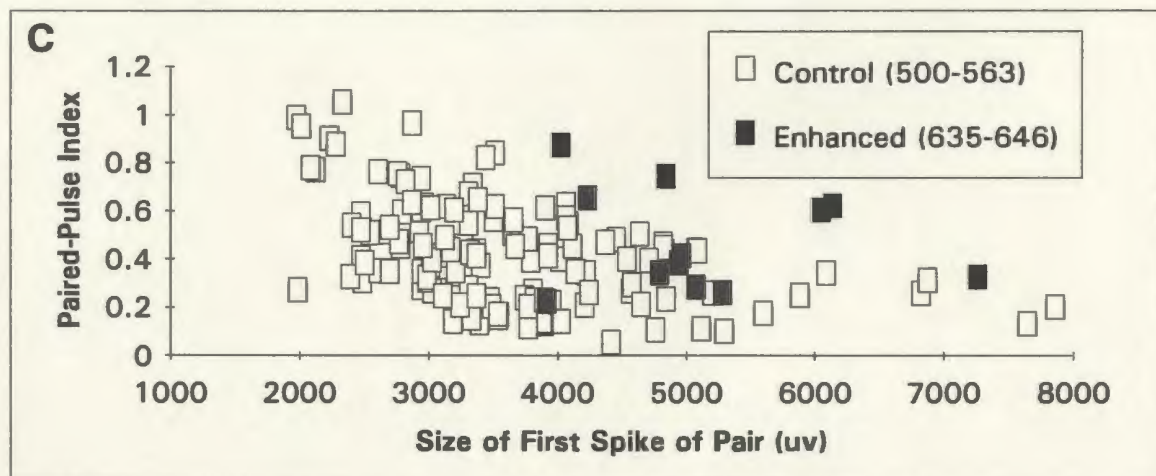
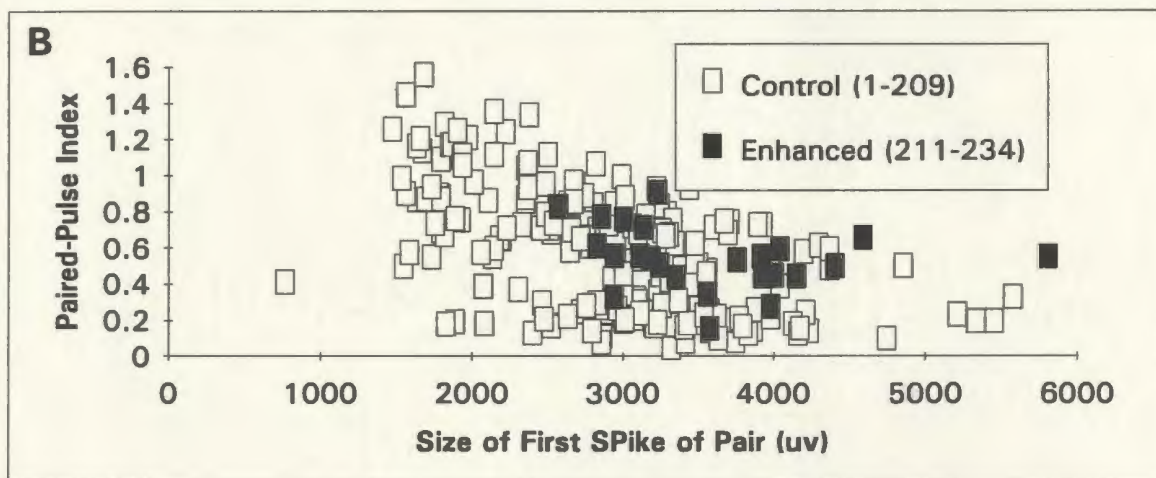
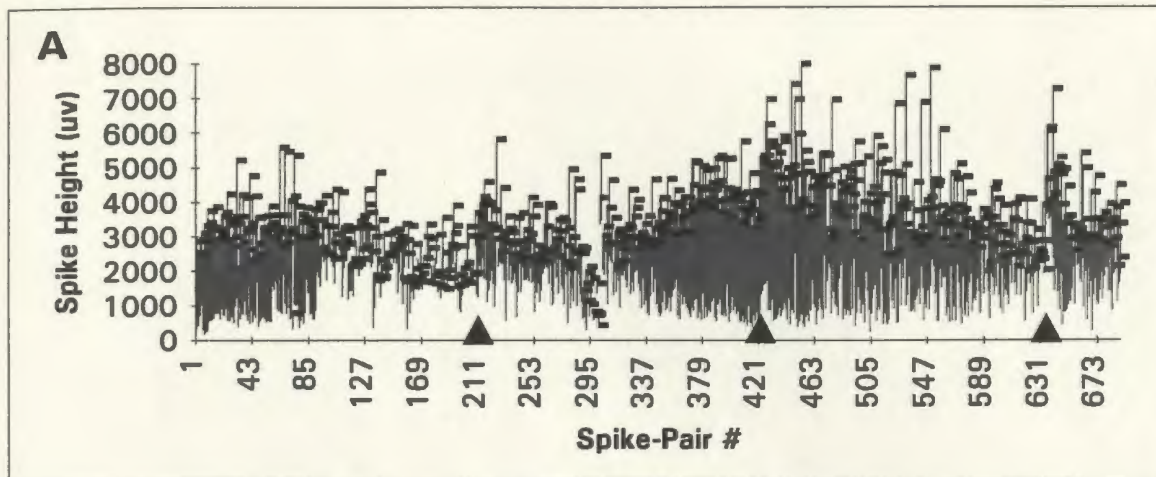
Bursting cells were scrutinized for evidence of complex bursting, where each successive spike in a burst decreases in amplitude. A burst was defined as 2 or more action potentials with interspike intervals of less than 6 ms. Complex bursts are indicative of pyramidal cells (Fox and Ranck, 1975; Fox and Ranck, 1981), although CA3 pyramidal cells may burst in a non-complex manner as well (Scharfman, 1992). Complex bursting was only observed in units MS1510-1a and MS0110-6c. Bursting cells that were excited by glutamate ejection to the MSC were scrutinized for a possible increase in bursting above that indicated by an increase in frequency. While bursting did increase, it was never above the proportional increase in frequency. There was no evidence that the number of spikes within a burst increased in number as a result of MSC activation as well.

The 5 non-bursting, low frequency (< 5 Hz) units, putatively identified as granule cells in chapter 2, were either excited (2) or inhibited (3). The rest of the cells, putative non-granule cells demonstrated mixed effects with 8 inhibited 6 excited, and 4 not responding.

The evoked potential at the molecular layer was recorded in 4 animals that exhibited population spike enhancement as a result of 8 different glutamate ejections to the MSC. Of the 8, 6 exhibited a brief ($\bar{X} = 2$ min) but significant enhancement of the EPSP slope measured at the cell layer and 7 showed a brief ($\bar{X} = 2$ min) but significant increase in the negative slope measured at the molecular layer ($\bar{X} = 106\%$). Therefore, for one ejection, the molecular layer slope was significantly increased, when the granule cell layer EPSP exhibited no significant increase.

Of the five animals subjected to paired-pulse stimuli following the multiparameter investigation, results from 3 demonstrated a significant population enhancement due to glutamate ejection to the MSC, and 2 did not, perhaps as a consequence of repeated ejections to the same site. Repeated ejections in animals given only single pulses however reliably reproduced an enhancement, although of shorter duration. This suggests a possible interaction between paired-pulse stimulation and the ability of MSC activation to induce population spike enhancement. Only one of the 'enhanced' studies showed evidence of a reduction in feed-back inhibition.

FIG. 3-6 A. Population spike size is plotted for each paired-pulse pair and a line connects the two points. Paired-pulse inhibition is evidenced by the reduced size of the second population spike. Arrows indicate the time of glutamate ejection to the medial septum complex. **B.** The ratio of the size of the second population spike to that of the first (paired-pulse index) is plotted against the size of the first. The data are taken from first glutamate ejection shown in 3-6A. **C.** The data are taken from the second glutamate ejection shown in 3-6A. Numbers in the legends of B and C represent spike pairs numbered in A.



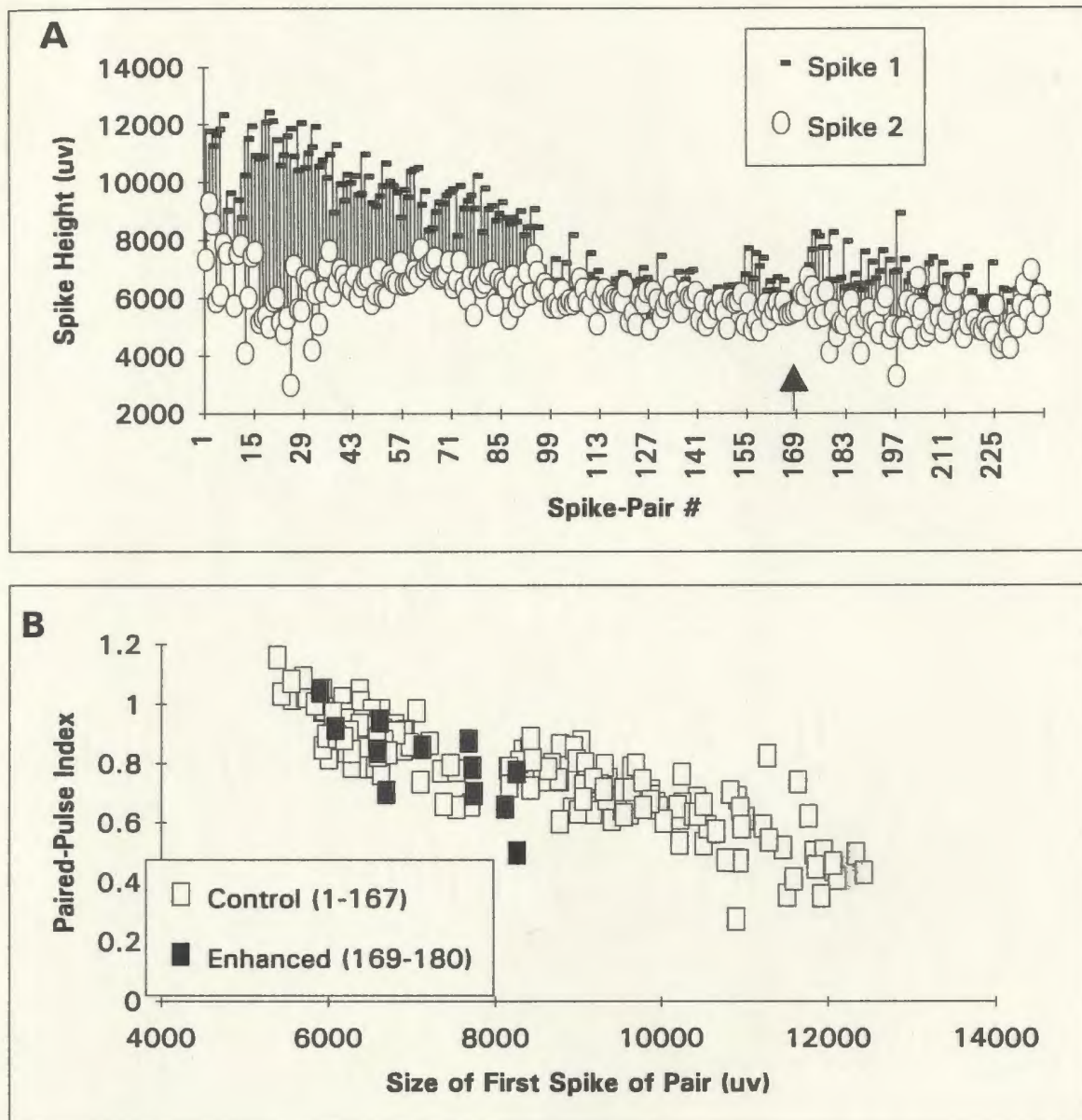


FIG. 3-7. See Fig. 3-6 for explanation of graphs. A. One glutamate ejection to the medial septal complex is indicated by the arrow in A. B. The data are taken from the glutamate ejection illustrated in 3-7A. Paired-pulse indexes for the enhanced group fall within those of the control group, indicating no reduction in feed-back inhibition.

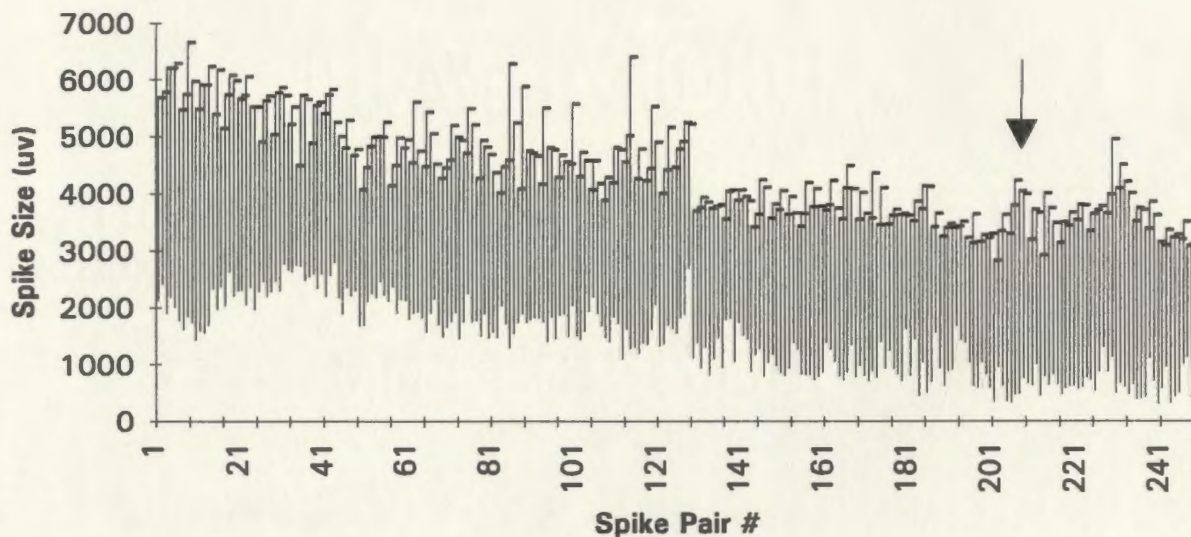


FIG. 3-8. Population spike height is plotted for each paired-pulse pair and a line connects the two points. Glutamate ejection to the medial septum complex, indicated by the arrow, did not induce an enhancement of the amplitude of the first spike and did not affect the magnitude of paired-pulse inhibition.

The results from this animal are shown in Fig. 3-6. Three MSC glutamate ejections were given during the course of the experiment as indicated by the arrows in Fig. 3-6A. In each instance a statistically significant enhancement of the first spike occurred. Paired-pulse ratio plots are shown in Fig. 3-6B and 3-6C for ejections 1 and 3 illustrated in Fig. 3-6A. The first ejection elicited an equivocally marginal reduction in feed-back inhibition with two ratios falling above those with equivalent first spike sizes (paired-pulse index: control $\bar{X} = 0.30 \pm 0.14$; enhanced $\bar{X} = 0.47 \pm 0.21$). Results from the third ejection (Fig. 3-6C) found almost half of the ratios falling above those from the control group with an equivalent range in first spike sizes (paired-pulse index: control $\bar{X} = 0.44 \pm 0.26$; enhanced $\bar{X} = 0.55 \pm .18$). Fig. 3-7 shows the results from another experiment where an enhancement of the first spike occurred, but there was no evidence of disinhibition (paired-pulse index: control $\bar{X} = 0.88 \pm 0.09$; enhanced $\bar{X} = 0.79 \pm .15$). Of the 2 paired-pulse experiments where no statistically significant enhancement of the first population spike of the pair was induced, there was no evidence of disinhibition. Fig. 3-8 shows the results from one of these experiments.

Table 3-1. Listing of each unit recorded, its spontaneous firing rate, whether it fired in bursts, whether it fired rhythmically in the theta frequency, the effects of glutamate ejection in the medial septum complex, and the magnitude of the accompanying population spike facilitation.

Cell ID	Freq. (Hz)	Burst	Rhythmic	Effect (maximum magnitude)	Spike (magnitude)
MS2507 3a	0.50	mild	no	excitation (x4)	136
MS2507 3b	14.4	no	no	excitation (x2)	136
MS2507 2a	.70	no	no	excitation (x20)	160
MS2811 3a	5.0	mild	no	none	111
MS02 5a	2.4	yes	no	excitation (x2)	164
MS02 6a	9.2	yes	no	excitation (x2)	156
MS02 7a	9.5	mild	no	none	137
MS02 2a	5.9	mild	no	inhibition (complete)	176
MS04 5a	3.1	yes	no	inhibition (x0.1)	160
MS05 1a	0.6	no	no	inhibition (complete)	185
MS1204 10a	0.6	no	no	excitation (x2)	152
MS0105 1a	8.4	no	yes	inhibition (x0.5)	129
MS0105 2a	1.5	mild	no	inhibition (x0.3)	162

Cell ID	Freq. (Hz)	Burst	Rhythmic	Effect (maximum magnitude)	Spike (magnitude)
MS0105 2b	13.5	no	yes	excitation (x1.5)	162
MS0105 2c	0.9	no	no	inhibition (complete)	162
MS0105 3a	9.8	mild	no	excitation (x2)	173
MS0105 3b	8.3	mild	yes	inhibition (x0.3)	173
MS0105 4a	8.8	yes	no	inhibition (x0.3)	123
MS0105 5a	5.5	mild	no	inhibition (x0.1)	138
MS0105 6a (repeat)	3.3	mild	no	inhibition (x0.1)	120
MS0105 6b	0.6	yes	no	inhibition (complete)	120
MS0805 1c	2.4	no	no	inhibition (x0.3)	135
MS1510 1a	2.0	yes	no	none	112
MS0110 6a	6.7	mild	no	none	143
MS0110 6b	12.2	yes	no	inhibition (x0.5)	143
MS0110 6c	3.1	yes	no	inhibition (x0.5)	143

Table 3-2. Listing of each unit recorded and its relationship in time to the population spike enhancement and EEG (if it was recorded, - indicates no recording).

Cell ID	Time of Unit effect (sec)	Time of max. effect (sec)	Spike enhance. time (sec)	Time of max. effect (sec)	Time of EEG effect (sec)
MS2507 3a	0-5	0-5	25-600	180-240	-
MS2507 3b	0-15	0-5	25-600	180-240	-
MS2507 2a	0-130	0-15	15-480	60-120	-
MS2811 3a	-	-	15(s)- 58(min)	60-120	no effect
MS02 5a	30- 500+	55-60	15-180	15-60	5-85
MS02 6a	105- 500+	170-175	25-120	25-60	no effect
MS02 7a	-	-	25-120	60-120	-
MS02 2a	5-600+	5-450	25-480	120-180	-
MS04 5a	0-30	10-25	25-60	25-60	10-35
MS05 1a	5-400	5-60	60-600	60-120	no effect
MS1204 10a	15-70	15-20	15-70	15-60	-
MS0105 1a	0-260+	0-50	25-120	60-120	-
MS0105 2a	0-40	0-40	45-1560	60-120	-

Cell ID	Time of Unit effect (sec)	Time of max. effect (sec)	Spike enhance. time (sec)	Time of max. effect (sec)	Time of EEG effect (sec)
MS0105 2b	30-100	40-85	45-1560	60-120	-
MS0105 2c	5-25	5-10	45-1560	60-120	-
MS0105 3a	0-80	0-10	35-2940	240-300	-
MS0105 3b	0-45	0-15	35-2940	240-300	-
MS0105 4a	0-50	10-15	45-720	240-300	-
MS0105 5a	0-45	20-30	5-2280	60-120	-
MS0105 6a (repeat)	5-35	20-25	35-420	60-120	-
MS0105 6b	5-40	5-40	35-420	60-120	-
MS0805 1c	5-25	10-25	60-1980	180-240	-
MS1510 1a	-	-	25-180	60-120	no effect
MS0110 6a	-	-	35-60	35-60	0-25
MS0110 6b	0-80	5-20	35-60	35-60	0-25
MS0110 6c	0-80	0-15	35-60	35-60	0-25

3.4 Conclusion

Theoretical mechanisms by which activation of the MSC may enhance the physiology of the dentate gyrus will be explored in chapter 4. The following represents a summary of the experimental findings.

Glutamate ejection in or immediately adjacent to the MSC produced a significant increase in amplitude of the perforant path-evoked population spike in the dentate gyrus. A similar finding was reported using electrical stimulation of the MSC (Fantie and Goddard, 1982; Bilkey and Goddard, 1985; Robinson and Racine, 1986b; Mizumori et al., 1989). A brief (2 min. or less) enhancement of the population EPSP slope in over 80% of the experiments associated with a population spike enhancement indicates that MSC activation increases the synaptic drive at the perforant path synapse. Recording from the molecular layer confirmed the existence of an EPSP increase indicated by the increase in EPSP slope measured at the granule cell layer. The fact that the increase in synaptic drive was relatively short lived, compared to population spike enhancement, indicates that a growth in synaptic drive may play a role in the induction of this heterosynaptic short-lasting (2-20 min) or long-lasting (>20 min.) potentiation, but does not underlie its maintenance.

Electrical stimulation of the MSC produces an increased population spike without an increase in the amplitude of the EPSP (Fantie and Goddard, 1982;

Bilkey and Goddard, 1985; Robinson and Racine, 1986b; Mizumori et al., 1989). The discrepancy between this study and the electrical stimulation studies indicates that glutamate activation might stimulate the neural elements of the MSC differently, perhaps because of its avoidance of fibres of passage, through an unknown preference for a chemically distinct subset of neurons, or by inducing a sustained burst pattern. These possibilities will be explored further in chapter 4.

Scopolamine (1 mg/kg, ip) failed to block MSC activation-induced population spike enhancement and did not statistically attenuate its duration, although a larger sample size and higher doses will be necessary to rule out the participation of acetylcholine. High doses of scopolamine (4 to 40 mg/kg, iv) were needed to abolish the medial septum stimulation produced enhancement of population spikes evoked in area CA1 by commissural path stimulation (Krnjevic and Ropert, 1982). However, scopolamine, at the dose used here, has been observed to suppress LTP in the hippocampus (Ito et al., 1988) and impair learning on a variety of tasks (Berz et al., 1992; Bianchi and Panerai, 1993; Bresnahan et al., 1992; File et al., 1990; Fishkin et al., 1993; Lukaszewska, 1993; Matsuoka et al., 1992; McNamara and Skelton, 1992; Riekkinen et al., 1991). Fantie and Goddard (1982) found that cholinergic antagonists failed to block the population spike enhancement produced by electrical stimulation of the MSC.

The duration of neurotransmitter release from the MSC afferents as a result of glutamate stimulation cannot be ascertained. It is unlikely, however, that the duration of neurotransmitter release due to glutamate-induced MSC cell activation matches the duration of population spike facilitation, as discussed in chapter 2. Concurrent monitoring of MSC cell activity would be of interest.

Glutamate activation differs from electrical stimulation of the MSC, as it does with electrical stimulation of the SUML, in the time course of their effects on evoked potentials in the dentate gyrus. Electrical stimulation only produces an enhancement if given within 100 to 1000 ms prior to the perforant path stimulus, optimally 5 ms prior to the stimulus (Fantie and Goddard, 1982; Robinson and Racine, 1986b; Mizumori et al., 1989). Units recorded in the dentate gyrus during MSC electrical stimulation were affected for typically 10-15 ms (Mizumori et al., 1989). Both units and evoked potentials were modulated for minutes in this experiment, as a result of a brief pulse of glutamate to the MSC. Furthermore, a 30 s delay between the glutamate pulse and the increase in spike amplitude was common in the present experiments.

Glutamatergic stimulation of the MSC inhibited 52% and excited 32% of the cells recorded in the dentate gyrus for an average of 125s. Most responded immediately, prior to the spike amplitude enhancement. As in the

SUML study, the time course of unit modulation rarely correlated with the time course of the spike enhancement. While this implies that changes in the spontaneous activity of the units recorded do not reflect the critical events that underlie the enhanced population spike, only a few cells were sampled from a large population. It is possible that the unit population response would reflect a mixture of unit responses in time, and hence their combined average may directly underlie the changes in the population spike amplitude.

Electrical stimulation of the MSC prior to perforant path stimulation resulted in a decrease in putative inhibitory local-circuit neuron activity in the dentate gyrus and an increase in putative granule cell activity (Mizumori et al., 1989). This effect suggests a disinhibition mechanism mediates the population spike facilitation produced by MSC stimulation (Mizumori et al., 1989). Stimulation of the MSC during a narrow time window associated with the first population spike elicited by the first pulse in a paired-pulse stimulation disinhibited the second population spike (Bilkey and Goddard, 1985), supporting the disinhibition theory. Units recorded in this experiment were not identified by the rigorous response properties employed by Mizumori et al. (1989). As suggested in chapter 2, we may assume that granule cells, in relation to non-granule cells found in the dentate gyrus, fire spontaneously at low rates (Mizumori et al., 1989; Scharfman, 1992), and are characterized by an absence of burst firing (Misgeld et al., 1992a; Scharfman, 1992). Of

the 5 non-bursting cells that fired at a frequency of less than 5 Hz, 3 were inhibited and 2 were excited by MSC activation, suggesting mixed effects on putative granule cells. A larger number of units sampled, coupled with the rigorous response properties employed by Mizumori et. al. (1989), would be more informative.

The mechanism by which the MSC influences hippocampal throughput was explored in this study using paired-pulse stimulation with interpulse intervals of 20-30 ms. Evidence for a disinhibition mechanism associated with MSC activation was variable, and may be indicative of two prominent neurotransmitter systems (acetylcholine and GABA) being activated in different proportions with each glutamate ejection.

Glutamatergic activation of the MSC induced a brief theta rhythm recorded at the molecular layer of the dentate gyrus in 70% of the experiments associated with a concomitant enhancement of the population spike. As pointed out in chapter 2, enhancement of the perforant path-dentate evoked potential has been correlated with the induction of theta through sensory stimulation (Herreras et al., 1988) and the theta rhythm may play a modulating role in the induction of LTP in the dentate gyrus (Pavlidis et al., 1988a; Ford et al., 1989). The production of theta is not necessary for the enhancement of the population spike here, given that the theta rhythm was not induced in 30% of the experiments. When induced, the theta rhythm

lasted for a brief period in time (20-112 s) relative to population spike enhancement, therefore if it did play a role in spike enhancement, it was restricted to the induction of the event alone, and not the maintenance of the spike enhancement.

It is well established that the MSC plays a critical role in the generation of hippocampal theta, specifically the type 2 theta that is left intact in urethane anaesthetized animals (Bland, 1986; Smythe et al.,1992; Vertes, 1986). Electrical stimulation of the MSC induces theta (Bland, 1986) and electrolytic lesions of the MSC disrupts theta activity in the hippocampus (Sainsbury and Bland, 1981). More importantly, in confirmation that type 2 theta is controlled by the MSC and not axons of passage, Type 2 theta is abolished by the cholinergic antagonist, atropine sulfate (Kramis et al.,1975). The induction of hippocampal theta by glutamatergic activation of the MSC reported here confirms the ability of the MSC, and not axons of passage, to generate type 2 theta production. More recently it has been proposed that the activities of both the GABAergic and cholinergic systems of the MSC are required to generate hippocampal theta (Smythe et al.,1992). Direct microinfusions of the cholinergic agonist, carbachol, into the hippocampus can induce theta (Malisch and Ott, 1982; Rowntree and Bland, 1986) but inactivation of the MSC by local infusion of procaine hydrochloride blocks carbachol-induced theta (Smythe et al.,1992).

While the MSC projects directly to neurons within the dentate gyrus, one cannot rule out the possibility that the modulatory effects on hippocampal physiology produced here were mediated through a multisynaptic pathway or through other indirect means. Stimulation of the septal complex by glutamate has been shown to increase the blood flow in the hippocampus (Cao et al., 1989). The response started about 1 min after glutamate ejection, peaked at about 3-5 min, and gradually returned within 30-60 min. The increase in blood flow induced by MSC activation was completely abolished by the nicotinic receptor blocker, mecamylamine. The concurrent monitoring of local blood flow in the hippocampus, and a test of the ability of a nicotinic receptor blocker to block MSC activation effects on the dentate gyrus population spike, are indicated for future experiments.

CHAPTER 4: DISCUSSION

These experiments were initially concerned with whether or not cell-selective glutamate activation would give similar results to those seen previously with electrical stimulation preceding the dentate gyrus-perforant path evoked potential. Further experiments attempted to address the relationship between different indices of electrophysiological or functional change following such activation, i.e. possible contemporaneous effects on EEG responses, cellular activity and evoked potentials. In addition, experiments were initiated to probe suggested mechanisms by looking at alterations in local circuit inhibition through an assessment of paired-pulse inhibition change following glutamate ejection.

The results of this research demonstrate that glutamate ejection in the SUML or MSC (and at medial thalamic sites) can significantly influence hippocampal physiology in the urethane-anaesthetized rat. Short- and long-lasting potentiation of the population spike were the most consistent results. A relatively brief increase in the population EPSP was seen after MSC (and medial thalamic) stimulation but not after SUML stimulation. Other putative modulatory systems enhance the population spike generated in the dentate gyrus as a result of perforant path stimulation.

Enhancement of the population spike has been obtained after stimulation of the locus coeruleus (Harley et al., 1989; Harley and Milway, 1986), the raphe nucleus (Winson, 1980; Assaf and Miller, 1978) and the substantia nigra (Shin et al., 1987). Glutamatergic activation of the locus coeruleus can produce a similar long-lasting potentiation of the population spike (Harley and Milway, 1986) as observed with MSC and SUML glutamatergic activation here.

The population spike enhancement produced by electrical stimulation of the midbrain raphe nucleus is not affected by prior depletion of brain serotonin (Srebro et al., 1982), the raphe system's primary neurotransmitter. The population spike enhancement produced by locus coeruleus electrical stimulation is not blocked by a noradrenergic beta receptor blocker (Harley et al., 1989), which has been shown to prevent population spike enhancements produced by glutamatergic activation of the locus coeruleus (Harley and Milway, 1986) and by norepinephrine applied to the slice (Lacaille and Harley, 1985). These two examples suggest electrical stimulation may not be particularly selective to the modulatory system targeted, and emphasize the need to evaluate the effects of a more cell-selective mode of activation as stated in the introduction.

There are clear differences between the results produced by electrical activation and glutamate activation of these structures. Electrical activation

of the MSC and SUML must be given within a narrow time window prior to the perforant path-induced population spike, and will only enhance the population spike associated with this time window (Fantie and Goddard, 1982; Mizumori et al., 1989; Robinson and Racine, 1986b). Glutamate activation of these structures was not temporally paired with perforant-path stimulation, since it was pressure-ejected randomly in time between the perforant path stimuli given every 10 s, and produced short and long-lasting enhancement of the population spike that often took 30 s to develop. Electrical stimulation of the MSC does not produce an enhancement of the field EPSP (Fantie and Goddard, 1982; Mizumori et al., 1989), whereas glutamate activation of the MSC consistently produced a brief (1-2 min) enhancement. Electrical stimulation of the MSC and SUML produces changes in the unit activity of dentate gyrus cells that can only be measured in ms (Mizumori et al., 1989; Segal, 1979), whereas the changes in spontaneous unit activity produced by glutamate activation in this study often lasted minutes. Some of these differences may be a result of the possibly nonselective nature of electrical stimulation mentioned above.

Pharmacological investigations of the specificity of these effects would be impossible, in the case of the SUML studies, given a primary neurotransmitter has not been identified to date. Pharmacological study of the MSC is problematic since at least 2 primary neurotransmitters have been

identified, acetylcholine and GABA, the latter also occurring in abundance intrinsically in the hippocampus. Hence, any attempt to block the GABAergic septohippocampal projection pharmacologically in the hippocampus would also severely disrupt the local inhibitory network. The ability of MSC electrical stimulation to enhance the dentate population spikes is resistant to the effects of both nicotinic and muscarinic cholinergic antagonists (Fantie and Goddard, 1982), suggesting that acetylcholine does not play a role in this facilitation. Preliminary results given here show that the enhancement of the population spike by glutamate activation of the MSC was not blocked by a relatively low dose of the muscarinic antagonist scopolamine.

The temporal relationship between population spike potentiation produced by glutamate activation of these structures and the other parameters measured is puzzling, and cannot be explained by simple network properties. When a theta rhythm is induced it is usually immediate and short-lived when compared to the population spike enhancement. The lack of temporal correspondence between the induction of a theta rhythm and the enhancement of the population spike suggests that these two manifestations arising from SUML or MSC activation reflect independent events. This interpretation is supported by the fact that a spike enhancement can occur in the absence of theta induction. The brief induction of a theta rhythm may be indicative of the length of time that the respective synaptic components

are active, and indicate that the spike enhancement outlasts synaptic activity arising from the SUML or MSC. The spontaneous unit activity, not just the evoked responses, were affected by SUML and MSC activation. Spontaneous unit activity is immediately affected by glutamate activation of these structures despite the delayed enhancement of the population spike. The duration of individual unit rate changes does not covary with population spike enhancement but may be just as long lasting. A closer look at unit changes will be necessary before possible changes in subsets of the local network can be elucidated. The rigorous response properties evaluated by Mizumori et. al. (1989) would help to differentiate between granule cells and nongranule cells.

Another puzzling finding is the effect glutamate activation of these structures had on paired-pulse inhibition. MSC activation could produce evidence of disinhibition, but this finding was not consistent. In other words, MSC activation-induced population spike enhancement may, or may not, be accompanied by evidence of a reduction in feed-back inhibition. In the SUML study, the reproduction of the population spike enhancement following a repeat ejection of glutamate to the SUML was difficult to produce when paired-pulses were given, and yet evidence for a reduction of feed-back inhibition was demonstrated despite this lack of a population spike enhancement.

The transient potentiation produced by electrical stimulation of the SUML (Mizumori et al., 1989) and the MSC (Fantie and Goddard, 1982; Mizumori et al., 1989; Robinson and Racine, 1986b) coupled with the short interpulse interval of 10-15 ms in the SUML study (Mizumori et al., 1989) and 5 ms in the MSC studies (Fantie and Goddard, 1982; Mizumori et al., 1989) required for maximal population spike facilitation, suggests an immediate ionotropic mechanism initiated by the release of each structure's respective neurotransmitter(s). Since the primary neurotransmitter of the SUML neurons has not been identified, speculation as to the possible ionotropic events underlying the SUML-activation-induced population spike enhancement is impossible.

Activation of the MSC would release acetylcholine and GABA at their respective synapses in the dentate gyrus. As reviewed in the introduction of chapter 3, cholinergic innervation of the dentate gyrus involves both symmetric and asymmetric synapses onto both local-circuit neurons and granule cells. Therefore activation of this system is likely to produce a complex mixture of events. The physiological mechanisms of acetylcholine in the hippocampus have recently been reviewed (Halliwell, 1990). In the rat hippocampus, acetylcholine and cholinergic agonists have produced various effects such as slow depolarization and a reduction of the slow afterhyperpolarization [e.g. (Misgeld and Muller, 1988)], effects that could

lead to increased cell excitability. However, Fantie and Goddard (1982) demonstrated that population spike enhancement induced by electrical stimulation of the MSC was not blocked by various muscarinic and nicotinic receptor antagonists. Their results suggest that population spike enhancement induced by electrical stimulation of the MSC is mediated by the GABAergic component of the septohippocampal projection.

A reduction in feed-back inhibition (Bilkey and Goddard, 1985), the blockade of MSC effects by the GABA antagonist picrotoxin (Fantie and Goddard, 1982), and the inhibition of putative local-circuit neurons (Mizumori et al., 1989), together suggest that electrical stimulation of the MSC enhances population spike amplitude by reducing the feed-forward inhibition elicited by perforant path stimulation. The MSC-GABA projection to the dentate gyrus preferentially innervates non-granule cells, many of which are immunoreactive for GABA (Freund and Antal, 1988), providing an anatomical basis for this disinhibition theory. The failure to reduce paired-pulse inhibition by MSC electrical stimulation in the study by Robinson and Racine (1986), however, needs to be reconciled. Since electrical stimulation of the SUML also inhibits putative local-circuit neurons, Mizumori et. al. (1989) hypothesize a similar disinhibition mechanism for SUML-induced population spike enhancement.

The long-lasting enhancement of the population spike produced by glutamate activation of the SUML and MSC, in contrast to the transient enhancement produced by electrical stimulation, could be most easily explained by a long-lasting activation of the SUML or MSC neurons that correlates with the length of population spike enhancement. This scenario is unlikely, although the recording from neurons near the glutamate ejection site should be undertaken in order to determine the length of activation. Glutamate is rapidly taken up by glutamatergic neurons and astrocytes in the CNS (Schousboe et al., 1990). In one study, where cells were recorded at the ejection site in the rat locus coeruleus, glutamate ejections of similar volume and concentrations to those used here, elicited a 250-450 ms burst of cell activity, followed by a depression of unit activity lasting 4.6 min on average (Harley and Sara, 1992). Ejections of similar volume and concentration into the nucleus retroambigualis of the cat and rabbit produced an increase in the firing rate of neurons within 0.2 mm of the ejection site, lasting for an average of 12 s, followed by a reduction in activity lasting 11.5 min on average (Lipski et al., 1988). The results from these two studies suggest that glutamate activation of neurons of the SUML and MSC should be short lived in comparison to the duration of population spike enhancement found in the dentate gyrus. The short burst activity generated by glutamatergic activation of the locus coeruleus elicited an enhancement of the evoked population

spike recorded in the dentate gyrus after stimulation of the perforant path that lasted minutes, and occasionally hours (Harley and Sara, 1992). Intravenous injections of clonidine produced silence or a depression of locus coeruleus cell firing lasting 3-5 min with no accompanying change in the dentate population spike. These results suggest that the glutamatergic burst of cell activity was responsible for the population spike enhancement, rather than the depression of unit activity that followed. It is therefore likely that activation of the two systems studied here produce an increase in the response of granule cells to perforant path stimulation that lasts well beyond the duration of probable glutamate-induced activation of the input cells.

One mechanism, that would distinguish electrical stimulation from glutamate activation, is the finding that peptide cotransmitters and "classical" transmitters found in the same neurons are released differentially based on the pattern of the induced action potentials (Lundberg et al., 1986). It is possible that glutamate activation of the MSC or SUML releases a greater amount of peptide cotransmitters, which have been found to produce slow postsynaptic potentials that can last as long as 30 min [for a review see (Libet, 1986)]. The existence of peptide neurotransmitters in SUML and MSC neurons have been demonstrated, as reviewed in the introduction to chapters 2 and 3.

The long-lasting potentiation produced here share some characteristics with LTP, briefly reviewed in chapter 1. There is a delay between the initiating event and its manifestation in both LTP and the potentiation seen here. LTP in the dentate gyrus does not start to manifest itself until a few seconds after the induction event, and thereafter grows approximately linearly for about 30 s (Hanse and Gustafsson, 1992a). Furthermore, a weak tetanization intensity produces a potentiation that falls short of long-term (defined by most researchers as lasting > 60 min), and may decay completely within 5-30 min (Hanse and Gustafsson, 1992a), potentiation durations that fall within the duration of long-lasting effects produced here. Cholinergic agonists in the slice (Burgard and Sarvey, 1990) and electrical stimulation of the MSC *in vivo* (Robinson, 1986a; Robinson and Racine, 1986b) enhance LTP generated in the dentate gyrus by perforant path tetanization.

The well characterized role that NMDA receptors play in synaptic plasticity make them tempting targets when trying to elucidate possible mechanisms of long-lasting enhancements seen here. The long-lasting effects of norepinephrine on perforant path-dentate gyrus evoked population spikes is blocked by NMDA antagonists in the hippocampal slice (Burgard et al., 1989; Stanton et al., 1989). A possible link between the amplification of NMDA currents and SUML activation was seen in the paired-pulse data in chapter

2. The size of the second spike in a pair is a reflection of the lingering influence from the generation of the first spike. In review, short perforant path stimulus intervals (approximately 10-40 ms) produce an early period of inhibition (Andersen et al., 1971a), where both the population EPSP and the population spike of the second field potential are depressed (Adamec et al., 1981; Sundstrom and Mellanby, 1990). The second phase is characterized by a facilitation of the second spike, and occurs with perforant path stimulus intervals of approximately 30 to 200 ms (Racine and Milgram, 1983). The results shown in Fig. 2-12 clearly demonstrate an overlap between the feed-back, early inhibition phase, and the facilitation phase. SUML activation changed the response to the second stimulus from a reduction of the size of the second spike to an increase. If feed-back inhibition did not overlap with the facilitatory process, and SUML activation simply abolished feed-back inhibition, then one would expect the second population spike amplitude to be equal to the first. It is possible, therefore, that any reduction in the size of the second population spike is due to either a reduction in feed-back inhibition or an increase in facilitation, or both. The net effect would reflect the sum of these competing events. In fact it has been suggested that the early and late phases of paired-pulse inhibition represent one prolonged GABA-dependent process that is superimposed on an independent facilitatory process (Steffensen and Henriksen, 1991).

It has recently been demonstrated that the NMDA glutamate receptor plays a dominant role in the paired-pulse facilitatory phase. Paired-pulse facilitation of the population spike is attenuated or blocked by the administration of NMDA receptor-ion channel blockers (Joy and Albertson, 1993). One possible interpretation of the SUML results is that SUML activation amplified the facilitatory process mediated by NMDA receptors, as seen in the paired-pulse experiments, and that the short- and long-lasting enhancements of the population spike demonstrated here are mediated through an NMDA-associated mechanism. The results from the MSC paired-pulse experiments were too variable to suggest a similar mechanism, however, acetylcholine has been found to enhance an NMDA-evoked calcium rise in pyramidal neurons of the hippocampus (Segal, 1992).

The alternate explanation for the SUML paired-pulse results is that SUML activation produces a disinhibition of granule cells (Mizumori et al., 1989). Since depolarization of the postsynaptic membrane is critical to the induction of LTP, bringing the membrane potential to a level where magnesium ions no longer block the NMDA receptor channels, it follows that interneuron-mediated inhibition, which limits postsynaptic depolarization during a stimulus train, may determine the threshold at which LTP can be induced. When inhibition is blocked with picrotoxin, a GABA-A receptor antagonist, depolarization during a stimulus train is enhanced, facilitating LTP induction

(Wigstrom and Gustafsson, 1983). Disinhibition produced by SUML activation may increase calcium flow through NMDA channels activated by the low-frequency stimulation of the perforant path. Further research testing the involvement of NMDA receptors in the heterosynaptic potentiation observed here needs to be done. Would NMDA receptor or channel blockers obstruct the population spike potentiation produced by MSC or SUML activation, and would they block the apparent reduction in feed-back inhibition observed after SUML activation?

The heterosynaptic short- and long-lasting potentiation demonstrated here may simply reflect a concomitant inhibition of dentate local circuit neurons, which inhibit granule cells. This would produce a disinhibition of granule cells and subsequently increase their response to perforant path stimulation. The inhibition of granule cells by local circuit neurons can occur in a tonic fashion, as a result of spontaneous activity, or may occur as a result of perforant path stimulation. The evoked response could occur through a perforant path-local circuit neuron synapse (feed-forward route) or through a granule cell mossy fibre-local circuit neuron synapse (feed-back route). The paired-pulse paradigm, using short interpulse intervals of about 10-30 ms, only measures the inhibition due to the feed-back route, since both tonic and feed-forward inhibition should be present during both evoked potentials. It is often assumed that a reduction in feed-back inhibition measured by a

paired-pulse also reflects a reduction in feed-forward and tonic inhibition. The overview of the local circuitry given in chapter 1 supports the view that the same neurons are responsible for both feed-forward and feed-back inhibition since most of these neurons send dendrites into the molecular layer and receive mossy fibre innervation. Hence, a general inhibition of these cells at the time of perforant path stimulation should reduce both feed-back and feed-forward inhibition.

Results from this study and others suggest that feed-forward and feed-back inhibition may work in a more independent fashion. In the hippocampal slice, two types of IPSPs are found in granule cells, fast Cl-dependent IPSPs involving the GABA-A receptor, and a slow K-dependent IPSPs likely involving the GABA-B receptor (Misgeld et al., 1992b). These potentials can occur independently of each other, suggesting that Cl- and K-dependent IPSPs are generated by different sets of neurons (Muller and Misgeld, 1990; Misgeld et al., 1992b). It has been proposed that different GABAergic local circuit neurons mediate feed-forward and feed-back inhibition to varying degrees (Miettinen and Freund, 1992a) and that subcortical inputs to the dentate gyrus may selectively influence one form of inhibition over the other (Miettinen and Freund, 1992a; Richter-Levin and Segal, 1990). The results of the SUML paired-pulse study support this concept, in that SUML activation could enhance the size of the second population spike without

altering the size of the first population spike. In other words, if SUML activation produced a reduction in both feed-forward and feed-back inhibition, then both the first and second population spikes should have increased. An increase in only the second population spike, where feed-back inhibition has been evoked, suggests that SUML activation had selectively reduced feed-back inhibition.

A selective effect upon feed-back inhibition does not explain how SUML-activation enhances the population spike during single, low-frequency stimulations to the perforant path. Only a reduction in tonic or feed-forward inhibition would enhance the population spike under these conditions. It is possible, however, that the threshold for a reduction in feed-forward inhibition is higher than that for feed-back inhibition. This might also explain similar results found during sensory stimulation of locally-anaesthetized rats (Herreras et al., 1988). While sensory stimulation (stroking the animals fur) produced an enhancement of the perforant path-evoked population spike in the dentate gyrus in 20 of the 33 animals tested, feed-back inhibition (measured by the paired-pulse paradigm) was reduced in 30 of the same 33 animals. In other words, 10 animals showed a reduction in feed-back inhibition without experiencing a sensory-evoked increase in the population spike.

The potentiation of population spikes recorded in the dentate gyrus was not accompanied by an enhancement of the population EPSP, after SUML activation, or was accompanied by a relatively short (1-2 min) population EPSP enhancement, after MSC activation. The magnitude of the EPSP slope reflects the size of the positive inward current generated at the granule cell dendrites. An enhancement may be due to such synaptic factors as an increase in glutamate release from the perforant path fibres, or an increase in the sensitivity of postsynaptic glutamate receptors. However, the resultant increase in the positive inward current, and hence the population EPSP, should have been observed for the course of the population spike enhancement. Since this did not occur, then the reduced firing threshold of the granule cells must have been caused by an increase in EPSP-spike coupling, where the neuron's ability to generate an action potential is enhanced without a change in the synaptic drive. For instance, an increase in the resistance of the granule cells dendritic shaft would allow an increased amount of synaptic current, generated by perforant path activation, to reach the spike generating zone in the soma without concurrently producing a detectable alteration of the EPSP. An increase in spike-coupling might also occur through the facilitation of voltage-gated ion channels linked to the generation of an action potential, as opposed to the chemically-gated ion channels on the postsynaptic membrane.

A reduction in the tonic or feed-forward inhibition, is a third example where an increase in EPSP-spike coupling could occur. An increase in EPSP-spike coupling has been observed as a property of LTP, along with the increase in the EPSP, and the two components may reflect independent processes (Bliss and Gardner-Medwin, 1973). In fact, the high frequency train required to produce LTP may produce a disproportionate enhancement of the population spike with either no change or a small increase in the EPSP (Bliss and Lomo, 1973; Abraham et al., 1985), as seen here after SUML or MSC activation. An increase in EPSP-spike coupling using a high-frequency train can be produced heterosynaptically (Abraham et al., 1985), whereas an enhancement of the synaptic component is only observed along the tetanized pathway (McNaughton and Barnes, 1977). The increase in EPSP-spike coupling observed in dentate LTP appears to be due, at least in part, to a reduction in feed-forward inhibition (Chavez-Noriega et al., 1990; Tomasulo et al., 1991; Tomasulo and Ramirez, 1993). A reduction in feed-forward inhibition would increase the efficiency with which dendritic depolarization translates into action potentials following perforant path stimulation.

While much attention has been focused on the action of glutamate, and its role in LTP, as a model system for synaptic plasticity changes that may

occur during learning and memory, other systems that mediate nonspecific states of "arousal" or "motivation" are likely to be important. An important role for such modulating systems on hippocampal plasticity is indicated by the significant impairment in the ability of the hippocampus to support long-term potentiation once the subcortical inputs to this structure are severed (Buzsaki and Gage, 1989; Valjakka et al., 1991; Abe et al., 1992).

If the physiological action of subcortical inputs to the hippocampus, such as those arising from the MSC and the SUML, were simply increasing the granule cell's response to any input during a given time period, then this may be likened to an attentional role in information processing. The putative sensory input arising from entorhinal afferents would be enhanced, presumably increasing the intensity of the experience of, or promoting attention to, the input.

The long-lasting enhancement of the population spike that can occur with MSC or SUML activation may simply reflect the length of this "arousal" state. Alternately, the arousal state may be of shorter duration, but the increased responsiveness of granule cells during this brief period may facilitate the induction of other forms of plasticity that would lengthen the duration of enhancement. These other synaptic changes may be associated with an LTP-like mechanism and should only occur at those synapses active during the early arousal state. The variability in duration of the induced spike

enhancements may reflect whether this second form of synaptic plasticity was established, and the strength of this establishment.

This hypothesis would necessitate a mechanism whereby the contemporaneous inputs arising from the entorhinal cortex during the SUML- or MSC-activated "aroused" state could be selectively strengthened by an increase in the EPSP-spike coupling observed here. Since the possible mechanisms by which such an EPSP-spike coupling could occur would presumably enhance all input, such a mechanism remains elusive (see discussion of putative mechanisms above). An increase in the resistance of the dendritic membrane, or a reduction in the feed-forward or tonic inhibition onto the granule cell, would enhance all perforant path input, rather than a selective few which may be paired with the SUML or MSC activation.

Further experiments could shed light on these important issues. The ability of NMDA antagonists to block MSC or SUML related population spike enhancements would resolve whether the long-lasting enhancements are due to an LTP-like mechanism. Varying the interval between SUML or MSC activation, and perforant path stimulation would shed light on whether long-lasting potentiation requires the contemporaneous activation of the perforant path during the early "aroused" state, and test the requirement of a putative second synaptic plasticity mechanism.

While the results published here clearly indicate that SUML- or MSC-activation can produce long-lasting increases in granule cell excitability, many questions remain about the mechanism of enhancement, and the role that these systems may play in hippocampal information processing.

REFERENCES

- Abe, K., Ishiyama, J. and Saito, H. (1992) Effects of epidermal growth factor and basic fibroblast growth factor on generation of long-term potentiation in the dentate gyrus of fimbria-fornix-lesioned rats. *Brain Research* 593:335-338.
- Abraham, W.C., Bliss, T.V.P. and Goddard, G.V. (1985) Heterosynaptic changes accompany long-term but not short-term potentiation of the perforant path in the anaesthetized rat. *Journal of Physiology* 363:335-349.
- Abraham, W.C. and Otani, S. (1991) Macromolecules and the maintenance of long-term potentiation. In: *Kindling and Synaptic Plasticity; The Legacy of Graham Goddard*, Ed. Morrell, F. Birkhauser, Boston. p. 92-109.
- Adamec, R., McNaughton, B., Racine, R. and Livingston, K. (1981) Effects of diazepam (Valium) on hippocampal excitability in the rat: action in the dentate area. *Epilepsia* 22:205-215.
- Aggleton, J.P., Hunt, P.R. and Shaw, C. (1990) The effects of mammillary body and combined amygdalar-fornix lesions on tests of delayed non-matching-to-sample in the rat. *Behavioural Brain Research* 40:145-157.
- Albertson, T.E. and Joy, R.M. (1987) Increased inhibition in dentate gyrus granule cells following exposure to GABA-uptake blockers. *Brain Research* 435:283-292.
- Alkon, D.L., Amaral, D.G., Bear, M.F., Black, J., Carew, T.J., Cohen, N.J., Disterhoft, J.F., Eichenbaum, H., Golski, S., Gorman, L.K., Lynch, G., McNaughton, B.L., Mishkin, M., Moyer, J.R., Jr., Olds, J.L., Olton, D.S., Otto, T., Squire, L.R., Staubli, U., Thompson, L.T. and Wible, C. (1991) Learning and memory. *Brain Research Reviews* 16:193-220.
- Alvarez-Leefmans, F.J. and Gardner-Medwin, A.R. (1975) Influences of the septum on the hippocampal dentate area which are which are unaccompanied by field potentials. *Journal of Physiology* 249:14P-16P.

- Alvarez-Leefmans, F.J. (1976) Functional synaptic organization of inhibitory pathways in the dentate gyrus of the rabbit. *Experimental Brain Research Supplement* 1:229-234.
- Amaral, D.G. (1978) A Golgi study of cell type in the hilar region of the hippocampus of the rat. *Journal of Comparative Anatomy* 182:851-914.
- Amaral, D.G. and Kurz, J. (1985) An analysis of the origins of the cholinergic and non-cholinergic septal projections to the hippocampal formation in the rat. *Journal of Comparative Neurology* 240:37-59.
- Amaral, D.G. and Witter, M.P. (1989) The three-dimensional organization of the hippocampal formation: a review of anatomical data. *Neuroscience* 31:571-591.
- Amaral, D.G., Ishizuka, N. and Claiborne, B. (1990) Neurons, numbers and the hippocampal network. *Progress in Brain Research* 83:1-11.
- Andersen, P., Holmqvist, B. and Voorhoeve, P.E. (1966a) Entorhinal activation of dentate granule cells. *Acta Physiologica Scandinavica* 66:448-460.
- Andersen, P., Blackstad, T.W. and Lomo, T. (1966b) Location and identification of excitatory synapses on hippocampal pyramidal cells. *Experimental Brain Research* 1:236.
- Andersen, P., Eccles, J.C. and Loyning, Y. (1971a) Pathway of postsynaptic inhibition in the hippocampus. *Journal of Neurophysiology* 27:608-619.
- Andersen, P., Bliss, T.V.P. and Skrede, K.K. (1971b) Lamellar organization of hippocampal excitatory pathways. *Experimental Brain Research* 13:222-238.
- Andersen, P., Bliss, T.V.P. and Skrede, K.K. (1971c) Unit analysis of hippocampal population spikes. *Experimental Brain Research* 13:208-221.

- Aniksztejn, L., Otani, S. and Ben-Ari, Y. (1992) Quisqualate metabotropic receptors modulate NMDA currents and facilitate induction of long-term potentiation through protein kinase C. *European Journal of Neuroscience* 4:500-505.
- Assaf, S.Y. and Miller, J.J. (1978) Neuronal transmission in the dentate gyrus: role of inhibitory mechanisms. *Brain Research* 151:587-592.
- Austin, K.B., Bronzino, J.D. and Morgane, P.J. (1989) Paired-pulse facilitation and inhibition in the dentate gyrus is dependent on behavioral state. *Experimental Brain Research* 77:594-604.
- Baisden, R.H., Woodruff, M.L. and Hoover, D.B. (1984) Cholinergic and non-cholinergic septohippocampal projections: a double-label horseradish peroxidase-acetylcholinesterase study in the rabbit. *Brain Research* 290:146-151.
- Bakst, I., Avendano, C., Morrison, J.H. and Amaral, D.G. (1986) An experimental analysis of the origins of somatostatin-like immunoreactivity in the dentate gyrus of the rat. *Journal of Neuroscience* 6:1452-1462.
- Baskys, A. (1992) Metabotropic receptors and 'slow' excitatory actions of glutamate agonists in the hippocampus. *Trends in Neurosciences* 15:92-96.
- Behzadi, G., Kalen, P., Parvopassu, F. and Wiklund, L. (1990) Afferents to the median raphe nucleus of the rat: retrograde cholera toxin and wheat germ conjugated horseradish peroxidase tracing, and selective D-3Aspartate labelling of possible excitatory amino acid inputs. *Neuroscience* 37:77-100.
- Berger, T.W. and Orr, W.B. (1982) Role of the hippocampus in reversal learning of the rabbit nictitating membrane response. In: *Conditioning: Representation Of Involved Neural Function*, Ed. C.D. Woody, New York, Plenum Press.
- Berger, T.W., Semple-Rowland, S. and Basset, J. (1980) Hippocampal polymorph neurons are the cells of origin for ipsilateral association and commissural afferents to the dentate gyrus. *Brain Research* 215:329-336.

- Berz, S., Battig, K. and Welzl, H. (1992) The effects of anticholinergic drugs on delayed time discrimination performance in rats. *Physiology and Behavior* 51:493-9.
- Bianchi, M. and Panerai, A.E. (1993) Reversal of scopolamine-induced amnesia by the GABA-B receptor antagonist CGP 35348 in the mouse. *Cognitive Brain Research* 1:135-6.
- Bilkey, D.K. and Goddard, G.V. (1985) Medial septal facilitation of hippocampal granule cell activity is mediated by inhibition of inhibitory interneurons. *Brain Research* 361:99-106.
- Bland, B.H. and Wishaw, I.Q. (1976) Generators and topography of hippocampal theta (RSA) in the anaesthetized and freely moving rat. *Brain Research* 118:259-280.
- Bland, B.H., Andersen, P., Ganes, T. and Sveen, O. (1980) Automated analysis of rhythmicity of physiologically identified hippocampal formation neurons. *Experimental Brain Research* 38:205-219.
- Bland, B.H. (1986) The physiology and pharmacology of hippocampal formation theta rhythms. *Progress in Neurobiology* 26:1-54.
- Bliss, T.V.P. and Gardner-Medwin, A.R. (1973) Long-lasting potentiation of synaptic transmission in the dentate gyrus of the unanaesthetized rabbit following stimulation of the perforant path. *Journal of Physiology* 232:357-374.
- Bliss, T.V.P. and Lomo, T. (1973) Long-lasting potentiation of synaptic transmission in the dentate area of the anaesthetized rabbit following stimulation of the perforant path. *Journal of Physiology* 232:331-356.
- Bond, N.W., Walton, J. and Pruss, J. (1989) Restoration of memory following septo-hippocampal grafts: a possible treatment for Alzheimer's disease. *Biological Psychology* 28:67-87.
- Bortolotto, Z.A. and Collingridge, G.L. (1992) Activation of glutamate metabotropic receptors induces long-term potentiation. *European Journal of Pharmacology* 214:297-298.

- Bowery, N.G., Hill, D.R., Hudson, A.L., Doble, A., Middlemiss, D.N., Shaw, J. and Turnbull, M. (1980) (-)Baclofen decreases neurotransmitter release in the mammalian CNS by an action at a novel GABA receptor. *Nature* 283:92-94.
- Bramham, C.R., Torp, R., Zhang, N., Storm-Mathisen, J. and Ottersen, O.P. (1990) Distribution of glutamate-like immunoreactivity in excitatory hippocampal pathways: A semiquantitative electron microscopic study in rats. *Neuroscience* 39:405-417.
- Bramham, C.R., Milgram, N.W. and Srebro, B. (1991) Activation of AP5-sensitive NMDA receptors is not required to induce LTP of synaptic transmission in the lateral perforant path. *European Journal of Neuroscience* 3:1300-1308.
- Brashear, H.R., Zaborszky, L. and Heimer, L. (1986) Distribution of gabaergic and cholinergic neurons in the rat diagonal band. *Neuroscience* 17:439-451.
- Bresnahan, E.L., Wiser, P.R., Muth, N.J. and Ingram, D.K. (1992) Delayed matching-to-sample performance by rats in a new avoidance-motivated maze: response to scopolamine and fimbria- fornix lesions. *Physiology and Behavior* 51:735-46.
- Brucato, F.H., Morrisett, R.A., Wilson, W.A. and Swartzwelder, H.S. (1992) The GABA-B receptor antagonist, CGP-35348, inhibits paired-pulse disinhibition in the rat dentate gyrus in vivo. *Brain Research* 588:150-153.
- Burgard, E.C., Decker, G. and Sarvey, J.M. (1989) NMDA receptor antagonists block norepinephrine-induced long-lasting potentiation and long-term potentiation in rat dentate gyrus. *Brain Research* 482:351-355.
- Burgard, E.C. and Sarvey, J.M. (1990) Muscarinic receptor activation facilitates the induction of long-term potentiation (LTP) in the rat dentate gyrus. *Neuroscience Letters* 116:34-39.
- Burgard, E.C. and Sarvey, J.M. (1991) Long-lasting potentiation and epileptiform activity produced by GABA-B receptor activation in the

- dentate gyrus of rat hippocampal slice. *Journal of Neuroscience* 11:1198-1209.
- Buzsaki, G., Leung, L.-W.S. and Vanderwolf, C.H. (1983) Cellular basis of hippocampal EEG in the behaving rat. *Brain Research Reviews* 6:139-171.
- Buzsaki, G. (1984) Feed-forward inhibition in the hippocampal formation. *Progress in Neurobiology* 22:131-154.
- Buzsaki, G., Czopf, J., Konakor, I. and Kellenyi, L. (1986) Laminar distribution of hippocampal rhythmic slow activity (RSA) in the behaving rat: current source density analysis, effects of urethane and atropine. *Brain Research* 365:125-137.
- Buzsaki, G. and Czeh, G. (1992) Physiological function of granule cells: a hypothesis. In: *The Dentate Gyrus and Its Role in Seizures*, Eds. Ribak, C.E., Gall, C.M. and Mody, I. Elsevier. p. 281-290.
- Buzsaki, G. and Gage, F.H. (1989) Absence of long-term potentiation in the subcortically deafferented dentate gyrus. *Brain Research* 484:94-101.
- Cao, W.-H., Inanami, O., Sato, A. and Sato, Y. (1989) Stimulation of the septal complex increases local cerebral blood flow in the hippocampus in anesthetized rats. *Neuroscience Letters* 107:135-140.
- Carre, G.P. and Harley, C.W. (1990) Enhancement of dentate gyrus field potentials through glutamate-induced activation of the supramammillary nucleus (SUM) in rats. *Society for Neuroscience Abstracts* 16:1097. (Abstract)
- Carre, G.P. and Harley, C.W. (1991) Population spike facilitation in the dentate gyrus following glutamate to the lateral supramammillary nucleus. *Brain Research* 568:307-310.
- Chandler, J.P. and Crutcher, K.A. (1983) The septo-hippocampal projection in the rat: an electronmicroscopic horseradish peroxidase study. *Neuroscience* 10:685-696.
- Chavez-Noriega, L.E., Halliwell, J.V. and Bliss, T.V.P. (1990) A decrease in firing threshold observed after induction of the EPSP-spike (E-S)

component of long-term potentiation in rat hippocampal slices. *Experimental Brain Research* 79:633-641.

- Chavkin, C., Shoemaker, W.I., McGinty, J.F., Bayon, A. and Bloom, F.E. (1985) Characterization of the prodynorphin and proenkephalin neuropeptide system in rat hippocampus. *Journal of Neuroscience* 5:808-816.
- Clarke, D.J. (1985) Cholinergic innervation of the rat dentate gyrus: an immunocytochemical and electron microscopical study. *Brain Research* 360:349-354.
- Collingridge, G.L., Kehl, S.J. and McLennan, H. (1983) Excitatory amino acids in synaptic transmission in the Schaffer collateral-commissural pathway of the rat hippocampus. *Journal of Physiology* 334:33-46.
- Cotman, C.W., Monaghan, D.T. and Ottersen, O.P. (1987) Anatomical organization of excitatory amino acid receptors and their pathways. *Trends in Neurosciences* 10:273-280.
- Crunelli, V., FORDA, S. and Kelly, J.S. (1983) Blockade of amino acid-induced depolarizations and inhibition of excitatory post-synaptic potentials in rat dentate gyrus. *Journal of Physiology* 341:627-640.
- Crutcher, K.A., Madison, R. and Davis, J.W. (1981) A study of the rat septo-hippocampal pathway using anterograde transport of horseradish peroxidase. *Neuroscience* 6:1961-1973.
- Dahl, D. and Winson, J. (1985) Action of norepinephrine in the dentate gyrus. I. Stimulation of the locus coeruleus. *Experimental Brain Research* 59:491-496.
- Davies, S. and Kohler, C. (1985) The substance P innervation of the rat hippocampal region. *Anatomy and Embryology* 173:45-52.
- Deller, T. and Leranth, C. (1990) Synaptic connections of neuropeptide Y (NPY) immunoreactive neurons in the hilar area of the rat hippocampus. *Journal of Comparative Neurology* 300:433-447.
- Dent, J.A., Galvin, N.J., Stanfield, B.B. and Cowan, W.M. (1983) The mode of termination of the hypothalamic projections to the dentate gyrus: an EM autoradiographic study. *Brain Research* 258:1-10.

- deToledo-Morrell, L., Geinisman, Y. and Morrell, F. (1988) Age-dependent alterations in hippocampal synaptic plasticity: relation to memory disorders. *Neurobiology of Aging* 9:581-590.
- Dingledine, R. (1983) N-methyl aspartate activates voltage-dependent calcium conductance in rat hippocampal pyramidal cells. *Journal of Physiology* 343:385-405.
- Dolphin, A.C. and Scott, R.H. (1974) Calcium channel currents and their inhibition by (-)baclofen in rat sensory neurons: modulation by guanine nucleotides. *Journal of Physiology* 386:1-17.
- Eberhard, H.B., Schwerdtfeger, W.K. and Germroth, P. (1989) New anatomical approaches to reveal afferent and efferent hippocampal circuitry. In: *The Hippocampus - New Vistas*, Eds. Alan R. Liss. p. 71-83.
- Eccles, J.C. (1988) Mechanisms of learning in complex neural systems. In: *Handbook of Physiology - The Nervous System V*. p. 137-167.
- Errington, M.L., Lynch, M.A. and Bliss, T.V. (1987) Long-term potentiation in the dentate gyrus: induction and increased glutamate release are blocked by D(-)aminophosphonovalerate. *Neuroscience* 20:279-284.
- Fantie, B.D. and Goddard, G.V. (1982) Septal modulation of the population spike in the fascia dentata produced by perforant path stimulation in the rat. *Brain Research* 252:227-237.
- Fifkova, E. (1975) Two types of terminal degeneration in the molecular layer of the dentate fascia following lesions of the entorhinal cortex. *Brain Research* 96:169-175.
- File, S.E., Mabbutt, P.S. and Toth, E. (1990) A comparison of the effects of diazepam and scopolamine in two positively reinforced learning tasks. *Pharmacology, Biochemistry and Behavior* 37:587-92.
- Fischer, B.O., Ottersen, O.P. and Storm-Mathisen, J. (1986) Implantation of D-4H aspartate loaded gel particles permits restricted uptake sites for transmitter-selective axonal transport. *Experimental Brain Research* 63:620-626.

- Fishkin, R.J., Ince, E.S., Carlezon, W.A., Jr. and Dunn, R.W. (1993) D-cycloserine attenuates scopolamine-induced learning and memory deficits in rats. *Behavioral and Neural Biology* 59:150-7.
- Ford, R.D., Colom, L.V. and Bland, B.H. (1989) The classification of medial septum-diagonal band cells as theta- on or theta-off in relation to hippocampal EEG states. *Brain Research* 493:269-282.
- Fox, S.E. and Ranck, J.B., Jr. (1975) Localization and anatomical identification of theta and complex-spike cells in the dorsal hippocampal formation of rats. *Experimental Neurology* 49:299-313.
- Fox, S.E. and Ranck, J.B., Jr. (1981) Electrophysiological characteristics of hippocampal complex-spike and theta cells. *Experimental Brain Research* 41:399-410.
- Fredens, K., Steengaard-Pedersen, K. and Larsson, L.I. (1984) Localization of enkephalin and cholecystokinin immunoreactivities in the perforant path terminal fields of the rat hippocampal formation. *Brain Research* 304:255-263.
- Freund, T.F. (1989) GABAergic septohippocampal neurons contain parvalbumin. *Brain Research* 478:375-381.
- Freund, T.F. and Antal, M. (1988) GABA-containing neurons in the septum control inhibitory interneurons in the hippocampus. *Nature* 336:170-173.
- Frotscher, M., Seress, L., Schwerdtfeger, W.K. and Buhl, E. (1991) The mossy cells of the fascia dentata: A comparative study of their fine structure and synaptic connections in rodents and primates. *Journal of Comparative Neurology* 312:145-163.
- Frotscher, M. and Zimmer, J. (1983) Lesion-induced mossy fibers to the molecular layer of the rat fascia dentata: identification of postsynaptic granule cells by the Golgi/EM technique. *Journal of Comparative Neurology* 215:299-311.
- Frotscher, M. and Leranth, C. (1986) The cholinergic innervation of the rat fascia dentata: identification of target structures on granule cells by

- combining choline acetyltransferase immunocytochemistry and Golgi impregnation. *Journal of Comparative Anatomy* 243:58-70.
- Frotscher, M. (1992) Application of the Golgi/electron microscopy technique for cell identification in immunocytochemical, retrograde labeling, and developmental studies of hippocampal neurons. *Journal of Microscopy Research and Technique* 23:306-323.
- Gahwiler, B.H. and Brown, D.A. (1985) GABA-B-receptor-activated K⁺ current in voltage-clamped CA3 pyramidal cells in hippocampal cultures. *Proceedings of the National Academy of Sciences* 82:1558-1562.
- Gall, C., Brecha, N., Karten, H.J. and Chang, K.J. (1981) Localization of enkephalin-like immunoreactivity to identified axonal and neuronal populations of the rat hippocampus. *Journal of Comparative Neurology* 198:335-350.
- Gall, C. and Selawski, L. (1984) Supramammillary afferents to guinea pig hippocampus contains substance P-like immunoreactivity. *Neuroscience Letters* 51:171-176.
- Gamble, E. and Koch, C. (1987) The dynamics of free calcium in dendritic spines in response to repetitive synaptic input. *Science* 236:1311-1315.
- Gamrani, H., Ontenienti, P., Seguela, P., Geffard, M. and Calas, A. (1986) Gamma-aminobutyric acid-immunoreactivity in the rat hippocampus. A light and electron microscopic study with anti-GABA antibodies. *Brain Research* 364:30-38.
- Gasic, G.P. and Hollmann, M. (1992) Molecular neurobiology of glutamate receptors. *Annual Review of Neuroscience* 54:507-536.
- Geeraedts, L.M., Nieuwenhuys, R. and Veening, J.G. (1990) Medial forebrain bundle of the rat: IV. Cytoarchitecture of the caudal (lateral hypothalamic) part of the medial forebrain bundle bed nucleus. *Journal of Comparative Neurology* 294:537-568.

- Germroth, P., Schwerdtfeger, W.K. and Buhl, E.H. (1989) GABAergic neurons in the entorhinal cortex project to the hippocampus. *Brain Research* 494:187-192.
- Germroth, P., Schwerdtfeger, W.K. and Buhl, E.H. (1991) Ultrastructure and aspects of functional organization of pyramidal and nonpyramidal entorhinal projection neurons contributing to the perforant path. *Journal of Comparative Neurology* 305:215-231.
- Goodchild, A.K., Dampney, R.A.L. and Bandler, R. (1982) A method for evoking physiological responses by stimulation of cell bodies, but not axons of passage, within localized regions of the central nervous system. *Journal of Neuroscience Methods* 6:351-363.
- Grandes, P. and Streit, P. (1991) Effect of perforant path lesion on pattern of glutamate-like immunoreactivity in rat dentate gyrus. *Neuroscience* 41:391-400.
- Greenstein, Y.J., Pavlides, C. and Winson, J. (1988) Long-term potentiation in the dentate gyrus is preferentially induced at theta rhythm periodicity. *Brain Research* 438:331-334.
- Gulyas, A.I., Gorcs, T.J. and Freund, T.F. (1990) Innervation of different peptide-containing neurons in the hippocampus by GABAergic septal afferents. *Neuroscience* 37:31-44.
- Gulyas, A.I., Miettinen, R., Jacobowitz, D.M. and Freund, T.F. (1992) Calretinin is present in non-pyramidal cells of the rat hippocampus--I. A new type of neuron specifically associated with the mossy fibre system. *Neuroscience* 48:1-27.
- Gustafsson, B., Wigstrom, H., Abraham, W.C. and Huang, Y.-Y. (1987) Long-term potentiation in the hippocampus using depolarizing current pulses as the conditioning stimulus to single volley synaptic potentials. *Journal of Neuroscience* 7:774-780.
- Haberly, L.B. and Price, J.L. (1978) Association and commissural fiber systems of the olfactory cortex in the rat. I. Systems originating in the piriform cortex and adjacent areas. *Journal of Comparative Neurology* 178:711-740.

- Haglund, L., Swanson, L.W. and Kohler, C. (1984) The projection of the supramammillary nucleus to the hippocampal formation: an immunohistochemical and anterograde transport study with the lectin PHA-L in the rat. *Journal of Comparative Neurology* 229:171-185.
- Halliwel, J.V. (1990) Physiological mechanisms of cholinergic action in the hippocampus. *Progress in Brain Research* 84:255-272.
- Hanse, E. and Gustafsson, B. (1992a) Postsynaptic, but not presynaptic, activity controls the early time course of long-term potentiation in the dentate gyrus. *Journal of Neuroscience* 12:3226-3240.
- Hanse, E. and Gustafsson, B. (1992b) Long-term potentiation and field EPSPs in the lateral and medial perforant paths in the dentate gyrus in vitro: A comparison. *European Journal of Neuroscience* 4:1191-1201.
- Harley, C., Milway, J.S. and Lacaille, J.C. (1989) Locus coeruleus potentiation of dentate gyrus responses: evidence for two systems. *Brain Research Bulletin* 22:643-650.
- Harley, C.W., Lacaille, J.-C. and Galway, M. (1983) Hypothalamic afferents to the dorsal dentate gyrus contain acetylcholinesterase. *Brain Research* 270:335-339.
- Harley, C.W. and Milway, J.S. (1986) Glutamate ejection in the locus coeruleus enhances the perforant path-evoked population spike in the dentate gyrus. *Experimental Brain Research* 63:143-150.
- Harley, C.W. and Sara, S.J. (1992) Locus coeruleus bursts induced by glutamate trigger delayed perforant path spike amplitude potentiation in the dentate gyrus. *Experimental Brain Research* 89:581-587.
- Harris, E.W. and Cotman, C.W. (1985) Effects of synaptic antagonists on perforant path paired-pulse plasticity: differentiation of pre- and postsynaptic antagonism. *Brain Research* 334:348-353.
- Harris, E.W. and Cotman, C.W. (1986) Long-term potentiation of guinea pig mossy fiber responses is not blocked by N-methyl D-aspartate antagonists. *Neuroscience Letters* 70:132-137.

- Herkenham, M. (1978) The connections of the nucleus reuniens thalami: evidence for a direct thalamo-hippocampal pathway in the rat. *Journal of Comparative Neurology* 177:589-610.
- Herreras, O., Solis, J.M., Munoz, M.D., Martin-del-Rio, R. and Lerma, J. (1988) Sensory modulation of hippocampal transmission. I. Opposite effects on CA1 and dentate gyrus synapses. *Brain Research* 461:290-302.
- Hjorth-Simonsen, A. (1972) Projection of the lateral part of the entorhinal area to the hippocampus and fascia dentata. *Journal of Comparative Neurology* 146:219-232.
- Hjorth-Simonsen, A. and Laurberg, S. (1977) Commissural connections of the dentate area in the rat. *Journal of Comparative Neurology* 174:591-606.
- Hoff, S.F., Scheff, S.W., Bernardo, L.S. and Cotman, C.W. (1982) Lesion induced synaptogenesis in the dentate gyrus of aged rats: I. Loss and reacquisition of normal synaptic density. *Journal of Comparative Neurology* 205:246-252.
- Houser, C.R., Crawford, R.P., Barber, R.P., Salvaterra, P.M. and Vaughn, J.E. (1983) Organization and morphological characteristics of cholinergic neurons: an immunocytochemical study with monoclonal antibody to choline acetyltransferase. *Brain Research* 266:97-119.
- Ino, T., Itoh, K., Sugimoto, T., Kaneko, T., Kamiya, H. and Mizuno, N. (1988) The supramammillary region of the cat sends substance P-like immunoreactive axons to the hippocampal formation and the entorhinal cortex. *Neuroscience Letters* 90:259-264.
- Ito, T., Miura, Y. and Kadokawa, T. (1988) Effects of physostigmine and scopolamine on long-term potentiation of hippocampal population spikes in rats. *Canadian Journal of Physiology and Pharmacology* 66:1010-1016.
- Jerusalinsky, D., Ferreira, M.B.C., Walz, R., Da Silva, R.C., Bianchin, M., Ruschel, A.C., Zanatta, M.S., Medina, J.H. and Izquierdo, I. (1992) Amnesia by post-training infusion of glutamate receptor antagonists

into the amygdala, hippocampus, and entorhinal cortex. *Behavioral and Neural Biology* 58:76-80.

Johnston, D., Williams, S., Jaffe, D. and Gray, R. (1992) NMDA-receptor-independent long-term potentiation. *Annual Review of Physiology* 54:489-505.

Joy, R.M. and Albertson, T.E. (1993) NMDA receptors have a dominant role in population spike-paired pulse facilitation in the dentate gyrus of urethane-anesthetized rats. *Brain Research* 604:273-282.

Katsumaru, H., Kosaka, T., Heizmann, C.W. and Hama, K. (1988) Immunocytochemical study of GABAergic neurons containing the calcium-binding protein parvalbumin in the rat hippocampus. *Experimental Brain Research* 72:347-362.

Kesner, R.P. (1988) Reevaluation of the contribution of the basal forebrain cholinergic system to memory. *Neurobiology of Aging* 9:609-616.

Kirk, I.J. and McNaughton, N. (1991) Supramammillary cell firing and hippocampal rhythmical slow activity. *Neuroreport* 2:723-725.

Kitajima, T. and Hara, K. (1991) A model of the mechanism of cooperativity and associativity of long-term potentiation in the hippocampus: A fundamental mechanism of associative memory and learning. *Biological Cybernetics* 64:365-371.

Klanchnik, J.M. and Phillips, A.G. (1991) Modulation of synaptic plasticity in the dentate gyrus of the rat by electrical stimulation of the median raphe nucleus. *Brain Research* 557:236-240.

Kimble, D.P. (1968) Hippocampus and internal inhibition. *Psychological Bulletin*, 70:285-295.

Kohler, C., Chan-Palay, V. and Wu, J.-Y. (1984) Septal neurons containing glutamic acid decarboxylase immunoreactivity project to the hippocampal region in the rat brain. *Anatomy and Embryology* 169:41-44.

- Kohler, C. (1985a) Intrinsic projections of the retrohippocampal region in the rat brain. I. The subicular complex. *Journal of Comparative Neurology* 236:504-522.
- Kohler, C. (1985b) A projection from the deep layers of the entorhinal area to the hippocampal formation in the rat brain. *Neuroscience Letters* 56:13-19.
- Kohler, C., Eriksson, L., Davies, S. and Chan-Palay, V. (1986) Neuropeptide Y innervation of the hippocampal region in the rat and monkey brain. *Journal of Comparative Neurology* 244:384-400.
- Kohler, C., Eriksson, L.G., Davies, S. and Chan-Palay, V. (1987) Colocalization of neuropeptide Y and somatostatin immunoreactivity in neurons of individual subfields of the rat hippocampal region. *Neuroscience Letters* 78:1-6.
- Konopacki, J., Bland, B.H. and Roth, S.H. (1987) Cholinergic theta rhythm in transected hippocampal slices: independent CA1 and dentate generators. *Brain Research* 436:217-222.
- Kosaka, T., Wu, J.Y. and Benoit, R. (1988) GABAergic neurons containing somatostatin-like immunoreactivity in the rat hippocampus and dentate gyrus. *Experimental Brain Research* 71:388-398.
- Kosel, K.C., Van Hoesen, G.W. and West, J.R. (1981) Olfactory bulb projections to the parahippocampal area of the rat. *Journal of Comparative Neurology* 198:467-482.
- Kramis, R., Vanderwolf, C.H. and Bland, B.H. (1975) Two types of hippocampal rhythmical slow activity in both the rabbit and the rat: relations to behavior and effects of atropine, diethylether, urethane, and pentobarbital. *Experimental Neurology* 49:58-85.
- Krnjevic, K. and Ropert, N. (1982) Electrophysiological and pharmacological characteristics of facilitation of hippocampal population spikes by stimulation of the medial septum. *Neuroscience* 7:2165-2183.
- Krug, M., Koch, M., Schoof, E., Wagner, M. and Matthies, H. (1989) Methylglucamine orotate, a memory-improving drug, prolongs

- hippocampal long-term potentiation. *European Journal of Pharmacology* 173:223-226.
- Krug, M., Jork, R., Reymann, K., Wagner, M. and Matthies, H. (1991a) The amnesic substance 2-deoxy-D-galactose suppresses the maintenance of hippocampal LTP. *Brain Research* 540:237-242.
- Krug, M., Bergado, J. and Ruethrich, H. (1991b) Long-term potentiation and postconditioning potentiation - the same mechanism?. *Biomedica Biochimica Acta* 49:273-279.
- Kuba, K. and Kumamoto, E. (1990) Long-term potentiations in vertebrate synapses: A variety of cascades with common subprocesses. *Progress in Neurobiology* 34:197-269.
- Kudo, Y. and Ogura, A. (1986) Glutamate-induced increase in intracellular Ca^{2+} concentration in isolated hippocampal neurones. *British Journal of Pharmacology* 89:191-198.
- Lacaille, J.-C. and Harley, C.W. (1985) The action of norepinephrine in the dentate gyrus: Beta-mediated facilitation of evoked potentials in vitro. *Brain Research* 358:210-220.
- Laroche, S., Bergis, O., Doyere, V. and Bloch, V. (1988) Parallel studies on learning and LTP in the dentate gyrus. In: *Synaptic Plasticity in the Hippocampus*, Eds. Haas, H.L. and Buzsaki, G. Springer-Verlag, Berlin: p. 208-211.
- Laroche, S., Bloch, V., Doyere, V. and Redini-Del Negro, C. (1991) Significance of long-term potentiation for learning and memory. In: *Kindling and Synaptic Plasticity; The Legacy of Graham Goddard*, Ed. Morrell, F. Birkhauser, Boston. p. 12-37.
- Larson, J. and Lynch, G. (1986) Induction of synaptic potentiation in hippocampus by patterned stimulation involves two events. *Science* 232:985-988.
- Larson, J. and Lynch, G. (1988) Role of N-methyl-D-aspartate receptors in the induction of synaptic potentiation by burst stimulation patterned after the hippocampal theta-rhythm. *Brain Research* 441:111-118.

- Larson, J., Wong, D. and Lynch, G. (1986) Patterned stimulation at the theta frequency is optimal for the induction of hippocampal long-term potentiation. *Brain Research* 368:347-350.
- Larson, J. and Lynch, G. (1989) Theta pattern stimulation and the induction of LTP: the sequence in which synapses are stimulated determines the degree to which they potentiate. *Brain Research* 489:49-58.
- Laurberg, S. and Sorensen, K.E. (1981) Associational and commissural collaterals of neurons in the hippocampal formation (hilus fasciae dentatae and subfield CA3). *Brain Research* 212:287-300.
- Lavond, D.G., McCormick, D.A., Clark, G.A., Holmes, D.T., and Thompson, R.F. (1981) Effects of ipsilateral rostral pontine reticular lesions on retention of classically conditioned nictitating membrane and eyelid responses. *Physiological Psychology*, 9:335-339.
- Leranth, C. and Frotscher, M. (1987) Cholinergic innervation of hippocampal GAD- and somatostatin-immunoreactive commissural neurons. *Journal of Comparative Anatomy* 261:33-47.
- Leranth, C., Malcolm, A.J. and Frotscher, M. (1990) Afferent and efferent synaptic connections of somatostatin- immunoreactive neurons in the rat fascia dentata. *Journal of Comparative Neurology* 295:111-122.
- Leung, L.-W.S. (1990) Field potentials in the central nervous system; recording, analysis and modeling. In: *Neuromethods, Vol. 15: Neurophysiological Techniques: Applications to Neural Systems*, Eds. Boulton, A.A., Baker, G.B. and Vanderwolf, C.H. The Humana Press Inc., Clifton, NJ. p. 277-312.
- Li, Y.J., Simon, J.R. and Low, W.C. (1992) Intrahippocampal grafts of cholinergic-rich striatal tissue ameliorate spatial memory deficits in rats with fornix lesions. *Brain Research Bulletin* 29:147-155.
- Libet, B. (1986) Nonclassical synaptic functions of transmitters. *Federation Proceedings* 45:2678-2686.
- Lingenhohl, K. and Finch, D.M. (1991) Morphological characterization of rat entorhinal neurons in vivo: Soma-dendritic structure and axonal domains. *Experimental Brain Research* 84:57-74.

- Lipski, J., Bellingham, M.C., West, M.J. and Pilowsky, P. (1988) Limitations of the technique of pressure microinjection of excitatory amino acids for evoking responses from localized regions of the CNS. *Journal of Neuroscience Methods* 26:169-179.
- Lomo, T. (1971) Patterns of activation in a monosynaptic corticalthpaway: the perforant path input to the dentate area of the hippocampal formation. *Experimental Brain Research* 12:18-45.
- Lopes da Silva, F.H., Witter, M.P., Boeijinga, P.H. and Lohman, A.H.M. (1990) Anatomic organization and physiology of the limbic cortex. *Physiological Reviews* 70:453-512.
- Lothman, E.W., Bertram, E.H., III and Stringer, J.L. (1991) Functional anatomy of hippocampal seizures. *Progress in Neurobiology* 37:1-82.
- Lubbers, K. and Frotscher, M. (1987) Fine structure and synaptic connections of identified neurons in the rat fascia dentata. *Anatomy and Embryology* 177:1-14.
- Lukaszewska, I. (1993) Scopolamine affects response-to-change test involving 20-min retention interval after locomotor exploration in rats. *Physiology and Behavior* 53:763-7.
- Lundberg, J.M., Rudehill, A., Sollevi, A., Theodorsson-Norheim, E. and Hamberger, B. (1986) Frequency-dependent and reserpine-dependent chemical coding of sympathetic neurotransmission-Differential release of noradrenaline and neuropeptide Y from pig spleen. *Neuroscience Letters* 63:96-100.
- Lynch, G., Larson, J., Kelso, S., Barrionuevo, G. and Schottler, F. (1983) Intracellular injections of EGTA block induction of hippocampal long-term potentiation. *Nature* 305:719-721.
- Magloczky, Z., Acsady, L. and Freund, T.F. (1991) Innervation of the hippocampal formation by hypothalamic afferents. *European Journal of Neuroscience, Supplement* 4:159.
- Malenka, R.C., Kauer, J.A., Zucker, R.J. and Nicoll, R.A. (1988) Postsynaptic calcium is sufficient for potentiation of hippocampal synaptic transmission. *Science* 242:81-84.

- Malenka, R.C. (1991) The role of postsynaptic calcium in the induction of long-term potentiation. *Molecular Neurobiology* 5:289-295.
- Malisch, R. and Ott, T. (1982) Rhythmical slow wave electroencephalographic activity elicited by hippocampal injection of muscarinic agents in the rat. *Neuroscience Letters* 28:113-118.
- Massicotte, G. and Baudry, M. (1991) Triggers and substrates of hippocampal synaptic plasticity. *Neuroscience and Biobehavioral Reviews* 15:415-423.
- Matsuoka, N., Maeda, N., Yamazaki, M., Ohkubo, Y. and Yamaguchi, I. (1992) Effect of FR121196, a novel cognitive enhancer, on the memory impairment of rats in passive avoidance and radial arm maze tasks. *Journal of Pharmacology and Experimental Therapeutics* 263:436-44.
- Matsuoka, N., Maeda, N., Ohkubo, Y. and Yamaguchi, I. (1991) Differential effects of physostigmine and pilocarpine on the spatial memory deficits produced by two septo-hippocampal deafferentations in rats. *Brain Research* 559:233-240.
- Matthews, D.A., Cotman, C.W. and Lynch, G. (1976) An electron microscopic study of lesion induced synaptogenesis in the dentate gyrus of the adult rat. I. Magnitude and time course of degeneration. *Brain Research* 115:1-21.
- Matthews, D.A., Salvaterra, P.M., Crawford, G.D., Houser, C.R. and Vaughn, J.E. (1987) An immunocytochemical study of choline acetyltransferase-containing neurons and axon terminals in normal and partially deafferented hippocampal formation. *Brain Research* 402:30-43.
- Matthies, H., Frey, U., Reymann, K., Krug, M., Jork, R. and Schroeder, H. (1990) Differential mechanisms and multiple stages of LTP. *Advances in Experimental Medicine and Biology* 268:359-368.
- Mayer, M.L., Westbrook, G.L. and Guthrie, P.B. (1984) Voltage-dependent block by Mg^{++} of NMDA responses in spinal cord neurones. *Nature* 309:261-263.

- McGuinness, N., Anwyl, R. and Rowan, M. (1991) The effects of trans-ACPD on long-term potentiation in the rat hippocampal slice. *Neuroreport* 2:688-690.
- McNamara, R.K. and Skelton, R.W. (1992) Assessment of a cholinergic contribution to chlordiazepoxide-induced deficits of place learning in the Morris water maze. *Pharmacology, Biochemistry and Behavior* 41:529-38.
- McNaughton, B.L. and Barnes, C.A. (1977) Physiological identification and analysis of dentate granule cell responses to stimulation of the medial and lateral perforant pathways in the rat. *Journal of Comparative Neurology* 175:439-454.
- McNaughton, B.L., Douglas, R.M. and Goddard, G.V. (1978) Synaptic enhancement in fascia dentata: cooperativity among coactive afferents. *Brain Research* 157:277-293.
- Melander, T., Staines, W.A., Hokfelt, T., Rokaeus, A., Eckenstein, F., Salvaterra, P.M. and Wainer, B.H. (1985) Galanin-like immunoreactivity in cholinergic neurons of the septum-basal forebrain complex projecting to the hippocampus of the rat. *Brain Research* 360:130-138.
- Mellgren, S.I. and Srebro, B. (1973) Changes in acetylcholinesterase and distribution of degenerating fibres in the hippocampal region after septal lesions in the rat. *Brain Research* 52:19-36.
- Mesulam, M.-M. (1988) Central cholinergic pathways: neuroanatomy and some behavioral implications. In: *Neurotransmitters and Cortical Function*, Eds. Avoli, M., Reader, T.A., Dykes, R.W. and Gloor, P. Plenum Press, New York. p. 237-260.
- Miettinen, R. and Freund, T.F. (1992a) Convergence and segregation of septal and median raphe inputs onto different subsets of hippocampal inhibitory interneurons. *Brain Research* 594:263-272.
- Miettinen, R. and Freund, T.F. (1992b) Neuropeptide Y-containing interneurons in the hippocampus receive synaptic input from median raphe and gabaergic septal afferents. *Neuropeptides* 22:185-193.

- Miettinen, R., Gulyas, A.I., Baimbridge, K.G., Jacobowitz, D.M. and Freund, T.F. (1992) Calretinin is present in non-pyramidal cells of the rat hippocampus--II. Co-existence with other calcium binding proteins and GABA. *Neuroscience* 48:29-43.
- Misgeld, U. and Muller, W. (1988) The role of M1 and M2 receptors in slow muscarinic excitation of hippocampal neurons. In: *Synaptic Plasticity in the Hippocampus*, Eds. Haas, H.L. and Buzsaki, G. Springer-Verlag, Berlin. p. 137-139.
- Misgeld, U., Bijak, M., Brunner, H. and Dembowski, K. (1992a) K-dependent inhibition in the dentate-CA3 network of guinea pig hippocampal slices. *Journal of Neurophysiology* 68:1548-1557.
- Misgeld, U., Bijak, M. and Brunner, H. (1992b) Granule cell inhibition and the activity of hilar neurons. In: *The Dentate Gyrus and its Role in Seizures*, Eds. Ribak, C.E., Gall, C.M. and Mody, I. Elsevier, New York. p. 113-118.
- Mizumori, S.J., McNaughton, B.L. and Barnes, C.A. (1989) A comparison of supramammillary and medial septal influences on hippocampal field potentials and single-unit activity. *Journal of Neurophysiology* 61:15-31.
- Mody, I. and Heinemann, U. (1986) Laminar profiles of the changes in extracellular calcium concentration induced by repetitive stimulation and excitatory amino acids in the rat dentate gyrus. *Neuroscience Letters* 69:137-142.
- Monaghan, D.T. and Cotman, C.W. (1985) Distribution of N-methyl-D-aspartate-sensitive L-[3H]glutamate-binding sites in rat brain. *Journal of Neuroscience* 5:2909-2919.
- Morris, R.G.M., Anderson, E., Lynch, G.S. and Baudry, M. (1986) Selective impairment of learning and blockade of long-term potentiation by an N-methyl-D-aspartate receptor antagonist, AP5. *Nature* 319:774-776.
- Mosko, S., Lynch, G. and Cotman, C.W. (1973) The distribution of septal projections to the hippocampus of the. *Journal of Comparative Neurology* 152:163-174.

- Mott, D.D. and Lewis, D.V. (1991) Facilitation of the induction of long-term potentiation by GABA-B receptors. *Science* 252:1718-1720.
- Muller, W. and Misgeld, U. (1990) Inhibitory role of dentate hilus neurons in guinea pig hippocampal slice. *Journal of Neurophysiology* 64:46-56.
- Nafstad, P.H.J. (1967) An electron microscope study on the termination of the perforant path fibres in the hippocampus and the fascia dentata. *Z.Zellforsch.* 76:532-542.
- Naumann, T., Linke, R. and Frotscher, M. (1992) Fine structure of rat septohippocampal neurons: I. Identification of septohippocampal projection neurons by retrograde tracing combined with electron microscopic immunocytochemistry and intracellular staining. *Journal of Comparative Neurology* 325:207-218.
- Nitsch, R., Soriano, E. and Frotscher, M. (1990) The parvalbumin-containing nonpyramidal neurons in the rat hippocampus. *Anatomy and Embryology* 181:413-425.
- Nowak, L., Bregestovski, P., Ascher, P., Herbert, A. and Prochiantz, A. (1984) Magnesium gates glutamate-activated channels in mouse central neurones. *Nature* 307:462-465.
- Nyakas, C., Luiten, P.G.M., Spencer, D.G. and Traber, J. (1987) Detailed projection patterns of septal and diagonal band efferents to the hippocampus in the rat with emphasis on innervation of CA1 and dentate gyrus. *Brain Research Bulletin* 18:533-545.
- O'Keefe, J., and Nadel, L. (1978) *The Hippocampus As A Cognitive Map*. Oxford: Clarendon Press
- Olton, D.S. (1983) Memory functions and the hippocampus. In: *Neurobiology Of The Hippocampus*. Ed. Seifert, W., London, Academic Press.
- Otani, S. and Ben-Ari, Y. (1991) Metabotropic receptor-mediated long-term potentiation in rat hippocampal slices. *European Journal of Pharmacology* 205:325-326.

- Pakhomova, A.S. (1992) Diencephalic afferents of the rat hippocampus. *Neurophysiology* 13:267-273.
- Pasqualotto, B.A. and Vincent, S.R. (1991) Galanin and NADPH-diaphorase coexistence in cholinergic neurons of the rat basal forebrain. *Brain Research* 551:78-86.
- Pasquier, D.A. and Reinoso-Suarez, F. (1976) Direct projections from hypothalamus to hippocampus in the rat demonstrated by retrograde transport of horseradish peroxidase. *Brain Research* 108:165-169.
- Pasquier, D.A. and Reinoso-Suarez, F. (1978) The topographic organization of hypothalamic and brain stem projections to the hippocampus. *Brain Research Bulletin* 3:373-389.
- Pavlidis, C., Greenstein, Y.J., Grudman, M. and Winson, J. (1988a) Long-term potentiation in the dentate gyrus is induced preferentially on the positive phase of theta-rhythm. *Brain Research* 439:383-387.
- Pavlidis, C., Greenstein, Y.J. and Winson, J. (1988b) Comparative extracellular current flow at dendrites and soma of dentate granule cells during long-term potentiation. *Neuroscience Letters* 92:177-181.
- Paxinos, G. and Watson, C. (1986) *The Rat Brain in Stereotaxic Coordinates*. Academic Press, New York.
- Potashner, S.J. (1978) Baclofen: effects on amino acid release. *Canadian Journal of Physiology and Pharmacology* 56:150-154.
- Racine, R., Milgram, N.W. and Hafner, S. (1983) Long-term potentiation phenomena in the rat limbic forebrain. *Brain Research* 260:217-231.
- Racine, R.J. and Milgram, N.W. (1983) Short-term potentiation phenomena in the rat limbic forebrain. *Brain Research* 260:201-216.
- Ramirez, O.A., Orsingher, O.A. and Carrer, H.F. (1988) Differential threshold for long-term potentiation in the hippocampus of rats with inborn high or low learning capacity. *Neuroscience Letters* 92:275-279.

- Ranck, J.B., Jr. (1975) Which elements are excited in electrical stimulation of mammalian central nervous system: a review. *Brain Research* 98:417-440.
- Rawlins, J.N.P. and Green, K.F. (1977) Lamellar organization in the rat hippocampus. *Experimental Brain Research* 28:335-344.
- Ribak, C.E. and Seress, L. (1983) Five types of basket cells in the hippocampal dentate gyrus. A combined Golgi and electron microscopic study. *Journal of Neurocytology* 12:577-597.
- Ribak, C.E., Vaughn, J.E. and Saito, K. (1978) Immunocytochemical localization of glutamic acid decarboxylase in neuronal somata following colchicine inhibition of axonal transport. *Brain Research* 140:315-332.
- Ribak, C.E., Seress, L. and Amaral, D.G. (1985) The development, ultrastructure and synaptic connections of the mossy cells of the dentate gyrus. *Journal of Neurocytology* 14:835-857.
- Richter-Levin, G. and Segal, M. (1990) Effects of serotonin releasers on dentate granule cell excitability in the rat. *Experimental Brain Research* 82:199-207.
- Riekkinen, P., Jr., Sirvio, J., Valjakka, A., Miettinen, R. and Riekkinen, P. (1991) Pharmacological consequences of cholinergic plus serotonergic manipulations. *Brain Research* 552:23-6.
- Riley, J.N. and Moore, R.Y. (1981) Diencephalic and brainstem afferents to the hippocampal formation of the rat. *Brain Research Bulletin* 6:437-444.
- Robinson, G.B. (1986a) Enhanced long-term potentiation induced in rat dentate gyrus by coactivation of septal and entorhinal inputs: temporal constraints. *Brain Research* 379:56-62.
- Robinson, G.B. and Racine, R.J. (1986b) Interactions between septal and entorhinal inputs to the rat dentate gyrus: facilitation effects. *Brain Research* 379:63-67.

- Rose, A.M., Hattori, T. and Fibiger, H.C. (1976) Analysis of the septo-hippocampal pathway by light and electronmicroscope autoradiography. *Brain Research* 108:170-174.
- Rose, G.M., Diamond, D. and Lynch, G.S. (1983) Dentate granule cells in the rat hippocampal formation have the behavioral characteristics of theta neurons. *Brain Research* 266:29-37.
- Rowntree, C.I. and Bland, B.H. (1986) An analysis of cholinceptive neurons in the hippocampus by direct microinfusion. *Brain Research* 362:98-113.
- Ruth, R.E., Collier, T.J. and Routtenberg, A. (1982) Topography between the entorhinal cortex and the dentate septotemporal axis in rats: I. Medial and intermediate entorhinal projection cells. *Journal of Comparative Neurology* 209:69-78.
- Ruth, R.E., Collier, T.J. and Routtenberg, A. (1988) Topographical relationship between the entorhinal cortex and the septo-temporal axis of the dentate gyrus in rats. II Cells projecting from lateral entorhinal subdivisions. *Journal of Comparative Neurology* 270:506-516.
- Ruthrich, H., Dorochoy, W., Pohle, W., Ruthrich, H.L. and Matthies, H. (1987) Colchicine-induced lesion of rat hippocampal granular cells prevents conditioned active avoidance with perforant path stimulation as conditioned stimulus, but not conditioned emotion. *Physiology and Behavior* 40:147-154.
- Rye, D.B., Wainer, B.H., Mesulam, M.-M., Mufson, E.J. and Saper, C.B. (1984) Cortical projections arising from the basal forebrain: a study of cholinergic and non-cholinergic components employing combined retrograde tracing and immunohistochemical localization of choline acetyltransferase. *Neuroscience* 13:627-643.
- Sainsbury, R.S. and Bland, B.H. (1981) Effects of selective septal lesions on theta production in the CA1 and dentate gyrus of the hippocampus. *Physiology and Behavior* 26:1097-1011.
- Sakanaka, M., Shiosaka, S., Takagi, H., Senba, E., Takatsuki, K., Inagaki, S., Yabuuchi, H., Matsuzaki, T. and Tohyama, M. (1980) Topographic organization of the projection from the forebrain subcortical areas to

- the hippocampal formation of the rat. *Neuroscience Letters* 20:253-257.
- Saper, C.B. (1985) Organization of cerebral cortical afferent systems in the rat. II. hypothalamic projections. *Journal of Comparative Neurology* 237:21-46.
- Saper, C.B. (1988) Diffuse cortical projection systems: anatomical organization and role in cortical function. In: *Handbook of Physiology - Nervous System V*. p. 169-210.
- Sara, S.J., Dyon-Laurent, C., Guibert, B. and Leviel, V. (1992) Noradrenergic hyperactivity after partial fornix section: Role in cholinergic dependent memory performance. *Experimental Brain Research* 89:125-132.
- Sarvey, J.M., Burgard, E.C. and Decker, G. (1989) Long-term potentiation: studies in the hippocampal slice. *Journal of Neuroscience Methods* 28:109-124.
- Scharfman, H.E., Kunkel, D.D. and Schwartzkroin, P.A. (1990) Synaptic connections of dentate granule cells and hilar neurons: Results of paired intracellular recordings and intracellular horseradish peroxidase injections. *Neuroscience* 37:693-707.
- Scharfman, H.E. (1991) Dentate hilar cells with dendrites in the molecular layer have lower thresholds for synaptic activation by perforant path than granule cells. *Journal of Neuroscience* 11:1660-1673.
- Scharfman, H.E. (1992) Differentiation of rat dentate neurons by morphology and electrophysiology in hippocampal slices: granule cells, spiny hilar cells and aspiny 'fast spiking' cells. In: *The Dentate Gyrus and Its Role in Seizures*, Eds. Ribak, C.E., Gall, C.M. and Mody, I. Elsevier, New York. p. 93-109.
- Scharfman, H.E. and Schwartzkroin, P.A. (1988) Electrophysiology of morphologically identified mossy cells of the dentate hilus recorded in guinea pig hippocampal slices. *Journal of Neuroscience* 8:3812-3821.

- Scharfman, H.E. (1992) Blockade of excitation reveals inhibition of dentate spiny hilar neurons recorded in rat hippocampal slices. *Journal of Neurophysiology* 68:978-984.
- Scharfman, H.E. and Schwartzkroin, P.A. (1990) Responses of cells of the rat fascia dentata to prolonged stimulation of the perforant path: Sensitivity of hilar cells and changes in granule cell excitability. *Neuroscience* 35:491-504.
- Schmechel, D.E., Vickrey, B.G., Fitzpatrick, D. and Elde, R.P. (1984) GABAergic neurons of mammalian cerebral cortex. Widespread subclass defined by somatostatin content. *Neuroscience Letters* 47:227-232.
- Schoepp, D., Bockaert, J. and Sladeczek, F. (1990) Pharmacological and functional characteristics of metabotropic excitatory amino acid receptors. *Trends in Pharmacological Sciences* 11:508-515.
- Schoepp, D.D. (1993) The biochemical pharmacology of metabotropic glutamate receptors. *Biochemical Society Transactions* 21:97-102.
- Schofield, P.R., Darlison, M.G., Fujita, N., Burt, D.R., Stephenson, F.A., Rodriguez, H., Rhee, L.M., Ramachandran, J., Reale, V., Glencore, T.A., Seeburg, P.H. and Barnard, E.A. (1987) Sequence and functional expression of the GABA-A receptors shows a ligand-gated receptor super-family. *Nature* 328:221-227.
- Schousboe, A., Larsson, O.M., Frandsen, B.B., Pasantés-Morales, H. and Krosgaard-Larsen, P. (1990) Neuromodulatory actions of glutamate, GABA and taurine: regulatory role of astrocytes. In: *Plasticity and Regeneration of the Nervous System*, Ed. Timaras, P.S. Plenum Press, New York. p. 165-180.
- Schwartzkroin, P.A., Scharfman, H.E. and Sloviter, R.S. (1990) Similarities in circuitry between Ammon's horn and dentate gyrus: local interactions and parallel processing. *Progress in Brain Research* 83:269-286.
- Scoville, W.B., and Milner, B. (1957) Loss of recent memory after bilateral hippocampal lesions. *Journal of Neurology, Neurosurgery, and Psychiatry*, 20:11-21.

- Segal, M. (1979) A potent inhibitory monosynaptic hypothalamo-hippocampal connection. *Brain Research* 162:137-141.
- Segal, M. and Landis, S. (1974) Afferents to the hippocampus of the rat studied with the method of retrograde transport of horseradish peroxidase. *Brain Research* 78:1-15.
- Segal, M. (1992) Acetylcholine enhances NMDA-evoked calcium rise in hippocampal neurons. *Brain Research* 587:83-87.
- Senut, M.C., Menetrey, D. and Lamour, Y. (1989) Cholinergic and peptidergic projections from the medial septum and the nucleus of the diagonal band of Broca to dorsal hippocampus, cingulate cortex and olfactory bulb: a combined wheatgerm agglutinin-apohorseradish peroxidase-gold immunohistochemical study. *Neuroscience* 30:385-403.
- Seress, L. and Ribak, C.E. (1983) GABAergic cells in the dentate gyrus appear to be local circuit and projection neurons. *Experimental Brain Research* 50:173-182.
- Seress, L. and Ribak, C.E. (1984) Direct commissural connections to the basket cells of the hippocampal dentate gyrus: anatomical evidence for feed-forward inhibition. *Brain Research* 13:215-225.
- Shin, C., Scialabba, F.A. and McNamara, J.O. (1987) Stimulation of substantia nigra pars reticulata enhances dentate granule cell excitability. *Brain Research* 411:21-27.
- Sloviter, R.S. (1987a) Decreased hippocampal inhibition and a selective loss of interneurons in experimental epilepsy. *Science* 235:173-176.
- Sloviter, R.S. and Nilaver, G. (1987b) Immunocytochemical localization of GABA-, cholecystinin-, vasoactive intestinal polypeptide-, and somatostatin-like immunoreactivity in the area dentata and hippocampus of the rat. *Journal of Comparative Neurology* 256:42-60.
- Sloviter, R.S. (1991) Feedforward and feedback inhibition of hippocampal principal cell activity evoked by perforant path stimulation: GABA-

mediated mechanisms that regulate excitability in vivo. *Hippocampus* 1:31-40.

Smythe, J.W., Colom, L.V. and Bland, B.H. (1992) The extrinsic modulation of hippocampal theta depends on the coactivation of cholinergic and GABA-ergic medial septal inputs. *Neuroscience and Biobehavioral Reviews* 16:289-308.

Soriano, E. and Frotscher, M. (1989) A GABAergic axo-axonic cell in the fascia dentata controls the main excitatory hippocampal pathway. *Brain Research* 503:170-174.

Srebro, B., Azmitia, E.C. and Winson, J. (1982) Effect of 5-HT depletion of the hippocampus on neuronal transmission from PP through DG. *Brain Research* 235:142-147.

Stanton, P.K., Mody, I. and Heinemann, U. (1989) A role for N-methyl-D-aspartate receptors in norepinephrine-induced long-lasting potentiation in the dentate gyrus. *Experimental Brain Research* 77:517-530.

Stanton, P.K., Chattarji, S. and Sejnowski, T.J. (1991) 2-Amino-3-phosphonopropionic acid, an inhibitor of glutamate-stimulated phosphoinositide turnover, blocks induction of homosynaptic long-term depression, but not potentiation, in rat hippocampus. *Neuroscience Letters* 127:61-66.

Steffensen, S.C. and Henriksen, S.J. (1991) Effects of baclofen and bicuculline on inhibition in the fascia dentata and hippocampus regio superior. *Brain Research* 538:46-53.

Stengaard-Pedersen, K., Fredens, K. and Larsson, L.I. (1983) Comparative localization of enkephalin and cholecystokinin immunoreactivities and heavy metals in the hippocampus. *Brain Research* 273:81-96.

Steward, O. and Scoville, S.A. (1976) Cells of origin of entorhinal cortical afferents to the hippocampus and fascia dentata of the rat. *Journal of Comparative Neurology* 169:347-370.

Steward, O. (1976) Topographic organization of the projections from the entorhinal area to the hippocampal formation of the rat. *Journal of Comparative Neurology* 167:285-314.

- Storm-Mathisen, J., Leknes, A.K., Bore, A.T., Vaaland, J.L., Edminson, P., Haug, F.-M.S. and Ottersen, O.P. (1983) First visualization of GABA neurons by immunocytochemistry. *Nature* 301:517-520.
- Struble, R.G., Desmond, N.L. and Levy, W.B. (1978) Anatomical evidence for interlamellar inhibition in the fascia dentata. *Brain Research* 152:580-585.
- Su, H.-S. and Bentivoglio, M. (1990) Thalamic midline cell populations projecting to the nucleus accumbens, amygdala, and hippocampus in the rat. *Journal of Comparative Neurology* 297:582-593.
- Sundstrom, L.E. and Mellanby, J.H. (1990) Tetanus toxin blocks inhibition of granule cells in the dentate gyrus of the urethane-anaesthetized rat. *Neuroscience* 38:621-627.
- Sutherland, R.J. and Rodriguez, A.J. (1989) The role of the fornix/fimbria and some related subcortical structures in place learning and memory. *Behavioural Brain Research* 32:265-277.
- Swanson, L.W. (1982) The anatomy of the septohippocampal pathway. In: *Aging, Vol. 19, Alzheimer's Disease: A Report of Progress in Research*, Eds. Corkin, S., Davis, K.L., Growdon, J.H., Usdin, E. and Wurtman, R.J. Raven Press, New York. p. 207-212.
- Swanson, L.W., Kohler, C. and Bjorklund, A. (1987) The Limbic region. I: The septohippocampal system. In: *Handbook of Chemical Neuroanatomy, Vol. 5, Integrated systems of the CNS. Part I. Hypothalamus, Hippocampus, Amygdala, Retina*, Eds. Swanson, L.W., Kohler, C. and Bjorklund, A. Elsevier, Amsterdam. p. 125-277.
- Tanabe, Y., Masu, M., Ishii, T., Shigemoto, R. and Nakanishi, S. (1992) A family of metabotropic glutamate receptors. *Neuron* 8:169-179.
- Tomasulo, R.A., Levy, W.B. and Steward, O. (1991) LTP-associated EPSP/spike dissociation in the dentate gyrus: GABAergic and non-GABAergic components. *Brain Research* 561:27-34.
- Tomasulo, R.A. and Ramirez, J.J. (1993) Activity-mediated changes in feed-forward inhibition in the dentate commissural pathway: Relationship

- to EPSP/spike dissociation in the converging perforant path. *Journal of Neurophysiology* 69:165-173.
- Tuff, L.P., Racine, R.J. and Adamec, R. (1983) The effects of kindling on GABA-mediated inhibition in the dentate gyrus of the rat. I. Paired-pulse depression. *Brain Research* 277:79-90.
- Valjakka, A., Lukkarinen, K., Koivisto, E., Lammintausta, R., Airaksinen, M.M. and Riekkinen, P. (1991) Evoked field responses, recurrent inhibition, long-term potentiation and immobility-related nonrhythmical EEG in the dentate gyrus of fimbria-fornix-lesioned and control rats. *Brain Research Bulletin* 26:525-532.
- Van der Zee, E.A., Benoit, R., Strosberg, A.D. and Luiten, P.G.M. (1991) Coexistence of muscarinic acetylcholine receptors and somatostatin in nonpyramidal neurons of the rat dorsal hippocampus. *Brain Research Bulletin* 26:343-351.
- Vanderwolf, C.H. (1988) Cerebral activity and behaviour: control by central cholinergic and serotonergic systems. *International Review of Neurobiology* 30:225-339.
- Vertes, R.P. (1986) Brainstem modulation of the hippocampus: anatomy, physiology, and significance. In: *The Hippocampus, Volume 4*, Eds. Isaacson, R.L. and Pribram, K.H. Plenum Press, New York. p. 41-75.
- Vertes, R.P. (1992) PHA-L analysis of projections from the supramammillary nucleus in the rat. *Journal of Comparative Neurology* 326:595-622.
- Wainer, B.H., Levey, A.I., Rye, D.B., Mesulam, M.-M. and Mufson, E.J. (1985) Cholinergic and non-cholinergic septo-hippocampal pathways. *Neuroscience Letters* 54:45-52.
- Watanabe, Y., Himi, T., Saito, H. and Abe, K. (1992) Involvement of glycine site associated with the NMDA receptor in hippocampal long-term potentiation and acquisition of spatial memory in rats. *Brain Research* 582:58-64.
- Welzl, H., Tolle, T.R. and Huston, J.P. (1985) Intracranial application of substances in the unrestrained, awake rat by pressure ejection through glass micropipettes. *Journal of Neuroscience Methods* 13:1-8.

- West, M.J. and Andersen, A.H. (1980) An allometric study of the area dentata in the rat and mouse. *Brain Research Reviews* 2:317.
- White, W.F., Nadler, J.V., Hamberger, A. and Cotman, C.W. (1977) Glutamate as transmitter of hippocampal perforant path. *Nature* 270:356-357.
- Wible, C.G., Shiber, J.R. and Olton, D.S. (1992) Hippocampus, fimbria-fornix, amygdala, and memory: Object discriminations in rats. *Behavioral Neuroscience* 106:751-761.
- Wigstrom, H. and Gustafsson, B. (1983) Facilitated induction of hippocampal long-lasting potentiation during blockade of inhibition. *Nature* 301:603-604.
- Wigstrom, H., Gustafsson, B., Huang, Y.-Y. and Abraham, W.C. (1986) Hippocampal long-term potentiation is induced by pairing single afferent volleys with intracellularly injected depolarizing current pulses. *Acta Physiologica Scandinavica* 126:317-319.
- Winson, J. (1980) Influence of raphe nuclei on neuronal transmission from PP to DG. *Journal of Neurophysiology* 44:917-950.
- Witter, M.P. (1989a) Connectivity of the rat hippocampus. In: *The Hippocampus - New Vistas*. Alan R. Liss, Inc. p. 53-69.
- Witter, M.P., Groenewegen, H.J., Lopes da Silva, F.H. and Lohman, A.H.M. (1989b) Functional organization of the extrinsic and intrinsic circuitry of the parahippocampal region. *Progress in Neurobiology* 33:161-253.
- Woodhams, P.L., Kawano, H. and Raisman, G. (1991) The OM series of terminal field-specific monoclonal antibodies demonstrate innervation of the adult rat dentate gyrus by embryonic entorhinal transplants. *Neuroscience* 46:71-82.
- Woodhams, P.L., Kawano, H., Seeley, P.J., Atkinson, D.J., Field, P.M. and Webb, M. (1992) Monoclonal antibodies reveal molecular differences between terminal fields in the rat dentate gyrus. *Neuroscience* 46:57-69.

- Wouterlood, F.G., Saldana, E. and Witter, M.P. (1990) Projection from the nucleus reuniens thalami to the hippocampal region: Light and electron microscopic tracing study in the rat with the anterograde tracer Phaseolus vulgaris- leucoagglutinin. *Journal of Comparative Neurology* 296:179-203.
- Wyss, J.M., Swanson, L.W. and Cowan, W.M. (1979a) A study of subcortical afferents to the hippocampal formation of the rat. *Neuroscience* 4:463-476.
- Wyss, J.M., Swanson, L.W. and Cowan, W.M. (1979b) Evidence for an input to the molecular layer and the stratum granulosum of the dentate gyrus from the supramammillary region of the hypothalamus. *Anatomy and Embryology* 156:165-176.
- Wyss, J.M. (1981) An autoradiographic study of the efferent connections of the entorhinal cortex in the rat. *Journal of Comparative Neurology* 199:495-512.
- Yamano, M. and Luiten, P.G. (1989) Direct synaptic contacts of medial septal efferents with somatostatin immunoreactive neurons in the rat hippocampus. *Brain Research Bulletin* 22:993-1001.
- Yanagihara, M. and Niimi, K. (1989) Substance P-like immunoreactive projection to the hippocampal formation from the posterior hypothalamus in the cat. *Brain Research Bulletin* 22:689-694.
- Yeckel, M.F. and Berger, T.W. (1990) Feedforward excitation of the hippocampus by afferents from the entorhinal cortex: Redefinition of the role of the trisynaptic pathway. *Proceedings of the National Academy of Sciences* 87:5832-5836.
- Yoon, K.-W. and Rothman, S.M. (1991) The modulation of rat hippocampal synaptic conductances by baclofen and gamma-aminobutyric acid. *Journal of Physiology* 442:377-390.
- Yoshida, K. and Oka, H. (1990) Topographical distribution of septohippocampal projections demonstrated by the PHA-L immunohistochemical method in rats. *Neuroscience Letters* 113:247-252.

- Zheng, F. and Gallagher, J.P. (1992) Metabotropic glutamate receptors are required for the induction of long-term potentiation. *Neuron* 9:163-172.
- Zipp, F., Nitsch, R., Soriano, E. and Frotscher, M. (1989) Entorhinal fibers form synaptic contacts on parvalbumin-immunoreactive neurons in the rat fascia dentata. *Brain Research* 495:161-166.

APPENDIX I: ASYST program for evoked potential data acquisition.

```
ERROR.TRACE.ON
```

```
ECHO.OFF
```

```
\ written for RC A/D board
```

```
\ uses code.exe as external assembly code for fast read.
```

```
\ therefore code.exe must be in default drive.
```

```
\ program written to analyse dentate population spike.
```

```
7 1 FIX.FORMAT
```

```
: WAIT.FOR.KEY
```

```
KEY 0 = IF KEY DROP THEN ; \ loops until any key is pressed
```

```
integer dim[ 2400 ] array a1          \ to store data from A/D board
```

```
0 a1 :=
```

```
integer dim[ 40 ] array PROGRAM.ARRAY \ to store assembly read prog.
```

```
0 PROGRAM.ARRAY :=
```

```
PROGRAM.ARRAY LOAD.EXE c:\ASYST\CODE.EXE \ load assembly read program
```

```
integer scalar off.set      \ variables for read prog.
```

```
scalar defs
```

```
scalar data.offset
```

```
scalar data.seg
```

```
PROGRAM.ARRAY address off.set := defs :=
```

```
\ **** set display windows ****
```

```
3 4 5 78 WINDOW {HEADER1}
```

```
6 4 13 78 WINDOW {DATA1}
```

```
15 4 15 78 WINDOW {HEADER2}
```

```
16 4 18 78 WINDOW {DATA2}
```

```
20 4 20 78 WINDOW {HEADER3}
```

```
21 4 21 78 WINDOW {DATA3}
```

```
23 4 24 60 WINDOW {MESS}
```

```
23 61 24 78 WINDOW {FLAG}
```

```
\ **** setup RC data acquisition board ****
```

```
: trigger.setup      \ poke a machine language interrupt service
```

```
29931 def.seg \ routine into memory at the defined segment
```

```
30 0 poke \ (&h74EB). This routine stores a value of 1
```

```
87 1 poke \ into memory address &h74EE0 whenever a low
```

```
80 2 poke \ to high transition occurs on IRQ3.
```

```

184 3 poke
238 4 poke \ new address 74EE0 (478,944) for flag check
116 5 poke
142 6 poke
216 7 poke \ note, this routine is written in memory at
191 8 poke \ 478,896 to 478,944, high in the area that
0 9 poke \ ASYST reserves for the user dictionary, which
0 10 poke \ is unlikely to fill. Check with "?memory".
198 11 poke
5 12 poke
1 13 poke
176 14 poke
32 15 poke
230 16 poke
32 17 poke
88 18 poke
95 19 poke
31 20 poke
207 21 poke
\ set IRQ3 interrupt vector to &h74EB0
0 def.seg
0 44 poke
0 45 poke
235 46 poke
116 47 poke
\ enable interrupt request IRQ3
33 port.in dup 8 / integer
dup 2 / integer 2 *
< > if 8 - 33 port.out then ;

: disable.scope
0 779 port.out ; \ stop acquisition

: load.mux
8 0 do 0 784 port.out 1 784 port.out loop ; \ use input #1&2

: set.trigger
205 769 port.out \ set trigger threshold to 1 V (LSB,MSB)
8 770 port.out
9 794 port.out \ select trigger channel 2
0 785 port.out \ internal sample clock select
10 776 port.out ; \ trigger slope, internal trigger, positive polarity

: set.clock
116 775 port.out \ set internal clock to sample every 10 us
10 773 port.out \ LSB
0 773 port.out ; \ MSB

```

```

: set.burst
  50 775 port.out  \ sample both channels on each clock pulse
  2 772 port.out
  0 772 port.out ;

: set.post.trigger  \ sample 4096 points
  178 775 port.out
  0 774 port.out
  16 774 port.out ;

: set.bank.mem
  0 789 port.out  \ select bank B , manual bank switching
  04 795 port.out ; \ select 4K sample size for RC buffer

: trigger.flag  \ put a 0 into memory reserved for trigger flag status
  29934 def.seg
  0 0 poke ;

: start.acquisition  \ start reading data from channels 1 & 2
  0 778 port.out
  10 msec.delay
  0 780 port.out ;

: trigger.check  \ check mem for trigger flag status
  29934 def.seg
  begin 0 peek 0 < > until
  10 msec.delay ;

: new.read
  0 788 port.out call[ defs , off.set , 2400 , a1 ] ; \ read data

: setup.final  \ to initialize board
  trigger.setup
  disable.scope
  load.mux
  set.trigger
  set.clock
  set.burst
  set.post.trigger ;

\ **** remove trigger channel data from data array and place in waveform ****

integer scalar counter
integer dim[ 1200 ] array waveform

0.1 SET.CUTOFF.FREQ \ for smooth function

: fill.data  \ take info from channel 1 and place into array waveform

```

```

0 WAVEFORM :=
a1 SUB[ 1 , 1200 , 2 ] waveform := \ place every odd value into array
;

: GO          \ to start aquisition
  set.bank.mem
  trigger.flag
  start.acquisition
  trigger.check
  new.read
  fill.data ;

\ **** routines for spike delineation by user ****

INTEGER SCALAR MARK1
      SCALAR MARK2
      SCALAR MARK3 \ mark2 - mark1 = size of waveform.sub
      SCALAR GAIN

20 STRING FILENAME
8 STRING DRIVE

: INTRO
  NORMAL.DISPLAY
  SCREEN.CLEAR
  ." Enter the latencies (in us) necessary to calculate field" CR
  ." potential stats. Terminate each entry with <CR> . " CR
  CR ;

: GET.EPSP.START
  CR
  ." EPSP starts at:-->"
  BEGIN
  #INPUT NOT
  WHILE
  CR ." Invalid number, reenter: "
  REPEAT
  MARK1 :=
  CR ;

: GET.AMP.GAIN
  CR
  ." The amplifier gain is:-->"
  BEGIN
  #INPUT NOT
  WHILE
  CR ." Invalid number, reenter: "
  REPEAT

```

```

GAIN :=
CR ;

: USER.SETUP      \ get popspike delineators from user
INTRO
GET.EPSP.START
GET.AMP.GAIN
CR
." EPSP starts at      " MARK1 . CR
." Amp gain is        " GAIN . CR CR
." Are these numbers correct? (N = no, any other key = yes) "
KEY                \ if user responds with n or N, restart user.setup
CASE
  78 OF MYSELF ENDOF
  110 OF MYSELF ENDOF
    SCREEN.CLEAR
ENDCASE ;

\ **** create subarray after EPSP-start mark for data analysis ****

TOKEN WAVEFORM.SUB

: MAKE.SUB
MARK1 10 / MARK2 := \ change from time to index
1200 MARK2 - MARK3 :=
WAVEFORM SUB[ MARK2 , MARK3 , 1 ] BECOMES> WAVEFORM.SUB
WAVEFORM.SUB SMOOTH WAVEFORM.SUB :=
;

\ **** calculate parameters ****

INTEGER SCALAR POP.START
  SCALAR POP.START.INDEX
  SCALAR POP.PEAK
  SCALAR POP.PEAK.INDEX
  SCALAR POP.LATENCY
  SCALAR PEAK.LATENCY
  SCALAR POINTER1
  SCALAR POINTER2
  SCALAR POINTER
  SCALAR MARKER
  SCALAR B

REAL SCALAR POP.TALL
  SCALAR POP.HEIGHT
  SCALAR NUMER
  SCALAR NUMERV
  SCALAR EPSP.SLOPE

```

\ * variables for added parameters including pop size to line between 2 peaks

```

INTEGER SCALAR EPSP.PEAK
    SCALAR EPSP.PEAK.INDEX
INTEGER SCALAR CHECK
REAL SCALAR PEAK.DIFF
    SCALAR INDEX.DIFF
    SCALAR POINT1.LINE
    SCALAR POINT2.LINE
    SCALAR LINE.INC
    SCALAR START.VALUE.LINE
    SCALAR POP.SIZE.LINE
    SCALAR AREA

```

```

TOKEN PEAK.LINE
TOKEN RAM.LINE

```

```

REAL SCALAR POP.HEIGHT.LINE
    SCALAR EPSP.HEIGHT
    SCALAR EPSP.LATENCY

```

```

: CALC.POP \ find max point in pre-pop EPSP (CASE = 1) and store value and index
    \ find min point in popspike (CASE = 2) and store...index
    \ find max point in EPSP (CASE = 3) and store...index
1 POINTER := \ set flag = 1 so that it looks for max first
0 POP.START := \ to store max value, 0 so that orig. value never exceeds max
5000 POP.PEAK := \ to store min, 5000 so orig. value never lower than min
0 EPSP.PEAK :=
MARK3 1 DO
POINTER
CASE
1 OF \ find max
    WAVEFORM.SUB [ I ] POP.START > =
    IF
        WAVEFORM.SUB [ I ] POP.START := \ if greater than store new value
        I POP.START.INDEX :=
    ELSE \ if not greater, then we have peek
        2 POINTER :=
    THEN
ENDOF
2 OF \ same logic as in CASE = 1 but look now for min instead of max
    WAVEFORM.SUB [ I ] POP.PEAK < =
    IF
        WAVEFORM.SUB [ I ] POP.PEAK :=
        I POP.PEAK.INDEX :=
    ELSE
        3 POINTER :=

```

```

    THEN
    ENDOF
3 OF          \ find max of post-spike EPSP
    WAVEFORM.SUB [ I ] EPSP.PEAK > =
    IF
        WAVEFORM.SUB [ I ] EPSP.PEAK :=
        I EPSP.PEAK.INDEX :=
    ELSE
        LEAVE \ breakout of larger loop, min & max's found
    THEN
    ENDOF
ENDCASE
LOOP
;

: CALC.EPSP.SLOPE
POP.START.INDEX 75 - POINTER1 :=          \ get pt 750us behind onset
POP.START.INDEX 45 - POINTER2 :=          \ get pt 450us behind onset
POINTER1 1 <
IF
    1 POINTER1 :=
    30 POINTER2 :=
    {MESS} CR
    INTEN.ON
    ." " CR
    ." Slope narrow, took slope from first pt to 300th."
    INTEN.OFF
THEN
    WAVEFORM.SUB [ POINTER2 ] WAVEFORM.SUB [ POINTER1 ] - NUMER := \ find diff
    NUMER .001221 * GAIN / 1000000 * NUMERV :=          \ convert to millivolts
    NUMERV 0.3 / EPSP.SLOPE :=          \ slope in uv/ms
;

INTEGER SCALAR POINT1.INDEX
        SCALAR POINT2.INDEX

REAL SCALAR INC1
        SCALAR INC2
        SCALAR MAXV
\ SCALAR TIME.START

: FIND.LINE
POINT2.LINE POINT1.LINE - PEAK.DIFF :=
POINT2.INDEX POINT1.INDEX - INDEX.DIFF :=
PEAK.DIFF INDEX.DIFF / LINE.INC :=          \ slope of "tangent"
POINT1.LINE POINT1.INDEX LINE.INC * - START.VALUE.LINE :=
RAM.LINE LINE.INC * START.VALUE.LINE + BECOMES> PEAK.LINE
1 CHECK :=

```

```

1 MAXV :=
POINT1.INDEX 50 + POINT1.INDEX 50 - DO
  WAVEFORM.SUB [ I ] PEAK.LINE [ I ] - MAXV >
  IF
    WAVEFORM.SUB [ I ] PEAK.LINE [ I ] - MAXV :=
    1 POINT1.INDEX :=
    2 CHECK :=
  THEN
LOOP
MAXV INC1 :=
1 MAXV :=
POINT2.INDEX 50 + POINT2.INDEX 50 - DO
  WAVEFORM.SUB [ I ] PEAK.LINE [ I ] - MAXV >
  IF
    WAVEFORM.SUB [ I ] PEAK.LINE [ I ] - MAXV :=
    1 POINT2.INDEX :=
    2 CHECK :=
  THEN
LOOP
MAXV INC2 :=
\ REL.TIME TIME.START - 5000 >           \ check in case potential
\ IF                                     \ has no spike
\ STACK.CLEAR                           \
\ {MESS} ." Unable to find tangent" CR {DATA1} \
\ THEN                                   \
2 CHECK =
IF
  PEAK.LINE [ POINT1.INDEX ] INC1 + POINT1.LINE :=
  PEAK.LINE [ POINT2.INDEX ] INC2 + POINT2.LINE :=
  STACK.CLEAR
  MYSELF
THEN

ONERR: {DEF}
;

: FIND.AREA
0 AREA :=
POINT2.INDEX POINT1.INDEX DO
  PEAK.LINE [ I ] WAVEFORM.SUB [ I ] - AREA + AREA :=
LOOP
PEAK.LINE [ POP.PEAK.INDEX ] WAVEFORM.SUB [ POP.PEAK.INDEX ] -
  POP.SIZE.LINE :=
;

: CONVERT.PARAMS
POP.START POP.PEAK - POP.TALL :=

```

```

POP.TALL .001221 * GAIN / 1000000 * POP.HEIGHT := \ convert to microvolts
POP.START.INDEX 10 * MARK1 + POP.LATENCY := \ convert to microsecs
POP.PEAK.INDEX 10 * MARK1 + PEAK.LATENCY := \ convert to microsecs
POP.SIZE.LINE .001221 * GAIN / 1000000 * POP.HEIGHT.LINE :=
EPSP.PEAK .001221 * GAIN / 1000000 * EPSP.HEIGHT :=
EPSP.PEAK.INDEX 10 * MARK1 + EPSP.LATENCY :=
AREA .001221 * GAIN / 1000 * AREA := ; \ convert to millivolts

: GO2
MAKE.SUB
CALC.POP
CALC.EPSP.SLOPE
POP.START POINT1.LINE :=
POP.START.INDEX POINT1.INDEX :=
EPSP.PEAK POINT2.LINE :=
EPSP.PEAK.INDEX POINT2.INDEX :=
MARK3 REAL RAMP BECOMES> RAM.LINE \ create base array for tangent
\ REL.TIME TIME.START := \ used for time check in FIND.LINE
FIND.LINE
FIND.AREA
CONVERT.PARAMS ;

\ **** set display up ****

: WINDOWS.SET
NORMAL.DISPLAY
{DATA1} {BORDER}
{DATA2} {BORDER}
{DATA3} {BORDER}
{HEADER1} SCREEN.CLEAR ." POP# SLOPE POP PEAK POP EPSP POP
AREA" CR
                ."          START LATENCY SIZE LATENCY HEIGHT" CR
                ."          uv/ms us us uv us uv mv "
{HEADER2} SCREEN.CLEAR ." mean for 60 spikes prior to last flag (+ 95% conf.limits)"
{HEADER3} SCREEN.CLEAR ." mean for last 6 spikes"
INTEN.ON
{DEF}
1 1 GOTO.XY ." F:flag;"
    ." S:stop;"
    ." P:print spike;"
    ." M:mean last 6;"
    ." W:peek wave;"
    ." L:pause;"
    ." D:save prev. wave"
1 2 GOTO.XY ." Trends:"
    ." (1) slope "
    ." (2) start "

```

```

        ." (3) peak lat "
        ." (4)/(6) pop size "
        ." (5) late peak "
        ." (7) area"
{MESS}
." No message"
INTEN.OFF
{DATA1} CR ;

TEXT.BUFFER SCREEN.IMAGE \ to allow switching of video pages for peek at wave

: WAVEFORM.PEEK
SCREEN.IMAGE STORE.VIDEO \ store data screen
GRAPHICS.DISPLAY      \ plot present waveform
WAVEFORM.SUB Y.AUTO.PLOT
PEAK.LINE Y.DATA.PLOT
5000 MSEC.DELAY      \ display for 5 seconds
NORMAL.DISPLAY
SCREEN.IMAGE RESTORE.VIDEO ; \ restore data page as it was

INTEGER SCALAR POP#
    SCALAR COUNTER2
    SCALAR FLAG.INDEX
    SCALAR A
    SCALAR FLAG.MARKER

REAL    SCALAR SLOPE.MEAN
    SCALAR POP.SIZE.MEAN
    SCALAR START.POP.MEAN
    SCALAR PEAK.TIME.MEAN
    SCALAR SLOPE.DEV
    SCALAR SLOPE.UPPER.LIMIT
    SCALAR SLOPE.LOWER.LIMIT
    SCALAR START.POP.DEV
    SCALAR START.POP.UPPER.LIMIT
    SCALAR START.POP.LOWER.LIMIT
    SCALAR PEAK.TIME.DEV
    SCALAR PEAK.TIME.UPPER.LIMIT
    SCALAR PEAK.TIME.LOWER.LIMIT
    SCALAR POP.SIZE.DEV
    SCALAR POP.SIZE.UPPER.LIMIT
    SCALAR POP.SIZE.LOWER.LIMIT

INTEGER DIM[ 2000 ] ARRAY START.POP
INTEGER DIM[ 2000 ] ARRAY PEAK.TIME
REAL DIM[ 2000 ] ARRAY SLOPE
REAL DIM[ 2000 ] ARRAY POP.SIZE

```

```

INTEGER DIM[ 30 ] ARRAY FLAG      \ SETS LIMIT OF 30 FLAGS
REAL DIM[ 10 ] ARRAY ARRAY1
REAL DIM[ 10 ] ARRAY ARRAY3
INTEGER DIM[ 6 ] ARRAY ARRAY5
INTEGER DIM[ 6 ] ARRAY ARRAY7
INTEGER DIM[ 2 ] ARRAY KEEPER
REAL DIM[ 10 ] ARRAY ARRAY2
REAL DIM[ 10 ] ARRAY ARRAY4
REAL DIM[ 6 ] ARRAY ARRAY6
REAL DIM[ 6 ] ARRAY ARRAY8
O START.POP :=
O PEAK.TIME :=
O SLOPE :=
O POP.SIZE :=
O FLAG :=
O KEEPER :=

```

\ *variables for added parameters such as pop size to line between two curves

```

REAL SCALAR EPSP.PEAK.MEAN
  SCALAR EPSP.PEAK.DEV
  SCALAR EPSP.PEAK.UPPER.LIMIT
  SCALAR EPSP.PEAK.LOWER.LIMIT
  SCALAR EPSP.PEAK.TIME.MEAN
  SCALAR EPSP.PEAK.TIME.DEV
  SCALAR EPSP.PEAK.TIME.UPPER.LIMIT
  SCALAR EPSP.PEAK.TIME.LOWER.LIMIT
  SCALAR POP.SIZE.LINE.MEAN
  SCALAR POP.SIZE.LINE.DEV
  SCALAR POP.SIZE.LINE.UPPER.LIMIT
  SCALAR POP.SIZE.LINE.LOWER.LIMIT
  SCALAR AREA.MEAN
  SCALAR AREA.DEV
  SCALAR AREA.UPPER.LIMIT
  SCALAR AREA.LOWER.LIMIT

```

```

REAL DIM[ 2000 ] ARRAY EPSP.LAT
  DIM[ 2000 ] ARRAY POP.PERP.SIZE
  DIM[ 2000 ] ARRAY AREA.ARRAY
  DIM[ 10 ] ARRAY ARRAY10
  DIM[ 10 ] ARRAY ARRAY11
  DIM[ 10 ] ARRAY ARRAY15
  DIM[ 6 ] ARRAY ARRAY12
  DIM[ 6 ] ARRAY ARRAY13
  DIM[ 6 ] ARRAY ARRAY14
  DIM[ 6 ] ARRAY ARRAY16

```

```

0 EPSP.LAT :=
0 POP.PERP.SIZE :=
0 AREA.ARRAY :=

: WRITE.DATA
| 1 =
IF
  OUT>FILE C:\JUNK\DATA.TXT
ELSE
  OUT>FILE.CONT
THEN
{DATA1}
POP# .
1 SPACES
EPSP.SLOPE .
POP.LATENCY .
3 SPACES PEAK.LATENCY .
2 SPACES POP.HEIGHT .
2 SPACES EPSP.LATENCY .
2 SPACES POP.HEIGHT.LINE .
2 SPACES AREA . CR
CONSOLE
;

: CALC.PRE.MEAN
1 FLAG.MARKER = \ check to see if at least 1 flag has been set
IF
FLAG [ COUNTER2 ] 60 - FLAG.INDEX :=
1 COUNTER :=
FLAG [ COUNTER2 ] FLAG.INDEX DO \ fill array with 60 pts prior to last flag
START.POP SUB[ 1 , 6 , 1 ] MEAN ARRAY1 [ COUNTER ] :=
SLOPE SUB[ 1 , 6 , 1 ] MEAN ARRAY2 [ COUNTER ] :=
PEAK.TIME SUB[ 1 , 6 , 1 ] MEAN ARRAY3 [ COUNTER ] :=
POP.SIZE SUB[ 1 , 6 , 1 ] MEAN ARRAY4 [ COUNTER ] :=
EPSP.LAT SUB[ 1 , 6 , 1 ] MEAN ARRAY10 [ COUNTER ] :=
POP.PERP.SIZE SUB[ 1 , 6 , 1 ] MEAN ARRAY11 [ COUNTER ] :=
AREA.ARRAY SUB[ 1 , 6 , 1 ] MEAN ARRAY15 [ COUNTER ] :=
1 COUNTER + COUNTER :=
6 +LOOP
ARRAY1 MEAN START.POP.MEAN := \ calculate means for each variable
ARRAY2 MEAN SLOPE.MEAN :=
ARRAY3 MEAN PEAK.TIME.MEAN :=
ARRAY4 MEAN POP.SIZE.MEAN :=
ARRAY10 MEAN EPSP.PEAK.TIME.MEAN :=
ARRAY11 MEAN POP.SIZE.LINE.MEAN :=
ARRAY15 MEAN AREA.MEAN :=
ARRAY1 SAMPLE.VARIANCE SQRT START.POP.DEV :=
ARRAY2 SAMPLE.VARIANCE SQRT SLOPE.DEV :=

```

```

ARRAY3 SAMPLE.VARIANCE SQRT PEAK.TIME.DEV :=
ARRAY4 SAMPLE.VARIANCE SQRT POP.SIZE.DEV :=
ARRAY10 SAMPLE.VARIANCE SQRT EPSP.PEAK.TIME.DEV :=
ARRAY11 SAMPLE.VARIANCE SQRT POP.SIZE.LINE.DEV :=
ARRAY15 SAMPLE.VARIANCE SQRT AREA.DEV :=
  \ calc upper confidence limit for .95, two-tailed
SLOPE.DEV 5 SQRT / 2.57 * SLOPE.MEAN +
  SLOPE.UPPER.LIMIT :=
SLOPE.DEV 5 SQRT / 2.57 * SLOPE.MEAN -
  ABS SLOPE.LOWER.LIMIT :=
POP.SIZE.DEV 5 SQRT / 2.57 * POP.SIZE.MEAN +
  POP.SIZE.UPPER.LIMIT :=
POP.SIZE.DEV 5 SQRT / 2.57 * POP.SIZE.MEAN -
  ABS POP.SIZE.LOWER.LIMIT :=
START.POP.DEV 5 SQRT / 2.57 * START.POP.MEAN +
  START.POP.UPPER.LIMIT :=
START.POP.DEV 5 SQRT / 2.57 * START.POP.MEAN -
  ABS START.POP.LOWER.LIMIT :=
PEAK.TIME.DEV 5 SQRT / 2.57 * PEAK.TIME.MEAN +
  PEAK.TIME.UPPER.LIMIT :=
PEAK.TIME.DEV 5 SQRT / 2.57 * PEAK.TIME.MEAN -
  ABS PEAK.TIME.LOWER.LIMIT :=
EPSP.PEAK.TIME.DEV 5 SQRT / 2.57 * EPSP.PEAK.TIME.MEAN +
  EPSP.PEAK.TIME.UPPER.LIMIT :=
POP.SIZE.LINE.DEV 5 SQRT / 2.57 * POP.SIZE.LINE.MEAN +
  POP.SIZE.LINE.UPPER.LIMIT :=
AREA.DEV 5 SQRT / 2.57 * AREA.MEAN + AREA.UPPER.LIMIT :=
EPSP.PEAK.TIME.DEV 5 SQRT / 2.57 * EPSP.PEAK.TIME.MEAN -
  ABS EPSP.PEAK.TIME.LOWER.LIMIT :=
POP.SIZE.LINE.DEV 5 SQRT / 2.57 * POP.SIZE.LINE.MEAN -
  ABS POP.SIZE.LINE.LOWER.LIMIT :=
AREA.DEV 5 SQRT / 2.57 * AREA.MEAN - ABS AREA.LOWER.LIMIT :=
{DATA2} SCREEN.CLEAR      \ set window

```

```

." UPPER " SLOPE.UPPER.LIMIT . START.POP.UPPER.LIMIT . 3 SPACES
PEAK.TIME.UPPER.LIMIT . 2 SPACES POP.SIZE.UPPER.LIMIT .
2 SPACES EPSP.PEAK.TIME.UPPER.LIMIT . 2 SPACES
POP.SIZE.LINE.UPPER.LIMIT .
2 SPACES AREA.UPPER.LIMIT . CR

```

```

." MEAN " SLOPE.MEAN . START.POP.MEAN . 3 SPACES PEAK.TIME.MEAN .
2 SPACES POP.SIZE.MEAN .
2 SPACES EPSP.PEAK.TIME.MEAN . 2 SPACES
POP.SIZE.LINE.MEAN .
2 SPACES AREA.MEAN . CR

```

```

." LOWER " SLOPE.LOWER.LIMIT . START.POP.LOWER.LIMIT . 3 SPACES
PEAK.TIME.LOWER.LIMIT . 2 SPACES POP.SIZE.LOWER.LIMIT .

```

```

2 SPACES EPSP.PEAK.TIME.LOWER.LIMIT . 2 SPACES
POP.SIZE.LINE.LOWER.LIMIT .
2 SPACES AREA.LOWER.LIMIT .
ELSE
{MESS} CR \ if no flags have been set print message
INTEN.ON
." NO FLAG HAS BEEN SET YET "
INTEN.OFF
BELL
THEN ;

: CALC.LAST.MEAN \ same as above but calc mean of last six
POP# 6 - A :=
1 COUNTER :=
POP# A DO
START.POP [ I ] ARRAY5 [ COUNTER ] :=
SLOPE [ I ] ARRAY6 [ COUNTER ] :=
PEAK.TIME [ I ] ARRAY7 [ COUNTER ] :=
POP.SIZE [ I ] ARRAY8 [ COUNTER ] :=
EPSP.LAT [ I ] ARRAY13 [ COUNTER ] :=
POP.PERP.SIZE [ I ] ARRAY14 [ COUNTER ] :=
AREA.ARRAY [ I ] ARRAY16 [ COUNTER ] :=
1 COUNTER + COUNTER :=
LOOP
ARRAY5 MEAN START.POP.MEAN :=
ARRAY6 MEAN SLOPE.MEAN :=
ARRAY7 MEAN PEAK.TIME.MEAN :=
ARRAY8 MEAN POP.SIZE.MEAN :=
ARRAY13 MEAN EPSP.PEAK.TIME.MEAN :=
ARRAY14 MEAN POP.SIZE.LINE.MEAN :=
ARRAY16 MEAN AREA.MEAN :=
{DATA3} SCREEN.CLEAR \ set window
7 SPACES SLOPE.MEAN .
START.POP.MEAN . 3 SPACES
PEAK.TIME.MEAN . 2 SPACES
POP.SIZE.MEAN .
2 SPACES EPSP.PEAK.TIME.MEAN .
2 SPACES POP.SIZE.LINE.MEAN .
2 SPACES AREA.MEAN . ;

: SET.FLAG
I 60 <
IF
{MESS} CR
INTEN.ON
." YOU DON'T HAVE 60 POPSPIKES!
INTEN.OFF
BELL

```

```

ELSE
  COUNTER2 1 + COUNTER2 := \ if "F" pressed save pop spike #
  I FLAG [ COUNTER2 ] :=
  1 FLAG.MARKER :=          \ put 1 into var to denote flag placed
  4 1 FIX.FORMAT
  {FLAG} CR INTEN.ON ." FLAG#" COUNTER2 . ." POP#" I . INTEN.OFF
  7 1 FIX.FORMAT
  CALC.PRE.MEAN
  THEN ;

: PRINT.SCREEN
SCREEN.PRINT

ONERR: NORMAL.DISPLAY
  ." PRINTER ERROR!!!!"
  ." PRESS ANY KEY TO RETURN TO AQUISITION"
  BELL PCKEY DROP
;

: PRINT.POP
SCREEN.IMAGE STORE.VIDEO
NORMAL.DISPLAY
  ." MAKE SURE THAT TOSHIBA IS IN PROPRINTER EMULATION" CR
  ." AND HIT ANY KEY"
GRAPHICS.DISPLAY
WAVEFORM Y.AUTO.PLOT
5 23 GOTO.XY
  ." Date: " .DATE ." Pop #: " POP# .
PRINT.SCREEN \ word to print the screen with error routine to protect
  \ data accumulated.
NORMAL.DISPLAY
SCREEN.IMAGE RESTORE.VIDEO ;

REAL DIM[ 2000 ] ARRAY VAR
INTEGER SCALAR U
65 STRING TITLE

: SHOW.TREND          \ added 9/90
SCREEN.IMAGE STORE.VIDEO
GRAPHICS.DISPLAY
I 200 < IF
  1 U :=
  ELSE
  I 200 - U :=
  THEN
  " +" SYMBOL
VAR SUB[ U , 200 , 1 ] Y.AUTO.PLOT
NORMAL.COORDS

```

```

.20 .96 POSITION TITLE LABEL
WAIT.FOR.KEY
NORMAL.DISPLAY
SCREEN.IMAGE RESTORE.VIDEO
;

16 STRING FILENAME2
INTEGER DIM[ 1200 ] ARRAY WAVEFORM.2ND

: WAVE.TO.DISK \ save previous popspike to disk -added 10/90
LOAD.OVERLAY DATAFILE.SOV
" C:\JUNK\POP#"
I 1 - 100 <
IF
" 00" "CAT
2 0 FIX.FORMAT
ELSE
I 1 - 1000 <
IF
" 0" "CAT
3 0 FIX.FORMAT
ELSE
4 0 FIX.FORMAT
THEN
THEN
POP# "." "CAT FILENAME2 " := \ note: saves to subdir JUNK
FILE.TEMPLATE
1 COMMENTS
WAVEFORM.2ND []FORM.SUBFILE
END
FILENAME2 DEFER> FILE.CREATE
FILENAME2 DEFER> FILE.OPEN
1 SUBFILE WAVEFORM.2ND ARRAY>FILE
FILE.CLOSE
7 1 FIX.FORMAT ;

: MECHANICS
SETUP.FINAL
USER.SETUP
WINDOWS.SET
0 FLAG.MARKER := \ puts 0 into variable signifying no flag set yet
0 COUNTER2 := \ keeps track of # of flags
2000 1 DO \ note: sets upper limit of 2000 pop spikes
GO
GO2
POP.LATENCY START.POP [ I ] := \ fill data arrays
EPSP.SLOPE SLOPE [ I ] :=

```

```

PEAK.LATENCY PEAK.TIME [ 1 ] :=
POP.HEIGHT POP.SIZE [ 1 ] :=
EPSP.LATENCY EPSP.LAT [ 1 ] :=
POP.HEIGHT.LINE POP.PERP.SIZE [ 1 ] :=
AREA AREA.ARRAY [ 1 ] :=
I POP# := \ keep track of popspike #
?KEY IF \ check to see if a key was pressed
KEY \ if yes get the key's ASCII #
CASE \ check # with user "function" keys
  70 OF SET.FLAG ENDOF
  102 OF SET.FLAG ENDOF
  83 OF I KEEPER [ 1 ] := COUNTER2 KEEPER [ 2 ] := \ if "S" leave word and
    EXIT ENDOF \ store # of pops and
  115 OF I KEEPER [ 1 ] := COUNTER2 KEEPER [ 2 ] := \ flags
    EXIT ENDOF
  80 OF PRINT.POP ENDOF \ if "P" calc and display preflag mean
  112 OF PRINT.POP ENDOF
  76 OF {MESS} SCREEN.CLEAR ." Pause on, strike any key" WAIT.FOR.KEY
SCREEN.CLEAR
  ." Pause off" ENDOF \ if L then pause collection of data
  108 OF {MESS} SCREEN.CLEAR ." Pause on, strike any key" WAIT.FOR.KEY
SCREEN.CLEAR
  ." Pause off" ENDOF
  77 OF CALC.LAST.MEAN ENDOF \ if "M" calc and display mean of last 6
  109 OF CALC.LAST.MEAN ENDOF
  87 OF WAVEFORM.PEEK ENDOF \ if "W" show waveform
  119 OF WAVEFORM.PEEK ENDOF
  68 OF WAVE.TO.DISK ENDOF \ if "D" save previous wave to disk
  100 OF WAVE.TO.DISK ENDOF
\ following choices allow glancing at trend (last 200 points)
  49 OF SLOPE VAR :=
    " LAST 200 POINTS FOR SLOPE" TITLE " :=
    SHOW.TREND ENDOF
  50 OF START.POP VAR :=
    " LAST 200 POINTS FOR POP START" TITLE " :=
    SHOW.TREND ENDOF
  51 OF PEAK.TIME VAR :=
    " LAST 200 POINTS FOR PEAK LATENCY" TITLE " :=
    SHOW.TREND ENDOF
  52 OF POP.SIZE VAR :=
    " LAST 200 POINTS FOR SPIKE SIZE" TITLE " :=
    SHOW.TREND ENDOF
  53 OF EPSP.LAT VAR :=
    " LAST 200 POINTS FOR ADP PEAK TIME" TITLE " :=
    SHOW.TREND ENDOF
  54 OF POP.PERP.SIZE VAR :=
    " LAST 200 POINTS FOR SPIKE SIZE TO TANGENT" TITLE " :=
    SHOW.TREND ENDOF

```

```

55 OF AREA.ARRAY VAR :=
    " LAST 200 POINTS FOR AREA" TITLE ": =
    SHOW.TREND ENDOF
{MESS} CR          \ if key pressed but does not match
INTEN.ON
." KEY PRESSED HAS NO FUNCTION "
INTEN.OFF
BELL
ENDCASE
THEN
WRITE.DATA          \ write data to screen
WAVEFORM WAVEFORM.2ND := \ place wave in buffer in case prev wave needed
LOOP ;

```

```

: GET.DRIVE          \ to limit places to save data
NORMAL.DISPLAY
{DEF} SCREEN.CLEAR
." CHOOSE DRIVE:" CR
." 1 FOR A:" CR
." 2 FOR B:" CR
." 3 FOR C:\JUNK" CR
KEY
CASE
49 OF " A:" DRIVE ": = ENDOF
50 OF " B:" DRIVE ": = ENDOF
51 OF " C:\JUNK\" DRIVE ": = ENDOF
MYSELF
ENDCASE ;

```

```

: CREATE.DATA.FILE
LOAD.OVERLAY DATAFILE.SOV
{DEF} SCREEN.CLEAR
GET.DRIVE
." Enter a name for your data file (filename.ext). --> "
"INPUT FILENAME ": =
DRIVE FILENAME "CAT FILENAME ": =
FILE.TEMPLATE
4 COMMENTS
START.POP []FORM.SUBFILE
SLOPE []FORM.SUBFILE
PEAK.TIME []FORM.SUBFILE
POP.SIZE []FORM.SUBFILE
FLAG []FORM.SUBFILE
KEEPER []FORM.SUBFILE
EPSP.LAT []FORM.SUBFILE
POP.PERP.SIZE []FORM.SUBFILE

```

```

AREA.ARRAY []FORM.SUBFILE
END
{DEF} CR
CR ." SAVING DATA ... "
FILENAME DEFER> FILE.CREATE
FILENAME DEFER> FILE.OPEN
" 7 Arrays of 2000 " 1 >COMMENT
" 1 Array of 30 storing POP# for each flag" 2 >COMMENT
" 1 Array of 2 storing pop total # and # of flags" 3 >COMMENT
1 SUBFILE START.POP ARRAY>FILE \ save time of pop start for all spikes
2 SUBFILE SLOPE ARRAY>FILE \ save slope for each epsp
3 SUBFILE PEAK.TIME ARRAY>FILE \ save latencies for each spike
4 SUBFILE POP.SIZE ARRAY>FILE \ save size of each spike
5 SUBFILE FLAG ARRAY>FILE \ save flag indexes for each flag
6 SUBFILE KEEPER ARRAY>FILE \ save # of spikes and flags
7 SUBFILE EPSP.LAT ARRAY>FILE
8 SUBFILE POP.PERP.SIZE ARRAY>FILE
9 SUBFILE AREA.ARRAY ARRAY>FILE
FILE.CLOSE

ONERR: CR ." Error occurred, likely no disk, or full disk in drive specified"
CR ." Type CREATE.DATA.FILE to try again."

?FILE.OPEN IF FILE.CLOSE THEN
ABORT
;

REAL SCALAR DEEP

: LABEL.PRINT
5 22 GOTO.XY
." Date: " .DATE CR
." Depth: " CR
PRINT.SCREEN \ word to print the screen with error routine to protect
\ data accumulated.
;

: PROFILE \ stand alone word to print out waveforms at various depths
SCREEN.CLEAR
SETUP.FINAL
2000 1 DO
GO
GRAPHICS.DISPLAY
WAVEFORM .001221 * 100 / 1000000 * \ convert to uv
SUB[ 1 , 1199 , 1 ] Y.AUTO.PLOT \ plot
?KEY IF
KEY

```

```

CASE
  80 OF LABEL.PRINT ENDOF
  112 OF LABEL.PRINT ENDOF
  76 OF 5 22 GOTO.XY ." Pause on, strike any key"
    WAIT.FOR.KEY SCREEN.CLEAR
    5 22 GOTO.XY ."
    ENDOF \ if L then pause collection of data
  108 OF 5 22 GOTO.XY ." Pause on, strike any key"
    WAIT.FOR.KEY SCREEN.CLEAR
    5 22 GOTO.XY ."
    ENDOF \ if L then pause collection of data
  83 OF EXIT DISABLE.SCOPE ENDOF
  115 OF EXIT DISABLE.SCOPE ENDOF
ENDCASE
THEN
LOOP
;

: RUN
{DEF} SCREEN.CLEAR
MECHANICS
CREATE.DATA.FILE \ file.dump routine
{DEF} CR
INTEN.ON
." DATA SAVED, TYPE BYE TO SIGN OFF
INTEN.OFF
BELL
ABORT ;

BELL 200 MSEC.DELAY BELL

NORMAL.DISPLAY SCREEN.CLEAR ECHO.ON
\ PROGRAM: POP.PRG
\ DESCRIPTION: This program acquires the results of an evoked potential and
\ stores the EPSP slope, the time the population spike starts and
\ peaks, the size of the pop spike (taken from start to peak),
\ the area under the tangent of the two positive going curves,
\ the height of the pop spike from peak to tangent, and the time
\ the EPSP peaks.
\ The data is stored at the end of acquisition onto a disk in drive
\ A:. Sampling rate is at 100 KHz (every 10 us).
\ REQUIREMENTS: Asyst module must have "basic statistics" overlay (spfn.sov)
\ installed. User must have 5 1/4 inch floppy disk to store data.
\ The trigger should feed into channel 2 and the recording
\ electrode into channel 1. Gain should be about 100.
\ LIMITATIONS: The program will not handle more than 2,000 pop spikes and
\ 30 flags. The EPSP should start 750 us before the pop spike
\ starts.

```

\ TO BEGIN PROGRAM, TYPE: RUN (or PROFILE to print any waveform)
\
\ NOTE: If program "crashes" during acquisition and you want to save the data,
\ type CREATE.DATA.FILE, leave ASYST (BYE) and start over.

APPENDIX II: ASYST program for data analysis of evoked potential data acquired using program in Appendix I.

ECHO.OFF

ERROR.TRACE.ON

8 2 FIX.FORMAT

LOAD.OVERLAY DATAFILE.SOV

INTEGER SCALAR A

SCALAR B

SCALAR COUNTER

INTEGER DIM[2000] ARRAY START.POP \ to store pop start times (us)

INTEGER DIM[2000] ARRAY PEAK.TIME \ to store pop peak times (us)

REAL DIM[2000] ARRAY SLOPE \ to store slope values (uv/ms)

REAL DIM[2000] ARRAY POP.SIZE \ to store pop size (uv)

REAL DIM[2000] ARRAY EPSP.LAT \ to store epsp peak latency

REAL DIM[2000] ARRAY POP.PERP.SIZE \ to store pop size from tangent

REAL DIM[2000] ARRAY AREA.ARRAY \ area under tangent

REAL DIM[2000] ARRAY VAR \ to store one of above for calcs

REAL DIM[1000] ARRAY VAR2 \ to store second pulse in prdpulse exp.

REAL DIM[1000] ARRAY VAR3 \ to store 2nd pulse/ 1st in prdpulse exp.

INTEGER DIM[30] ARRAY FLAG \ stores pop # for each flag

INTEGER DIM[30] ARRAY FLAG.INDEX \ stores flag #s minus control period

INTEGER DIM[2] ARRAY KEEPER \ temp storage of pop# and flag#

INTEGER SCALAR POP# \ total # of pop spikes

INTEGER SCALAR FLAG# \ total number of flags

INTEGER SCALAR MEAN.SIZE \ stores size of sample means

INTEGER SCALAR MEAN.SIZE# \ stores number of samples in control

INTEGER SCALAR CONTROL.WIDTH \ stores length of control period

0 A :=

0 B :=

0 COUNTER :=

0 START.POP :=

0 PEAK.TIME :=

0 SLOPE :=

0 POP.SIZE :=

0 FLAG :=

0 FLAG.INDEX :=

0 KEEPER :=

0 POP# :=

0 FLAG# :=

6 MEAN.SIZE := \ set default sample size to 6

0 MEAN.SIZE# :=

60 CONTROL.WIDTH := \ set default control period to 60 points

```

64 STRING COMMENT1
64 STRING COMMENT2
64 STRING COMMENT3
64 STRING COMMENT4
20 STRING FILENAME
20 STRING FILENAME0
20 STRING FILENAME3
65 STRING TITLE
 8 STRING DRIVE
35 STRING VARIABLENAME
20 STRING YAXIS

```

```

20 2 24 78 WINDOW {WINDOW1}
0 2 15 14 WINDOW {WINDOW2}
7 20 18 70 WINDOW {WINDOW3}
2 03 23 15 WINDOW {WINDOW4}
24 2 24 78 WINDOW {WINDOW5}

```

```

: WAIT.FOR.KEY
  KEY 0 = IF KEY DROP THEN ; \ loops until any key is pressed

```

```

: INPUT.#
  BEGIN
  #INPUT NOT
  WHILE
  CR ." Invalid number, reenter: "
  REPEAT
;

```

```

: RESET.FLAGS
  4 0 FIX.FORMAT \ to change flag values from those
  {WINDOW4} SCREEN.CLEAR \ entered during experiment
  {WINDOW4} {BORDER}
  ." CURRENT FLAGS" CR
  31 1 DO
  0 FLAG [ I ] <>
  IF 2 SPACES I . 2 SPACES FLAG [ I ] . CR THEN
  LOOP
  ." POP# = " POP# .
  {WINDOW3} SCREEN.CLEAR
  {WINDOW3} {BORDER}
  ." INPUT FLAG # TO CHANGE -->"
  INPUT.#
  A :=
  CR
  ." INPUT POP # FOR FLAG #" A . ." -->"
  8 2 FIX.FORMAT
  INPUT.#

```

```

FLAG [ A ] :=
0 FLAG# :=          \ to reset number of flags
31 1 DO
FLAG [ I ] 0 <>      \ if pop # for flag I does not equal zero,
  IF                \ then increment flag # by 1, until a zero
    FLAG# 1 + FLAG# :=          \ is found, then leave loop.
  ELSE LEAVE
  THEN
LOOP ;

: CHANGE.SIZE          \ to allow the user to set the length of
NORMAL.DISPLAY        \ the control period, and the sample size.
{WINDOW3} {BORDER}
{WINDOW3} SCREEN.CLEAR
CR ." Enter # of points for preflag control. -->"
INPUT.#
CONTROL.WIDTH :=
CR ." Enter size of mean clusters. -->"
INPUT.#
MEAN.SIZE := ;

: GET.DRIVE
NORMAL.DISPLAY
{WINDOW3} {BORDER}
{WINDOW3} SCREEN.CLEAR
." CHOOSE DRIVE:" CR
." 1 FOR A:" CR
." 2 FOR B:" CR
." 3 FOR C:\JUNK" CR
KEY
CASE
49 OF " A:" DRIVE " := ENDOF
50 OF " B:" DRIVE " := ENDOF
51 OF " C:\JUNK\" DRIVE " := ENDOF
MYSELF
ENDCASE ;

INTEGER SCALAR PRDPULSE.OR.NOT

: CONVERT.FLAGS      \ in case of paired pulse experiment, flags must be
                    \ converted to reflect only first spike of pair
FLAG 1 + 2 / FLAG :=
CR ." Flags converted to single pulse equivalent" CR
FLAG# 1 + 1 DO
  FLAG [ I ] ." "
LOOP
;

```

```

: GET.PARAMS          \ to get file to be analyzed
NORMAL.DISPLAY
{WINDOW3} {BORDER}
{WINDOW3} SCREEN.CLEAR
." Enter the name for the file (filename.ext)." CR
." --> "
"INPUT FILENAME0 " := CR
DRIVE FILENAME0 "CAT
." Is this data single (1) or paired (2) pulse? --> "
INPUT.# ;

: READ.DATA.FILE      \ read scores from data file
LOAD.OVERLAY C:\ASYST\DATAFILE.SOV
FILE.TEMPLATE        \ note: template rigid, cannot be
4 COMMENTS           \ changed unless change acquisition
START.POP [ ]FORM.SUBFILE \ program.
SLOPE [ ]FORM.SUBFILE
PEAK.TIME [ ]FORM.SUBFILE
POP.SIZE [ ]FORM.SUBFILE
FLAG [ ]FORM.SUBFILE
KEEPER [ ]FORM.SUBFILE
EPSP.LAT [ ]FORM.SUBFILE
POP.PERP.SIZE [ ]FORM.SUBFILE
AREA.ARRAY [ ]FORM.SUBFILE
END
FILENAME DEFER> FILE.OPEN
1 SUBFILE START.POP FILE>ARRAY \ time of pop start for all spikes
2 SUBFILE SLOPE FILE>ARRAY     \ slope for each epsp
3 SUBFILE PEAK.TIME FILE>ARRAY \ latencies for each spike
4 SUBFILE POP.SIZE FILE>ARRAY  \ size of each spike
5 SUBFILE FLAG FILE>ARRAY      \ flag indexes for each flag
6 SUBFILE KEEPER FILE>ARRAY    \ # of spikes and flags
7 SUBFILE EPSP.LAT FILE>ARRAY  \ epsp peak latencies
8 SUBFILE POP.PERP.SIZE FILE>ARRAY \ spike size to tangent
9 SUBFILE AREA.ARRAY FILE>ARRAY \ area under tangent
FILE.CLOSE
KEEPER [ 1 ] POP# :=
KEEPER [ 2 ] FLAG# :=

ONERR: CR ." Error occurred, likely a nonexistent file. "
CR ." Type GO to restart."

?FILE.OPEN IF FILE.CLOSE THEN
ABORT
;

REAL DIM[ 30 ] ARRAY VAR.MEAN

```

```

REAL SCALAR VAR.DEV
REAL DIM[ 30 ] ARRAY VAR.UPPER.LIMIT
REAL DIM[ 30 ] ARRAY VAR.LOWER.LIMIT

O VAR.MEAN :=
O VAR.DEV :=
O VAR.UPPER.LIMIT :=
O VAR.LOWER.LIMIT :=

INTEGER SCALAR POPEND
INTEGER DIM[ 300 ] ARRAY MEAN#
REAL DIM[ 30 , 300 ] ARRAY VAR.MEANS
REAL DIM[ 60 ] ARRAY TEMP.ARRAY
INTEGER SCALAR 123.OR.NOT
O VAR.MEANS :=
O TEMP.ARRAY :=
O MEAN# :=
O POPEND :=

REAL DIM[ 300 ] ARRAY UPPER.PTS
      DIM[ 300 ] ARRAY LOWER.PTS
      DIM[ 300 ] ARRAY ARRAY.BUFFER
O UPPER.PTS :=
O LOWER.PTS :=

: WRITE.QUERY
LOAD.OVERLAY C:\ASYST\123IO.SOV
NORMAL.DISPLAY
{WINDOW3} {BORDER}
{WINDOW3} SCREEN.CLEAR
." CHOOSE CREATION OF LOTUS FILE OR NOT:" CR
." 1 FOR WRITE MEANS TO 123 FILE" CR
." 2 FOR WRITE MEANS IN % OF CONTROL TO 123 FILE:" CR
." 3 FOR DO NOT CREATE 123 FILE" CR
KEY
CASE
49 OF 1 123.OR.NOT := ENDOF
50 OF 2 123.OR.NOT := ENDOF
51 OF 3 123.OR.NOT := ENDOF
MYSELF
ENDCASE
123.OR.NOT 3 <
IF
GET.DRIVE
GET.PARAMS
FILENAME3 ": =           \ places string from get.params into var
FILENAME3 DEFER> 123FILE.CREATE
FILENAME3 DEFER> 123FILE.OPEN

```

```

THEN
;

: WRITE.TO.123FILE
LOAD.OVERLAY C:\ASYST\123IO.SOV
1 FLAG# + 1 DO
0 ARRAY.BUFFER :=
1 MEAN# [ I ] + 1 DO
  VAR.MEANS [ J , I ] ARRAY.BUFFER [ I ] :=
LOOP
123.OR.NOT 2 =
IF
ARRAY.BUFFER VAR.MEAN [ I ] / 100 * ARRAY.BUFFER :=
THEN
1 | 123WRITE.DOWN
ARRAY.BUFFER ARRAY > 123FILE
LOOP
123FILE.CLOSE
;

: GET.MEANS          \ get sample means and store
WRITE.QUERY          \ write to 123 file or not
CONTROL.WIDTH MEAN.SIZE / MEAN.SIZE# := \ # of samples in control
FLAG CONTROL.WIDTH - FLAG.INDEX :=      \ start of control period
1 FLAG# + 1 DO          \ get samples for each flag set
0 MEAN# [ I ] :=
1 COUNTER :=
| FLAG# <          \ if not the last flag
IF
1 | + A :=
FLAG [ A ] FLAG.INDEX [ I ] DO \ from start of control to next flag
  VAR SUB[ I , MEAN.SIZE , 1 ] MEAN \ get mean for each sample and
  VAR.MEANS [ J , COUNTER ] := \ store in var.means
  1 COUNTER + COUNTER :=
  1 MEAN# [ J ] + MEAN# [ J ] := \ keep track of number of samples
MEAN.SIZE + LOOP \ add sample size to loop index
ELSE \ when at the last flag set
300 MEAN.SIZE * FLAG.INDEX [ I ] \ check to make sure no more than 300
+ POP# MIN POPEND := \ samples are available
POPEND 2 - POPEND := \ so no sample ends past total pop#
PRDPULSE.OR.NOT 2 = IF POPEND 2 / POPEND := THEN \ added fpr prdpulse
POPEND FLAG.INDEX [ I ] DO \ from control start to last popspike
  VAR SUB[ I , MEAN.SIZE , 1 ] MEAN
  VAR.MEANS [ J , COUNTER ] :=
  1 COUNTER + COUNTER :=
  1 MEAN# [ J ] + MEAN# [ J ] :=
MEAN.SIZE + LOOP
THEN

```

```

1 MEAN.SIZE# + 1 DO \ for each flag, place means into a temporary array
  VAR.MEANS [ J , I ] TEMP.ARRAY [ I ] :=
LOOP
TEMP.ARRAY SUB[ 1 , MEAN.SIZE# , 1 ]
  MEAN VAR.MEAN [ I ] := \ get mean of samples in control period
VAR SUB[ FLAG.INDEX [ I ] , CONTROL.WIDTH , 1 ]
  SAMPLE.VARIANCE SQRT VAR.DEV := \ get standard deviation
VAR.DEV MEAN.SIZE 1 - SQRT / \ find confidence limits
  .975 MEAN.SIZE 1 - STUDENT-T.FRACTILE *
  VAR.MEAN [ I ] + VAR.UPPER.LIMIT [ I ] :=
VAR.DEV MEAN.SIZE 1 - SQRT /
  .975 MEAN.SIZE 1 - STUDENT-T.FRACTILE *
  VAR.MEAN [ I ] - ABS VAR.LOWER.LIMIT [ I ] :=
LOOP
123.OR.NOT 3 <
IF
  WRITE.TO.123FILE
THEN
;

VUPORT RIGHT.HALF
.30 .30 VUPORT.ORIG
.70 .70 VUPORT.SIZE

VUPORT RIGHT.HALF2
.00 .00 VUPORT.ORIG
.99 .99 VUPORT.SIZE

: LABEL.GRAPH
4 0 FIX.FORMAT
90 LABEL.DIR
90 CHAR.DIR
NORMAL.COORDS
.02 .35 POSITION YAXIS LABEL
0 LABEL.DIR 0 CHAR.DIR
.40 .02 POSITION " SAMPLE NUMBER" LABEL
1 1 POSITION
{WINDOW1} SCREEN.CLEAR
." FILENAME = " FILENAME "TYPE 10 SPACES
." VARIABLE = " VARIABLENAME "TYPE CR
." FLAG # = " I . 5 SPACES ." POP # = " FLAG [ I ] . CR
." CONTROL PERIOD LENGTH = " CONTROL.WIDTH .
5 SPACES ." SAMPLE SIZE = " MEAN.SIZE . CR
." CONTROL PERIOD ENDS AT X = " MEAN.SIZE# . CR
." CONFIDENCE LIMITS USE CONTROL PERIOD SAMPLING DISTRIBUTION FOR 95%
2-TAILED"
8 2 FIX.FORMAT ;

```

```

: PRINT.MEANS
." FILENAME = " FILENAME "TYPE ." VARIABLE = " VARIABLENAME "TYPE CR
4 0 FIX.FORMAT
." FLAG # = " I . 5 SPACES ." FLAG POP # = " FLAG [ I ] . CR
." CONTROL PERIOD LENGTH = " CONTROL.WIDTH .
5 SPACES ." SAMPLE.SIZE = " MEAN.SIZE . CR
8 2 FIX.FORMAT
." UPPER.LIMIT = " VAR.UPPER.LIMIT [ I ] . 4 SPACES
." LOWER LIMIT = " VAR.LOWER.LIMIT [ I ] . 4 SPACES
." MEAN = " VAR.MEAN [ I ] . CR CR
0 COUNTER :=
0 A :=
10 SPACES ." SAMPLE # SAMPLE PERCENTAGE" CR
10 SPACES ." MEAN OF CONTROL MEAN" CR
301 1 DO
  I 1 + A :=
  ARRAY.BUFFER [ A ] 0 =
  IF LEAVE THEN
    10 SPACES I . 4 SPACES ARRAY.BUFFER [ I ] . 6 SPACES
\ calculate percentage of control mean and print
  ARRAY.BUFFER SUB[ 1 , MEAN.SIZE# , 1 ] MEAN ARRAY.BUFFER [ I ]
  SWAP / 100 * . CR
  PAUSE
  LOOP ;

```

```

INTEGER SCALAR X
  SCALAR Y

```

```

: PRINT.RAW.Scores
NORMAL.DISPLAY
OUT>PRINTER
." FILENAME = " FILENAME "TYPE CR CR
." POP # EPSP POP POP POP EPSP POP/TAN AREA " CR
." SLOPE START PEAK SIZE PEAK SIZE UNDER" CR
." TIME TIME TAN " CR
." uv/ms us us uv us uv mv" CR
." -----" CR
Y X DO
0 START.POP [ I ] =
IF
  LEAVE
ELSE
  I . 3 SPACES SLOPE [ I ] . 1 SPACES START.POP [ I ] .
  3 SPACES PEAK.TIME [ I ] . 3 SPACES POP.SIZE [ I ] .
  3 SPACES EPSP.LAT [ I ] . 3 SPACES POP.PERP.SIZE [ I ] .
  3 SPACES AREA.ARRAY [ I ] . CR
THEN
LOOP

```

```

CONSOLE ;

: GET.RANGE
  SCREEN.CLEAR
  ." TOTAL # OF SAMPLES TAKEN = " POP# . CR
  ." (note: range must be less than 1600 if graphing)" CR
  CR ." SAMPLE # FOR START OF RANGE? "
  INPUT.#
  X :=
  CR ." SAMPLE # FOR END OF RANGE? "
  INPUT.#
  1 + Y :=
;

: RAW.Scores
{WINDOW3}
SCREEN.CLEAR
." PRINT (A)LL RAW SCORES, A (R)ANGE OF RAW SCORES, OR (E)XIT? (A/R/E) "
KEY
CASE
65 OF 1 X :=
  POP# 1 + Y :=
  PRINT.RAW.Scores END OF
97 OF 1 X :=
  POP# 1 + Y :=
  PRINT.RAW.Scores END OF
82 OF GET.RANGE
  PRINT.RAW.Scores END OF
114 OF GET.RANGE
  PRINT.RAW.Scores END OF
69 OF EXIT END OF
101 OF EXIT END OF
MYSELF
ENDCASE
MYSELF ;

: CHECK
." ARE YOU SURE YOU WANT TO PRINT RAW SCORES ??? (Y/N)"
KEY
CASE
121 OF PRINT.RAW.Scores END OF
89 OF PRINT.RAW.Scores END OF
ENDCASE ;

TEXT.BUFFER SCREEN.IMAGE \ to allow switching of video pages to see means

: PRINT.FORMAT? \ print means to screen or to printer
." To Screen (1) or to Printer (2)? (1/2)

```

```

KEY
CASE
  49 OF SCREEN.IMAGE STORE.VIDEO NORMAL.DISPLAY
    PRINT.MEANS GRAPHICS.DISPLAY SCREEN.IMAGE
    RESTORE.VIDEO ENDOF
  50 OF OUT>PRINTER PRINT.MEANS CONSOLE ENDOF
ENDCASE ;

: PRINTOUT
{WINDOW2} SCREEN.CLEAR
." Print graph?" CR ." (Y/N) "
KEY
CASE
  121 OF SCREEN.CLEAR SCREEN.PRINT ENDOF
  89 OF SCREEN.CLEAR SCREEN.PRINT ENDOF
ENDCASE
CR ." Print means?" CR ." (Y/N) "
KEY
CASE
  121 OF PRINT.FORMAT? ENDOF
  89 OF PRINT.FORMAT? ENDOF
ENDCASE ;

: PLOT.MEANS
1 FLAG# + A :=
A 1 DO
  0 ARRAY.BUFFER :=
  1 MEAN# [ I ] + B :=
  B 1 DO \ fill 1 dim array so it can be plotted
    VAR.MEANS [ J , I ] ARRAY.BUFFER [ I ] :=
  LOOP
  GRAPHICS.DISPLAY
  HORIZONTAL GRID.OFF
  VERTICAL GRID.OFF
  RIGHT.HALF
  " *" SYMBOL
  ARRAY.BUFFER SUB[ 1 , MEAN# [ I ] , 1 ] Y.AUTO.PLOT
  SOLID
  VAR.UPPER.LIMIT [ I ] UPPER.PTS :=
  VAR.LOWER.LIMIT [ I ] LOWER.PTS :=
  UPPER.PTS SUB[ 1 , MEAN# [ I ] , 1 ] Y.DATA.PLOT
  LOWER.PTS SUB[ 1 , MEAN# [ I ] , 1 ] Y.DATA.PLOT
  LABEL.GRAPH
  PRINTOUT
LOOP ;

INTEGER SCALAR RANGE1
  SCALAR RANGE2

```

```

SCALAR RANGE3
SCALAR RANGE4
SCALAR RANGE5
SCALAR RANGE6
SCALAR RANGE7
SCALAR RANGE8
SCALAR RANGE9
SCALAR PAIRED.POP#

```

```

: XYPLOT \ for paired pulse only
CR ." Remember that pop# represents the sequential # of the"
CR ." first spike only." CR
CR ." control start pop# = " INPUT.# RANGE1 :=
CR ." control end pop# = " INPUT.# RANGE2 :=
CR ." enhanced start pop# = " INPUT.# RANGE3 :=
CR ." enhanced end pop# = " INPUT.# RANGE4 :=
CR ." post enhanced start pop# = " INPUT.# RANGE5 :=
CR ." post enhanced end pop# = " INPUT.# RANGE6 :=
POP# 2 / PAIRED.POP# :=
PAIRED.POP# 1 + 1 DO
VAR2 [ 1 ] VAR [ 1 ] / VAR3 [ 1 ] :=
LOOP
RANGE2 RANGE1 - RANGE7 :=
RANGE4 RANGE3 - RANGE8 :=
RANGE6 RANGE5 - RANGE9 :=
GRAPHICS.DISPLAY
HORIZONTAL GRID.OFF
VERTICAL GRID.OFF
RIGHT.HALF2
{WINDOW5}
" " SYMBOL
VAR SUB[ 1 , PAIRED.POP# , 1 ] VAR3 SUB[ 1 , PAIRED.POP# , 1 ] XY.AUTO.PLOT
" 1" SYMBOL
VAR SUB[ RANGE1 , RANGE7 , 1 ] VAR3 SUB[ RANGE1 , RANGE7 , 1 ] XY.DATA.PLOT
" 2" SYMBOL
VAR SUB[ RANGE3 , RANGE8 , 1 ] VAR3 SUB[ RANGE3 , RANGE8 , 1 ] XY.DATA.PLOT
" 3" SYMBOL
VAR SUB[ RANGE5 , RANGE9 , 1 ] VAR3 SUB[ RANGE5 , RANGE9 , 1 ] XY.DATA.PLOT
4 0 FIX.FORMAT
90 LABEL.DIR 90 CHAR.DIR
NORMAL.COORDS
.02 .35 POSITION " SIZE OF SPIKE2/SPIKE1" LABEL
0 LABEL.DIR 0 CHAR.DIR
.40 .08 POSITION " SIZE OF SPIKE 1" LABEL
.20 .96 POSITION
" FILE = " FILENAME "CAT " " "CAT VARIABLENAME "CAT TITLE " :=
TITLE LABEL
.02 .04 POSITION ." RANGE 1 =" RANGE1 . ." -" RANGE2 .

```

```

                ." RANGE 2 =" RANGE3 ." -" RANGE4 .
                ." RANGE 3 =" RANGE5 ." -" RANGE6 .
\  CURSOR.OFF
   0 1 POSITION
   8 2 FIX.FORMAT
   KEY
   CASE
     80 OF SCREEN.CLEAR SCREEN.PRINT ENDOF
     112 OF SCREEN.CLEAR SCREEN.PRINT ENDOF
   ENDCASE ;

: XYPLOT? \ for paired pulse only
PRDPULSE.OR.NOT 2 =
IF
  NORMAL.DISPLAY
  CR ." Do you want to plot prdpluse XY plot? (Y/N) "
  KEY
  CASE
    121 OF XYPLOT ENDOF
    89 OF XYPLOT ENDOF
  ENDCASE
THEN ;

: CHECK.FLAG \ in case program crashed during acquisition and the
FLAG# 0 = \ number of flags and pops were not saved
IF
  30 1 DO
    FLAG [ I ] 0 <>
    IF
      FLAG# 1 + FLAG# :=
    ELSE LEAVE
    THEN
  LOOP
THEN
\ POP# 0 =
\ IF
0 POP# :=
2000 1 DO
  POP.SIZE [ I ] 0 <>
  IF
    POP# 1 + POP# :=
  ELSE LEAVE
  THEN
LOOP
\ THEN
;

: ANAL

```

```

NORMAL.DISPLAY
{WINDOW3} {BORDER}
{WINDOW3} SCREEN.CLEAR
GET.DRIVE
GET.PARAMS
FILENAME ": = \ places string from get.params into variable
BELL
CR ." READING DATA ... "
READ.DATA.FILE
CHECK.FLAG
  PRDPULSE.OR.NOT :=
PRDPULSE.OR.NOT 2 =
IF
  CONVERT.FLAGS
THEN
;

: RUN
GET.MEANS
PLOT.MEANS
XYPLOT? ;

: SLOPE.FILL
PRDPULSE.OR.NOT 2 =
IF
  SLOPE SUB[ 1 , 1000 , 2 ] VAR SUB[ 1 , 1000 , 1 ] :=
  SLOPE SUB[ 2 , 1000 , 2 ] VAR2 :=
ELSE
  SLOPE VAR :=
THEN
" EPSP SLOPE" VARIABLENAME ": =
" SLOPE uv/ms" YAXIS ": =
RUN
EXIT ;

: POP.START.FILL
PRDPULSE.OR.NOT 2 =
IF
  START.POP SUB[ 1 , 1000 , 2 ] VAR SUB[ 1 , 1000 , 1 ] :=
  START.POP SUB[ 2 , 1000 , 2 ] VAR2 :=
ELSE
  START.POP VAR :=
THEN
" START OF POPSPIKE" VARIABLENAME ": =
" TIME (us)" YAXIS ": =
RUN
EXIT ;

```

```

: PEAK.TIME.FILL
PRDPULSE.OR.NOT 2 =
IF
  PEAK.TIME SUB[ 1 , 1000 , 2 ] VAR SUB[ 1 , 1000 , 1 ] :=
  PEAK.TIME SUB[ 2 , 1000 , 2 ] VAR2 :=
ELSE
  PEAK.TIME VAR :=
THEN
  " TIME OF POP PEAK" VARIABLENAME " :=
  " TIME (us)" YAXIS " :=
RUN
EXIT ;

: POP.SIZE.FILL
PRDPULSE.OR.NOT 2 =
IF
  POP.SIZE SUB[ 1 , 1000 , 2 ] VAR SUB[ 1 , 1000 , 1 ] :=
  POP.SIZE SUB[ 2 , 1000 , 2 ] VAR2 :=
ELSE
  POP.SIZE VAR :=
THEN
  " SIZE OF POPSPIKE" VARIABLENAME " :=
  " AMPLITUDE (uv)" YAXIS " :=
RUN
EXIT ;

: EPSP.LAT.FILL
PRDPULSE.OR.NOT 2 =
IF
  EPSP.LAT SUB[ 1 , 1000 , 2 ] VAR SUB[ 1 , 1000 , 1 ] :=
  EPSP.LAT SUB[ 2 , 1000 , 2 ] VAR2 :=
ELSE
  EPSP.LAT VAR :=
THEN
  " LATENCY OF EPSP PEAK" VARIABLENAME " :=
  " TIME (us)" YAXIS " :=
RUN
EXIT ;

: POP.PERP.SIZE.FILL
PRDPULSE.OR.NOT 2 =
IF
  POP.PERP.SIZE SUB[ 1 , 1000 , 2 ] VAR SUB[ 1 , 1000 , 1 ] :=
  POP.PERP.SIZE SUB[ 2 , 1000 , 2 ] VAR2 :=
ELSE
  POP.PERP.SIZE VAR :=
THEN
  " SIZE OF POPSPIKE (TANGENT)" VARIABLENAME " :=

```

```

" AMPLITUDE (uv)" YAXIS ": =
RUN
EXIT ;

: AREA.ARRAY.FILL
PRDPULSE.OR.NOT 2 =
IF
  AREA.ARRAY SUB[ 1 , 1000 , 2 ] VAR SUB[ 1 , 1000 , 1 ] :=
  AREA.ARRAY SUB[ 2 , 1000 , 2 ] VAR2 :=
ELSE
  AREA.ARRAY VAR :=
THEN
" AREA UNDER THE TANGENT" VARIABLENAME ": =
" AMPLITUDE (mv)" YAXIS ": =
RUN
EXIT ;

: CHOOSE.VARIABLE
NORMAL.DISPLAY
{DEF} SCREEN.CLEAR
{WINDOW3} SCREEN.CLEAR
{WINDOW3} {BORDER}
." CHOOSE VARIABLE:" CR
." 1 FOR SLOPE" CR
." 2 FOR START OF POPSPIKE" CR
." 3 FOR TIME OF POP PEAK" CR
." 4 FOR POPSPIKE (PEAK TO PEAK) SIZE" CR
." 5 FOR EPSP PEAK LATENCY" CR
." 6 FOR POPSPIKE (PEAK TO TANGENT) SIZE" CR
." 7 FOR AREA UNDER THE TANGENT" CR
." 8 FOR EXIT TO MAIN MENU" CR
KEY
CASE
  49 OF ." CALCULATING MEANS..." SLOPE.FILL ENDOF
  50 OF ." CALCULATING MEANS..." POP.START.FILL ENDOF
  51 OF ." CALCULATING MEANS..." PEAK.TIME.FILL ENDOF
  52 OF ." CALCULATING MEANS..." POP.SIZE.FILL ENDOF
  53 OF ." CALCULATING MEANS..." EPSP.LAT.FILL ENDOF
  54 OF ." CALCULATING MEANS..." POP.PERP.SIZE.FILL ENDOF
  55 OF ." CALCULATING MEANS..." AREA.ARRAY.FILL ENDOF
  56 OF EXIT ENDOF
MYSELF
ENDCASE
MYSELF ;

20 STRING FILENAME2

: GET.PARAMS2

```

```

GET.DRIVE
NORMAL.DISPLAY
{DEF} SCREEN.CLEAR
." ENTER THE NAME FOR YOUR 123 DATA FILE (add extension .WKS)."
CR
"INPUT FILENAME2 " :=
DRIVE FILENAME2 "CAT FILENAME2 " := ;

```

INTEGER SCALAR PULSES

```

: WRITE.TO123
  CR
  ." Paired Pulse or Single Pulse Data? (2/1) "
  INPUT.#
  PULSES :=
  LOAD.OVERLAY 123IO.SOV
  FILENAME2 DEFER> 123FILE.CREATE
  FILENAME2 DEFER> 123FILE.OPEN
  2 PULSES =
  IF
  1 1 123WRITE.DOWN
  START.POP SUB[ 1 , 2000 , 2 ] ARRAY> 123FILE
  1 2 123WRITE.DOWN
  SLOPE SUB[ 1 , 2000 , 2 ] ARRAY> 123FILE
  1 3 123WRITE.DOWN
  PEAK.TIME SUB[ 1 , 2000 , 2 ] ARRAY> 123FILE
  1 4 123WRITE.DOWN
  POP.SIZE SUB[ 1 , 2000 , 2 ] ARRAY> 123FILE
  1 5 123WRITE.DOWN
  EPSP.LAT SUB[ 1 , 2000 , 2 ] ARRAY> 123FILE
  1 6 123WRITE.DOWN
  POP.PERP.SIZE SUB[ 1 , 2000 , 2 ] ARRAY> 123FILE
  1 7 123WRITE.DOWN
  AREA.ARRAY SUB[ 1 , 2000 , 2 ] ARRAY> 123FILE
  1 8 123WRITE.DOWN
  START.POP SUB[ 2 , 2000 , 2 ] ARRAY> 123FILE
  1 9 123WRITE.DOWN
  SLOPE SUB[ 2 , 2000 , 2 ] ARRAY> 123FILE
  1 10 123WRITE.DOWN
  PEAK.TIME SUB[ 2 , 2000 , 2 ] ARRAY> 123FILE
  1 11 123WRITE.DOWN
  POP.SIZE SUB[ 2 , 2000 , 2 ] ARRAY> 123FILE
  1 12 123WRITE.DOWN
  EPSP.LAT SUB[ 2 , 2000 , 2 ] ARRAY> 123FILE
  1 13 123WRITE.DOWN
  POP.PERP.SIZE SUB[ 2 , 2000 , 2 ] ARRAY> 123FILE
  1 14 123WRITE.DOWN
  AREA.ARRAY SUB[ 2 , 2000 , 2 ] ARRAY> 123FILE

```

```
ELSE
  1 1 123WRITE.DOWN
  START.POP ARRAY> 123FILE
  1 2 123WRITE.DOWN
  SLOPE ARRAY> 123FILE
  1 3 123WRITE.DOWN
  PEAK.TIME ARRAY> 123FILE
  1 4 123WRITE.DOWN
  POP.SIZE ARRAY> 123FILE
  1 5 123WRITE.DOWN
  EPSP.LAT ARRAY> 123FILE
  1 6 123WRITE.DOWN
  POP.PERP.SIZE ARRAY> 123FILE
  1 7 123WRITE.DOWN
  AREA.ARRAY ARRAY> 123FILE
  THEN
  123FILE.CLOSE
;

: 123
  GET.PARAMS2
  WRITE.TO123
;

INTEGER SCALAR Z
INTEGER SCALAR W
INTEGER SCALAR V
INTEGER SCALAR U
INTEGER SCALAR T
INTEGER DIM[ 2000 ] ARRAY HOLDING

: GET.SYMBOL
  CASE
    1 OF " 0" SYMBOL ENDOF
    2 OF " 1" SYMBOL ENDOF
    3 OF " 2" SYMBOL ENDOF
    4 OF " 3" SYMBOL ENDOF
    5 OF " 4" SYMBOL ENDOF
    6 OF " 5" SYMBOL ENDOF
    7 OF " 6" SYMBOL ENDOF
    8 OF " 7" SYMBOL ENDOF
    9 OF " 8" SYMBOL ENDOF
    10 OF " 9" SYMBOL ENDOF
    11 OF " 0" SYMBOL ENDOF
    12 OF " 1" SYMBOL ENDOF
    13 OF " 2" SYMBOL ENDOF
    14 OF " 3" SYMBOL ENDOF
    15 OF " 4" SYMBOL ENDOF
```

```

16 OF " 5" SYMBOL ENDOF
17 OF " 6" SYMBOL ENDOF
18 OF " 7" SYMBOL ENDOF
19 OF " 8" SYMBOL ENDOF
20 OF " 9" SYMBOL ENDOF
21 OF " 0" SYMBOL ENDOF
22 OF " 1" SYMBOL ENDOF
23 OF " 2" SYMBOL ENDOF
24 OF " 3" SYMBOL ENDOF
25 OF " 4" SYMBOL ENDOF
26 OF " 5" SYMBOL ENDOF
27 OF " 6" SYMBOL ENDOF
28 OF " 7" SYMBOL ENDOF
29 OF " 8" SYMBOL ENDOF
30 OF " 9" SYMBOL ENDOF
ENDCASE
;

: PLOT.EACH.POINT
2000 RAMP HOLDING :=
FLAG# 1 + 1 DO
  X FLAG [ I ] <
  IF
  I W :=
  LEAVE
  THEN
  LOOP
FLAG# 1 + 1 DO
  Y FLAG [ I ] >
  IF
  I V :=
  THEN
  LOOP
V 1 + W DO
I GET.SYMBOL \ leave I on stack and get corresponding symbol
W I = IF
  FLAG [ I ] X - U :=
  HOLDING SUB[ X , U , 1 ] VAR SUB[ X , U , 1 ] XY.DATA.PLOT
ELSE
V I = IF
  I 1 - T :=
  FLAG [ I ] FLAG [ T ] - U :=
  HOLDING SUB[ FLAG [ T ] , U , 1 ] VAR SUB[ FLAG [ T ] , U , 1 ]
  XY.DATA.PLOT
  I 1 + GET.SYMBOL \ leave I + 1 on stack and get corresponding symbol
Y FLAG [ I ] - U :=
HOLDING SUB[ FLAG [ I ] , U , 1 ] VAR SUB[ FLAG [ I ] , U , 1 ]
  XY.DATA.PLOT

```

```

ELSE
  I 1 - T :=
  FLAG [ I ] FLAG [ T ] - U :=
  HOLDING SUB[ FLAG [ T ] , U , 1 ] VAR SUB[ FLAG [ T ] , U , 1 ] XY.DATA.PLOT
  THEN
  THEN
  LOOP
;

: PLOT.RAW.SCORES
  GET.RANGE
  Y X - Z :=          \ # of points to plot
  GRAPHICS.DISPLAY
  HORIZONTAL GRID.OFF
  VERTICAL GRID.OFF
  RIGHT.HALF2
  {WINDOW5}
  " " SYMBOL
  2000 INTEGER RAMP X + 1 - SUB[ 1 , Z , 1 ] \ set up x-axis
  VAR SUB[ X , Z , 1 ] XY.AUTO.PLOT
  PLOT.EACH.POINT
  4 0 FIX.FORMAT
  90 LABEL.DIR
  90 CHAR.DIR
  NORMAL.COORDS
  .02 .35 POSITION YAXIS LABEL
  0 LABEL.DIR 0 CHAR.DIR
  .40 .08 POSITION " SAMPLE NUMBER" LABEL
  .20 .96 POSITION
  " FILE = " FILENAME "CAT " " "CAT VARIABLENAME "CAT TITLE " :=
  TITLE LABEL
  CURSOR.OFF
  0 1 POSITION
  8 2 FIX.FORMAT
  KEY
  CASE
    80 OF SCREEN.CLEAR SCREEN.PRINT ENDOF
    112 OF SCREEN.CLEAR SCREEN.PRINT ENDOF
  ENDCASE
;

: GET.RAW.SCORES
  NORMAL.DISPLAY
  {DEF} SCREEN.CLEAR
  {WINDOW3} SCREEN.CLEAR
  {WINDOW3} {BORDER}
  ." CHOOSE VARIABLE:" CR
  ." 1 FOR SLOPE" CR

```

```

." 2 FOR START OF POPSPIKE" CR
." 3 FOR TIME OF POP PEAK" CR
." 4 FOR POPSPIKE (PEAK TO PEAK) SIZE" CR
." 5 FOR EPSP PEAK LATENCY" CR
." 6 FOR POPSPIKE (PEAK TO TANGENT) SIZE" CR
." 7 FOR AREA UNDER THE TANGENT" CR
." 8 FOR EXIT TO MAIN MENU" CR

```

KEY

CASE

```

49 OF " EPSP SLOPE" VARIABLENAME ": =
    " SLOPE uv/ms" YAXIS ": =
    SLOPE VAR :=
    PLOT.RAW.SCORES ENDOF
50 OF " START OF POPSPIKE" VARIABLENAME ": =
    " TIME (us)" YAXIS ": =
    START.POP VAR :=
    PLOT.RAW.SCORES ENDOF
51 OF " POPSPIKE PEAK LATENCY" VARIABLENAME ": =
    " TIME (us)" YAXIS ": =
    PEAK.TIME VAR :=
    PLOT.RAW.SCORES ENDOF
52 OF " SPIKE HEIGHT(PEAK TO PEAK)" VARIABLENAME ": =
    " AMPLITUDE (uv)" YAXIS ": =
    POP.SIZE VAR :=
    PLOT.RAW.SCORES ENDOF
53 OF " POST-SPIKE PEAK LATENCY" VARIABLENAME ": =
    " TIME (us)" YAXIS ": =
    EPSP.LAT VAR :=
    PLOT.RAW.SCORES ENDOF
54 OF " SPIKE HEIGHT(PEAK TO TAN)" VARIABLENAME ": =
    " AMPLITUDE (uv)" YAXIS ": =
    POP.PERP.SIZE VAR :=
    PLOT.RAW.SCORES ENDOF
55 OF " AREA UNDER THE TANGENT" VARIABLENAME ": =
    " AMPLITUDE (mv)" YAXIS ": =
    AREA.ARRAY VAR :=
    PLOT.RAW.SCORES ENDOF
56 OF EXIT ENDOF

```

MYSELF

ENDCASE

MYSELF ;

: CHOOSE.ACTION

NORMAL.DISPLAY

{DEF} SCREEN.CLEAR

{WINDOW3} {BORDER}

{WINDOW3} SCREEN.CLEAR

```

." CHOOSE ACTION:" CR
." 1 FOR RESET FLAGS" CR
." 2 FOR RESET CONTROL AND SAMPLE SIZES" CR
."   (default = 60 and 6)" CR
." 3 FOR PROCEED WITH CHOICE OF VARIABLE" CR
." 4 FOR PRINT OUT OF RAW SCORES" CR
." 5 FOR SWITCHING DATA FILES" CR
." 6 FOR CREATING A 123 .WKS FILE" CR
." 7 FOR PLOTTING THE RAW SCORES" CR
." 8 FOR EXIT PROGRAM" CR
KEY
CASE
 49 OF RESET.FLAGS ENDOF
 50 OF CHANGE.SIZE ENDOF
 51 OF CHOOSE.VARIABLE ENDOF
 52 OF RAW.SCORES ENDOF
 53 OF STACK.CLEAR ANAL MYSELF ENDOF \ same as GO
 54 OF 123 ENDOF
 55 OF GET.RAW.SCORES ENDOF
 56 OF BYE ENDOF
MYSELF
ENDCASE
MYSELF ;

: GO
  STACK.CLEAR
  ANAL
  CHOOSE.ACTION ;

BELL 200 MSEC.DELAY BELL

NORMAL.DISPLAY SCREEN.CLEAR ECHO.ON

\ PROGRAM: POPANAL.PRG
\
\ DESCRIPTION: Program analyzes data obtained through the "pop.prg" data
\               acquisition program. Analysis is done around flags entered by the
\               user during data acquisition. Flags can be altered. Control
\               period size and sample size can be reset by user. This program
\               calculates the mean and 95% confidence limits (t statistic) for
\               each window of data deliniated by the flags (preflag control
\               period + experimental period from flag to next flag). Analysis
\               is menu driven.
\
\ REQUIREMENTS: Asyst module must have the "basic statistics"
\               overlay installed (spfn.sov).
\
\ TO BEGIN PROGRAM, TYPE: GO

```